Airway Dynamics and the Role of Zyxin

Airway Dynamics and the Role of Zyxin

A DISSERTATION PRESENTED
BY
SONIA REBECCA ROSNER
TO
THE COMMITTEE ON HIGHER DEGREES IN BIOLOGICAL SCIENCES IN PUBLIC HEALTH

IN PARTIAL FULFILLMENT OF THE REQUIREMENTS
FOR THE DEGREE OF
DOCTOR OF PHILOSOPHY
IN THE SUBJECT OF
BIOLOGICAL SCIENCES IN PUBLIC HEALTH

HARVARD UNIVERSITY
CAMBRIDGE, MASSACHUSETTS
APRIL 2014

Jeffrey J. Fredberg Sonia Rebecca Rosner

Airway Dynamics and the Role of Zyxin

Abstract

Morbidity and mortality attributable to asthma arise mainly from contraction of airway smooth muscle (ASM) and resulting bronchospasm. Bronchospasm that is induced in the laboratory is easily reversed by a spontaneous deep inspiration (DI) whereas bronchospasm that occurs spontaneously in asthma is not. In response to a spontaneous DI, contracted ASM fluidizes rapidly and then resolidifies slowly, but molecular mechanisms accounting for these salutary bronchodilatory responses –and their dramatic breakdown in asthma– are unknown. Using a multi-scale approach, I show here that both the baseline contractile force and the fluidization response of ASM are independent of the cytoskeletal protein zyxin, whereas the resolidification response is zyxin-dependent. At the levels of the stress fiber, the isolated cell, and the integrated airway, zyxin acts to stabilize the contractile apparatus and promote the resolidification response. More than just the motor of contraction, ASM is thus viewed in the broader context of a self-healing active material wherein resolidification and its molecular determinants contribute to the biology of bronchospasm.

Contents

List of Figures

List of Tables

This dissertation is dedicated to my beloved parents, Ronda and Jeff Rosner.

Author List

The following authors contributed to these chapters:

Chapter 1: Sonia R. Rosner

Chapter 2: Sonia R. Rosner

Chapter 3: Sonia R. Rosner

Chapter 4: Sonia R. Rosner, Sumati Ram-Mohan, Jesus R. Paez-Cortez, Tera L. Lavoie, Maria L. Dowell, Lei Yuan, Xingbin Ai, Alan Fine, William C. Aird, Julian Solway, Jeffrey J. Fredberg, and Ramaswamy Krishnan. This work was published online in *The American Journal of Respiratory Cell and Molecular Biology* in December 2013 and appeared in print May 2014, Volume 50, Number 5. Lungs were prepared by JRPC and XA. Figure 4.1 was generated by SRR and LY. Figure 4.3 was generated by XA. Figure 4.9 was generated by SRM. The remaining figures were generated by SRR. The manuscript was written by SRR, JS, JJF, and RK.

Chapter 5: Sonia R. Rosner, Elizabeth Blankman, Chris Jensen, Ramaswamy Krishnan, Mary Beckerle, Jeffrey J. Fredberg and Mark Smith. Figures 5.1 and 5.2 were generated by EB and MS. Figure 5.18 was generated by MS. Figures 5.19, 5.20, 5.21, and 5.22 were generated by SRR, EB, and MS. The remaining figures were generated by SRR. The chapter was written by SRR and JJF.

Chapter 6: Sonia R. Rosner, Elizabeth Blankman, Chris Jensen, Ramaswamy Krishnan, Mary Beckerle, Jeffrey J. Fredberg and Mark Smith. Lungs were obtained and precision cut lung slices prepared by CJ and MS. All figures were generated by SRR. The chapter was written by SRR and JJF.

Chapter 7: Sonia R. Rosner

Acknowledgments

This thesis has been a long and complex endeavor, and I owe thanks to many people for their help and support. First, I would like to thank Jeff Fredberg, my advisor and mentor these past four years. His inexhaustible enthusiasm kept me going through the multitude of setbacks encountered during my thesis research. He never doubted my ability to tackle a multi-scale interdisciplinary project, scaling from molecular measurements to *ex vivo* airway studies and drawing on diverse disciplines ranging from airway physiology to materials science. From him I received not only a substantial depth and breadth of knowledge about asthma, but also learned to be a better speaker, writer, and scientist.

Over these past 4 years, I have spent countless hours talking about science, planning experiments, seeking advice and building friendships with the members of the Fredberg lab. Thank you Chan, Dhananjay, Guilluame, Enhua, Jae, Bomi, Robert, Sanaz, Nadar, Jennifer, Corey, Jacob, Christalyn, Cheng, Ali and Emil. Special thanks to Jim Butler for teaching me lung physiology, putting up with all my questions in class, and breaking down complex mathematical concepts so I could understand them. Also, thanks to Chan for answering so many questions about cell culture, gel making, and OMTC. I am grateful to Guilluame for all his help with coding in MATLAB and analyzing OMTC data. Dhananjay also deserves a special thank you for answering so many of my programming questions over the years.

I also wish to thank Rama Krishnan, who was my first introduction to the Fredberg lab

when I rotated back in my first year. While my rotation project ended soon after, Rama's passion for science and generosity of spirit kept me seeking out collaborations with him for the entirety of my PhD. Without his help, the PCLS experiments in this thesis would not have been possible. His entire team at the Beth Israel Center for Vascular Biology Research (CVBR): Sumati Ram-Mohan, Kavitha Rajendran, Greeshma Manomohan, and Quyhn Dang were helpful and understanding of my itinerate presence in the lab. Sumati in particular was of great help with the PCLS studies, and contributed a great deal of work towards developing the cryopreservation method included in this thesis. Kavitha, who along with Sumati and Greeshma previously worked with me in the Fredberg lab, was very helpful in the early stages of my PhD, teaching me how to make polyacrylamide gels and and perform traction force microscopy. Thank you also to Lei Yuan at CVBR for her help with assaying cell viability for the cryopreservation studies.

I would like to also acknowledge the substantial contributions of my collaborators at the Huntsman Cancer Institute. Mark Smith has been a key contributor to the development of our hypothesis about zyxin and stretch. He not only produced beautiful images of zyxin localization, but he was willing to take on challenges and learn new techniques so that our plans might come to fruition. His partnership in this process has been invaluable. Special thanks to Mary Beckerle, who agreed to work with us on this project, and willingly shared cells and tissues from her zyxin knockout mice. Thanks also to Elizabeth Blankman, who aided with microscopy and analysis, and Chris Jensen, who learned how to insufflate mouse lungs for this study and did all of the lung extractions.

I would like to express my gratitude to my collaborators at the Boston University School of Medicine. First, thanks are due to Jesus Paez-Cortez for all of his help with PCLS, not

only for his contributions to our cryopreservation study, but also for teaching me how to insufflate mouse lungs in such great detail. Thank you also to Xingbin Ai, who assisted with obtaining mouse lungs as well as the beautiful immunohistology for our cryopreservation study. Lastly, thank you to Alan Fine for his support of this collaboration.

I also wish to thank Julian Solway and his lab for all of their help with PCLS, both for the zyxin project as well as our cryopreservation study. Thank you to Maria Dowell, for helping me to establish PCLS in the Krishnan lab. Thanks are also in order to Tera Lavoie for helping me learn how to work with PCLS.

I would also like to thank my Dissertation Advisory Committee, Dan Tschumperlin, Barbara Burleigh and John Hartwig. I would like especially to thank Dan for all of his help and advice over the years, I could not have asked for a better committee chair. Dan was always willing to open his lab and his office to me when I came seeking help. Thanks also to Barbara Burleigh for chairing my dissertation defense committee.

I also wish to thank Michael Sanderson from UMass Medical School, for his help with establishing PCLS in the Krishnan lab and for serving on my dissertation defense committee.

I have been fortunate to have found a home in the MIPS department. Several members of the department deserve special mention. Thank you to Jin-Ah Park for all the help with western blotting and allowing me to use space and equipment in her lab. Thank you to Stephanie Shore, for asking such good questions at all my talks, for serving on my

dissertation defense committee, and for her excellent comments on my proposals and papers. Thank you to Les Kobzik for putting up with all my questions in his pathophysiology course and helping me to secure funding to attend a biophysics conference in Israel. Thank you to Joe Brain for serving on my dissertation defense committee. Thank you Patrice, Carla, and Juliana for helping me with travel authorizations, reimbursements, booking rooms in HSPH, and making sure my training grant support was always renewed.

I would also like to express my gratitude for the funding that supported my PhD. I have received financial support from the NIH Training Grant in Interdisciplinary Pulmonary Sciences (5T32HL007118-32). I have also received substantial support from the Jere Mead Fellowship Fund and would like to express my gratitude to his widow, Dot Mead, for her continued support of this fund.

I am proud and grateful to have been a part of the Biological Sciences in Public Health Graduate Program. Thank you to program director Marianne Wessling-Resnick for her hard work making this program a diverse and supportive environment. Thank you also to interim director Brendan Manning for helping with administrative concerns this last year. Many thanks are owed to Holly Southern for processing DAC reports, delivering study cards, and answering all my questions about program administration.

On a more personal note, I would like to thank a few individuals on whose support I relied during this process. Thank you to Renata Cummins, my good friend going all the way back to Jordan Middle School, for her continued support. Even though we are now on opposite coasts, she has continued to be there for me through good times and bad. I

would also like to thank Gina Schaefer, who has been a good friend and teammate, and who inspired me to try out taekwondo back in my first year of graduate school, which was one of the best decisions I made at Harvard. I am also grateful to Marj Rosner and Arnold Trebach, for having me as a guest in their homes again and again, and making sure that I never had to spend a holiday alone.

I am so grateful to have such supportive parents, Ronda and Jeff Rosner. Since I first began to voice my aspirations, they have always encouraged me to think big and work hard to achieve my dreams. Their high expectations and continual encouragement, together with a good dose of humor, have made me the person I am today.

Last, but decidedly not least, I am so very fortunate to have met Kyle Karhohs, my fiancé and soon-to-be husband, here at Harvard. He has supported me throughout my PhD in every possible way including reading my proposals, listening to my talks, brainstorming solutions to my experimental roadblocks, teaching me about image processing in MATLAB, helping me to run a qPCR experiment, driving me home from lab late at night, and supplying me with frequent, delicious and varied dinners, baked goods, and other assorted foodstuffs. Most important, however, has been his continued belief in me and constant support of my aspirations. For that has made all the difference.

…when the breathing is inclined to be asthmatical…the spasm may be broken through, and the respiration for the time rendered perfectly free and easy, by taking a long, deep full, inspiration. In severe asthmatic breathing this cannot be done.

Henry Hyde Salter

1 Introduction

1.1 Bronchospasm, Deep Inspiration, and the Role of Zyxin

Of all known bronchodilators, the most effective are the deep inspirations (DIs) that occur spontaneously in humans roughly once every 6 minutes [1–3]. This salutary bronchodilating effect of a DI has been attributed to the manner in which stretch fluidizes the airway smooth muscle (ASM) cell and thereby ablates contractile force [4, 5]. In the face of appreciable ASM activation, airway patency *in vivo* is very much dependent upon the act of breathing itself and is therefore sustained dynamically, not

statically [4, 6–8]. Simply put, breathing is good for breathing [9].

During an asthmatic attack, however, this virtuous positive feedback can collapse [8, 10–12]. This collapse in asthma has been associated with increased contractile stimulus of airway smooth muscle (ASM), increased ASM mass, and decreased lung parenchymal tethering forces attributable to increased airway wall thickness and decreased lung recoil [8, 13–16]. Acting alone or in concert, each of these factors tends to cause ASM to stretch less with each DI [4, 8, 12, 17], fluidize less, and thus allow the ASM to become stiffer still. Eventually a tipping point is reached beyond which ASM can become so stiff that it cannot be stretched by parenchymal tethering forces and thus becomes virtually frozen in the so-called latch state [4, 18–21]. ASM would thereafter remain refractory to the salutary effects of a DI, and stuck in a shortened and stiffened static state until the contractile stimulus is removed or bronchodilator drugs take effect. Accordingly, this physical picture suggests dynamic equilibration driven by positive mechanical feedbacks on the one hand versus collapse to a static frozen state on the other (Figure 1.1). As such, it provides a plausible explanation of why a DI can be so effective in the normal lung but not in the asthmatic lung [22, 23]. Molecular mechanisms responsible for this stark difference remain less clear, however.

Relaxation of activated ASM in response to stretch is marked by disruption of actin-myosin interactions [21, 24] and other weak bonds together with rapid fluidization of the cytoskeleton through loss of actin stress fibers (SFs), with resulting reduction of cellular contractility and stiffness [5, 25]. The prompt fluidization response is followed by a slow and ATP-dependent resolidification response wherein cellular contractility, stiffness and structure return slowly to baseline levels [5, 25, 26]. Whereas fluidization

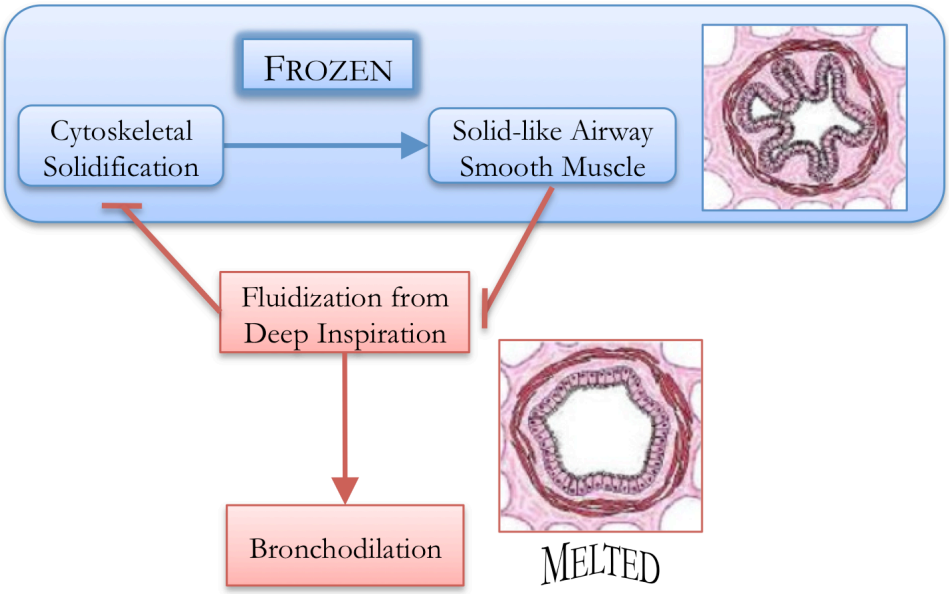

Figure 1.1: Schematic of the positive feedback loop of bronchospasm in the asthmatic airway. Increasingly solidified cytoskeleton in ASM cells promotes a more solid-like ASM. This more solid-like ASM is stiff enough to inhibit stretch-induced fluidization from a deep inspiration, which is necessary to reverse the solidification of the cytoskeleton. When fluidization is able to overcome a softer ASM, it promotes bronchodilation. Adapted from Krishnan et al, 2008 [23].

occurs on the timescale of seconds or less, resolidification occurs in an ATP-dependent manner on the timescale of minutes or more [5, 25]. Slow and ATP-dependent resolidification necessarily comprises reorganization, repolymerization and adaptation of focal adhesions, the cytoskeleton (CSK) and the contractile apparatus [5, 26–29], and thus implies active reassembly. Molecular determinants of that reassembly and its rate of progression could become interesting therapeutic targets because, were resolidification to be blocked, ASM would be unable to reassemble and contract. However, specific determinants of that reassembly remain to be identified.

I focus here on the LIM protein zyxin, a highly dynamic and mechano-responsive regulator of the actin cytoskeleton. In murine embryonic fibroblasts (MEFs) during isometric conditions, zyxin localizes predominantly to focal adhesions [30, 31]. After periodic cyclic stretches are imposed, however, zyxin localizes predominantly along actin stress fibers (SFs), which stabilize and thicken [31] as zyxin together with VASP and α-actinin are recruited to sites of highest SF strain [32]. Although the zyxin$^{-/-}$ mouse exhibits no known phenotype [33], I noted with interest that zyxin-mediated SF repair occurs on a timescale comparable to that of resolidification of ASM after stretch [5, 32]. Accordingly, here I used cells and tissues from wild type and zyxin$^{-/-}$ mice in a multi-scale approach to test the hypothesis that resolidification of ASM after stretch is dependent upon zyxin. During static isometric conditions I found that zyxin plays little or no role in determining ASM cell stiffness or net cell contractile force. However, during the resolidification following stretch-induced fluidization, zyxin impacts the dynamics of contractile force recovery.

1.2 A Multi-Scale, Interdisciplinary Approach to a Complex Problem

In order to explore the role of zyxin in airway smooth muscle, I developed a multi-scale, interdisciplinary approach, collecting data at the level of the actin stress fiber, the isolated ASM cell and the integrated airway *ex vivo*. This approach combined quantitative measurements of cell material properties and cell-exerted forces with physiological studies of the integrated airway from both wild type and zyxin$^{-/-}$ mice. Because bronchospasm is a complicated and multi-level emergent phenomenon, this systems approach allowed me to integrate my findings from molecule to tissue and allowed for greater insight than a traditional reductionist approach.

Executing this multi-scale project required the development of new methods, the adaptation of previous methods to focus on airway mechanics, and the partnership of expert collaborators. The work on imaging protein dynamics was made possible through a collaboration I established with Mark Smith in the Beckerle lab at the Huntsman Cancer Institute, and the work on precision cut lung slices (PCLS) was greatly advanced by collaborations I developed with the lab of Julian Solway at University of Chicago and the lab of Alan Fine at Boston University Medical School. The successful execution of both protein dynamics and PCLS experiments would not have been possible without the assistance of Ramaswamy Krishnan at the Center for Vascular Biology Research at Beth Israel.

To scale observations of ASM from molecule to cell to tissue required the use of a wide range of methods spanning cell biology, biophysics, and lung physiology. To measure protein dynamics immediately following transient stretch of physiologic magnitudes,

working with my collaborators Mark Smith and Rama Krishnan, we adapted the cell stretch system of Krishnan et al. [25] to work with high-resolution protein imaging on a spinning disk confocal microscope. This enabled us to observe for the first time zyxin localization as early as 5 seconds following a transient stretch. To measure nanoscale rearrangements of the cytoskeleton and cell cortical stiffness, I tracked nano-scale motions of beads adhered to the cytoskeleton and used optical magnetic twisting cytometry (OMTC) [34, 35]. This allowed me to see the contribution of zyxin to static cell mechanics at both subcellular and cellular levels. To measure static isometric and dynamic strain-responsive cell traction forces, I used Fourier Transform Traction Microscopy (FTTC) [25, 36]. This revealed the role of zyxin in modulating cell-exerted traction forces under both static isometric conditions and with dynamic strain. To measure airway responses to contractile agonists and physiologic stretch *ex vivo*, I measured contraction and dilation of airways in PCLS in response to contractile agonist stimuli and isotropic strain [8, 37, 38]. In order to bring these PCLS to our lab, I developed a method to cryopreserve PCLS for stable storage and transport [39]. These methodologies brought to light how our cell and molecular level observations translated to the integrated airway. Combining all of these findings gave a clearer picture of the dynamic role of zyxin in airway mechanics.

1.3 Organization of this Work

This work describes the role of zyxin in airway dynamics scaling from the level of molecular rearrangement to the integrated airway *ex vivo*. Chapters 2 and 3 comprise key background information relevant to the novel work presented in the thesis. Chapter 2 consists of a review of the literature on deep inspiration, airway smooth muscle, and zyxin, with a special focus on the innate heterogeneity in cell mechanical properties.

Chapter 3 provides an in depth overview of the methodology used in this thesis, and describes both how various tools and techniques work as well as why they were chosen for this particular work. Chapter 4 describes the discovery of a novel method to cryopreserve murine PCLS, which I developed in order to complete the integrated airway studies. Chapter 5 focuses on the role of zyxin at the subcellular and cellular level; zyxin's contribution to static isometric cell mechanics and zyxin's role in cellular responses to stretch. Chapter 6 focuses on the role of zyxin at the tissue level; how zyxin influences integrated airway responses to stimulation with contractile agonist and to physiologic stretch. Lastly, Chapter 7 summarizes these findings and draws conclusions on the role of zyxin in bronchospasm, as well as suggesting questions to explore in future studies.

2

Literature Review

Here I provide a concise overview of previous work on airway smooth muscle (ASM), deep inspiration, and the role of zyxin in cytoskeletal mechanics. Work in these fields constitutes the foundation of the ideas presented in this thesis. In this review I discovered an interesting gap of understanding separating this literature on cell mechanics compared with the emerging field of single cell biology. In the later part of this chapter I elaborate that gap and propose a hypothesis to unify existing observations.

2.1 Deep Inspiration and Airway Smooth Muscle

2.1.1 Asthma morbidity and mortality is a substantial problem for global health

Asthma is one of the world's most common chronic diseases, affecting an estimated 300 million people worldwide, predominantly in middle and high income countries [40]. Still, asthma deaths, estimated in 2009 at 250,000 worldwide, occur predominantly (over 80%) in low and lower-middle income countries [41]. However, this relatively low fatality rate minimizes the overall impact of asthma: the World Health Organization estimates that 15 million disability-adjusted life years (DALYs) are lost every year due to asthma, representing 1% of the total global disease burden (Figure 2.1)[41]. In the United States alone, 8.2% of adults and 9.5% of children are currently diagnosed with asthma. This disease burden results in 14.2 million physician office and 1.8 million emergency room visits every year [42]. Each year, about 1 in 2 people (about 12 million) diagnosed with asthma experience an asthma attack, suggesting that their current treatment is insufficient [42]. Additionally, asthma has a serious economic impact, costing the United States about $56 billion a year in medical costs and lost school and work days [42]. Although there are many treatments available to manage the symptoms of asthma, to date there is no cure. Worse yet, two of the most prescribed treatments for symptom management, β2 adrenergic receptor (β2AR) agonists and corticosteroids, do not work for all asthma patients. Despite extensive use of β2AR agonists, approximately 10% of asthma patients are unable to control their disease and exhibit severe symptoms [43]. Similarly concerning is the observation that even mild asthmatics who are treated long-term with β2AR agonists frequently develop a tolerance to its effects [44, 45]. This can lead to a reduced response to β2AR agonists treatment during emergent

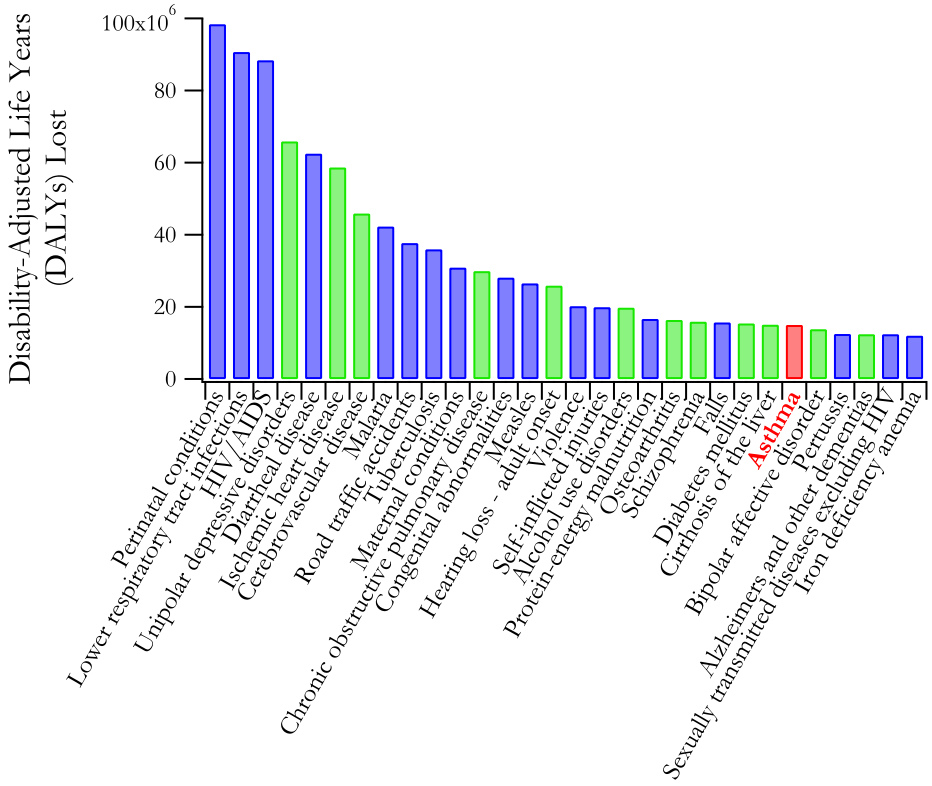

Figure 2.1: Asthma is the 25th leading cause of DALYs lost annually worldwide. Asthma is one of the most common chronic diseases in the world and has a comparable public health impact to diseases such as diabetes and cirrhosis of the liver [40]. Asthma DALYs lost are shown in red, other chronic non-infectious diseases are shown in green, and all other causes are in blue.

bronchospasm events [45]. This stems from changes in the β2AR including short-term phosphorylation and coupling with the Gi subunit, and long-term decreases in expression, which ultimitately lead to β2AR desensitization [46]. Further, 5-10% of asthma patients are refractory to corticosteroid treatment, another common treatment [47, 48]. These problems with current asthma treatments underscore the need to continue to develop new therapies for asthma. It is our hope that with a greater understanding of the physiological mechanisms that give rise to asthma, the tremendous burden of this disease can be reduced.

2.1.2 A brief history of deep inspirations

It was more than 150 years ago that Henry Hyde Salter [10] first noted that a spontaneous DI could reverse bronchospasm totally in mild asthma but not in severe asthma. But it took nearly a century until Nadel and Tierney [1] picked up that thread and showed that DIs temporarily reverse the increase in airway resistance induced by bronchospasm. Not long after, Bendixen et al. [2] suggested that DIs comprise an integral part of airway homeostasis and showed that DIs occur spontaneously in humans at a regular intervals –approximately once every 6 minutes–which is now seen to coincide roughly with the interval required for ASM resolidification (Figure 2.2). In controlled studies matched for the severity of airway obstruction across groups, Lim et al. [11] demonstrated that a DI reverses the obstruction that is induced in the laboratory, but not the obstruction that occurs in the spontaneous asthmatic attack, and even tends to exacerbate that spontaneous obstruction. These important observations notwithstanding, response to a DI was considered for the most part to be an epiphenomenon until Skloot et al. [12] demonstrated convincingly the central role of the DI in maintenance of airway patency –and the failure of the DI to reverse bronchospasm

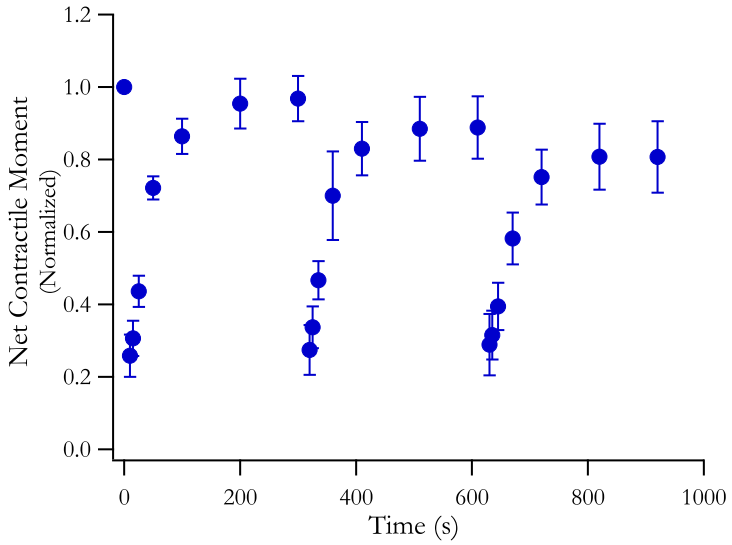

Figure 2.2: Deep inspiration frequency is the same timescale as resolidification of ASM. A experiment from this thesis showing normalized changes in net contractile moment in wild type murine primary ASM cells following a series of three stretches mimicking DIs at 0, 310 and 620 seconds.

in asthma– whereupon the phenomenon came to be widely appreciated as being a causal factor in asthmatic obstruction [49]. While certain evidence suggests otherwise [17, 50, 51], the preponderance of evidence now points to nonlinear positive mechanical feedbacks between the ASM and the dynamic mechanical load against which that ASM is contracting [4, 8, 24, 52]. Moreover, the isolated intact airway smooth muscle strip contracting against a dynamic physiological load expresses these very same dynamic behaviors, thus ruling out systemic mechanisms of neural or humoral origin [8, 21].

2.1.3 Airway smooth muscle as motor or material? Disordered, glassy, adaptable

All smooth muscles are defined by the absence of the ordered structure that is characteristic of striated muscle [53]. Nonetheless, for a long time smooth muscle was thought to operate functionally by some similar but hidden sliding filament mechanism,

with the main functional difference being merely that the unloaded shortening velocity in smooth muscle is far slower [54, 55]. The reason for this difference remained the central unanswered question in the field until Dillon and Murphy finally showed that unloaded shortening velocity in smooth muscle is time-dependent [56]. Unlike the control of acto-myosin cycling by the stearic switch-like action of tropomyosin in striated muscle, that cycling and its time dependence in smooth muscle was seen to be a regulated process under the action of phosphorylation of the 20 kDa myosin regulatory light chain. Murphy and colleagues then postulated the existence of a dephosphorylated but bound slowly cycling myosin bridge, which they termed the "latch bridge", and showed that latch could explain all data that was then available [56, 57]. But even with the new unifying concept of latch, all myosin II motors in smooth and striated muscle alike were imagined nonetheless to operate within the strict framework of stable sliding filaments [58–60], with its associated classical notions of optimal filament overlap, optimal muscle length, and optimal muscle force. To great surprise, these classical notions borrowed from striated muscle for application to smooth muscle were subsequently shown to be totally inapplicable. With the discovery of smooth muscle adaption [61] it became quickly appreciated that adhesions, cytoskeleton and contractile apparatus of ASM are highly dynamic, plastic, and adaptable structures characterized by high rates of turnover and remodeling. Such remodeling enables smooth muscle to adapt its microstructural configuration so as to produce virtually the same active force over a huge range of muscle lengths (Figure 2.3) [61]. If sliding thick and thin filaments exist at all in smooth muscle, the implication is that they must be evanescent [63]. Borrowing ideas from the physics of soft condensed matter, definitive biophysical studies subsequently showed that smooth muscle adaptation, when considered at a coarse-grained level, conforms closely to the notion of a glassy material perched close to a glass transition [5, 26, 35]. That is to say,

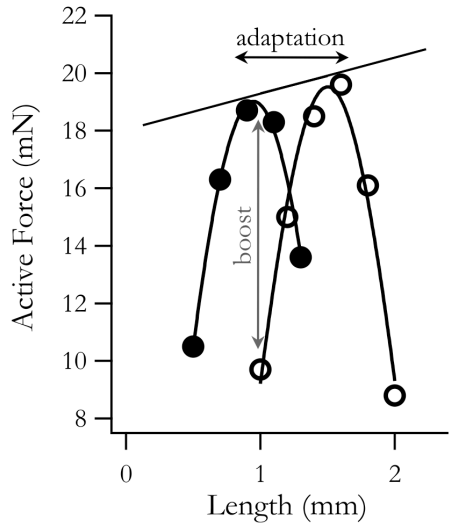

Figure 2.3: Force-length curves measured in the same muscle before and after adaptation. Length adaptation (black arrows) shifts the curve, which boosts the active force at shorter muscle lengths (grey arrow). This substantial effect is believed to be important in ASM hyperresponsiveness. The ASM can adapt to produce the same force over a broad range of muscle lengths. Accordingly, ASM has no optimal force or length. Adapted from Wang et al., 2001 [62].

smooth muscle structures, upon activation or imposed mechanical stretch, undergo a transition between fluid-like and solid-like glassy material states, with fluid-like states corresponding to the greatest rates of remodeling and adaptation, and solid-like states being far stiffer and corresponding to comparatively smaller rates of remodeling. In the transition from fluid-like to solid-like states following a transient stretch of physiological magnitude, moreover, ASM resolidification was shown to be dependent upon ATP [5], thus indicating the presence of active molecular processes but of non-specified kinds [5].

2.1.4 Understanding the regulation of actin cytoskeletal dynamics in the contractile cell

Much work has been done to understand myosin cross-bridge cycling and myosin ATPase activity in contractile cells [54–56]. The movement of myosin heads along actin

filaments to produce tension in a shortening cell has been well described [64]. However, smooth muscle contraction additionally requires the polymerization of actin [65–67]. Actin, the most abundantly expressed protein in the cell, forms filaments made up of double-stranded helical arrays of actin monomers, which are constantly being exchanged with the pool of soluble monomers in the cytosol. These actin filaments are anchored to the extracellular matrix by mechano-sensitive adhesion complexes [68, 69]. It has long been known that the inhibition of actin depolymerization suppresses tension generation in the contractile cell [65]. It has also been shown that contraction of the smooth muscle cell decreases the ratio of g-actin (soluble) to f-actin (filamentous), shifting more actin from the cytosol into actin filaments [67, 70]. Interestingly, while it does suppress tension generation, the inhibition of actin polymerization with cytochalasin D does not affect intracellular Ca^{2+}, myosin light chain phosphorylation, or myosin ATPase activity in the smooth muscle cell [66]. Additionally, the inhibition of N-WASp-induced actin polymerization inhibits tension without effecting myosin light chain phosphorylation [70]. However, the inhibition of myosin light chain kinase does not affect agonist-induced actin polymerization in smooth muscle [71]. Taken together, these studies suggest that the regulation of actin filaments exists in a parallel pathway to the conventional activation of smooth muscle contraction via myosin ATPase activity. Much work remains to be done to clarify the complex and dynamic regulation of actin filaments and the contractile scaffold. However, it appears clear that characterizing actin regulation in smooth muscle is essential our understanding of smooth muscle contraction, both in normal physiology and in disease states, including bronchospasm.

2.1.5 Zyxin in cell adaptation, resolidification and self-healing

Crawford and Beckerle [30] first characterized zyxin and later identified LIM and α-actinin binding sites as well as α-actinin, CRP and members of the Ena/VASP family as binding partners [72–75]. Zyxin is an 82 kDa protein that is found in cell-cell and cell-ECM adhesions, shows Arp2/3-independent actin-polymerization activity [76], and plays a role in cell spreading and proliferation [77]. When cells are mechanically stressed, zyxin mobilizes from focal adhesions to actin stress fibers [31], and contributes to strain-dependent remodeling of the actin cytoskeleton and force-dependent changes in zyxin binding affinities [31, 78], although the directionality of these shifts remains a matter of some dispute [79, 80]. Zyxin$^{-/-}$ cells have also been shown to have faster migration, increased adhesion to ECM proteins, and deficits in actin remodeling [81].

More recently, zyxin has been shown to be a key player in the repair and maintenance of actin stress fibers (SFs) [32, 82]. It was observed that actin SFs experience periodic strain events, where traction forces transiently increase followed by thinning of co-localized SFs, and lower traction forces [32]. Zyxin is preferentially recruited to these aforementioned sites of SF strain, where it facilitates the recruitment of α-actinin, an F-actin crosslinking protein, and VASP, an actin barbed-end-binding protein (Figure 2.4)[31, 32, 72]. Interestingly, the recruitment of α-actinin and VASP is significantly compromised in zyxin$^{-/-}$ murine embryonic fibroblasts (MEFs), while zyxin recruitment still occurs in the absence of α-actinin or VASP [31, 32]. By recruiting key proteins that stabilize SFs, zyxin prevents SF ruptures; zyxin$^{-/-}$ MEFs experience a significantly higher rate of SF breaks [32]. However, despite these myriad differences observed in zyxin$^{-/-}$ cells, the zyxin$^{-/-}$ mouse shows no apparent phenotype [33].

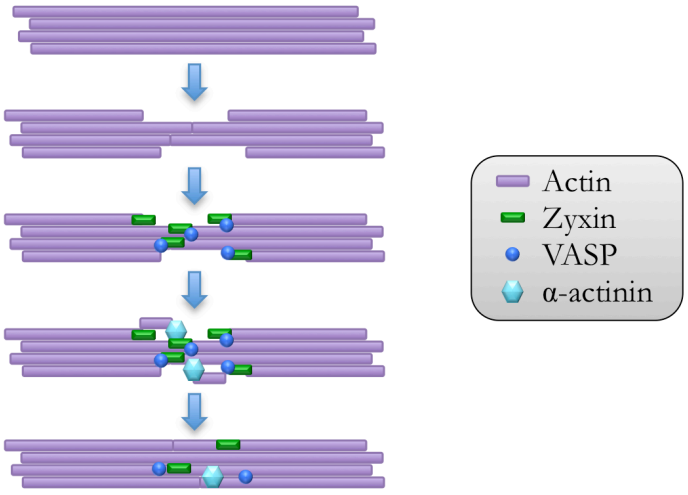

Figure 2.4: Zyxin facilitates stress fiber repair by recruiting VASP and α-actinin. Actin SFs periodically experience strain events, where the actin filaments begin come apart, weakening the stress fiber. When this occurs, zyxin is recruited to these sites, and brings along VASP, an actin barbed-end binding protein. Subsequently, zyxin facilitates the recruitment of α-actinin, an actin cross-linking protein. These proteins stabilize and repair the actin stress fiber. Adapted from Smith et al., 2010 ([32].

2.2 Single Cell Biology and Cell Mechanics

As researchers in our lab and others began to piece together a better picture of cell mechanics in ASM and other tissues, an interesting, and as yet unexplained phenomenon was identified. Adherent cells of many types and under a variety of conditions were found to have extremely heterogeneous mechanical phenotypes, even within clonal cell populations [5, 25, 83–86]. These distributions of cell stiffness and contractility were found to be log normal, which implies a fat tailed distribution with many more cells lying far from the mean than would be expected in a normal distribution [25, 83–85]. In this second part of the review, I will explore the possible causes of this phenomenon and suggest a new approach to elucidate the relationships between biochemical signaling events within the cell and emergent cell mechanical properties.

2.2.1 Innate heterogeneities in cell mechanics

The study of single cell mechanics has come a long way over the past two decades. Where once cell material properties were inferred from images of actin stress fibers and the wrinkling of flexible substrates [87, 88], now they are quantified using methods such as optical magnetic twisting cytometry (OMTC) and Fourier Transform Traction Microscopy (FTTM) [36, 83, 89]. While these advances have yielded answers to a wide range of questions, I focus here on the finding of large heterogeneities in cell mechanical properties.

Heterogeneity in single cell mechanics was first discussed in the work of Fabry et al. in 2001, where he demonstrated a log normal distribution of cell stiffness in cultured adherent human ASM cells [83]. Intriguingly, Fabry et al. showed that treatment with contracting and relaxing agonists did not substantially change this log normal distribution of cell stiffness [83]. Later work by Deng et al. confirmed the log normal distribution of cell stiffness, and showed further that while measures of the elastic (G') and viscous (G'') properties of individual cell varied according to a log normal distribution, the loss tangent (G'/G'') was far less variable, suggesting that variations in cell stiffness are pegged to the maintenance of a set level of hysteresivity [84]. Balland et al. subsequently confirmed the observation of log normal distribution and high variability of cell stiffness using optical trapping [85]. The work of Wang et al. further showed that measures of cell stiffness and contractility closely correlate with one another [34]. Recent advances in measuring cell-exerted forces in a higher-throughput manner have improved another tool in the field of single cell mechanics. In 2009, Krishnan et al used FTTM to measure contractile force in adherent human ASM cells and confirmed the same log normal distribution of net contractile moment in the isometric cell [25].

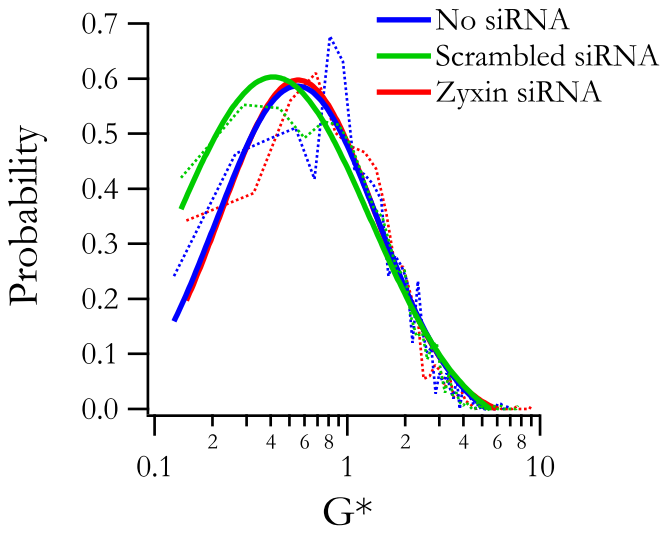

Figure 2.5: Cell stiffness is log normally distributed. The distribution of isometric stiffness of primary HASM cells (G*) is log normal for control, scrambled siRNA treatment, and zyxin siRNA knockdown. The raw data are shown by the dashed lines, and are fit by log normal curves shown by the solid lines.

Similarly, the work in this thesis shows log normal distributions of both cell stiffness and net contractile moment in MEFs and human ASMs with and without zyxin (Figure 2.5). From the above observations and others, it appears that the finding of log normal heterogeneity in cell mechanical measures is quite robust.

But what does it mean? The log normal distribution of cell stiffness and net contractile moment invites questions as to the physiologic significance of those cells in the long tail of the distribution. There exist many physiological processes, most notably in the growth and metastasis of neoplasms, driven by a distinct subset of cells rather than average cell behaviors [90, 91]. Could this stiffer and more contractile sub-population similarly promote disparate cell behaviors? What drives this wide range of cell stiffness and contractility? Very little work has been done to address these questions. In 2013, one group found that the stiffness of mesenchymal stem cells (MSC) correlated closely with

their differentiation into osteoblasts, with the stiffest subset of MSCs differentiating later than softer MSCs [92]. However, most studies examining a physiological role for cell mechanics still focus on average cell behaviors, ignoring so-called "outliers" in the long tail and failing to correlate individual cell mechanical measures with gene expression or cell behavioral measures in those same cells.

2.2.2 Hypotheses abound as to the cause of cell mechanical heterogeneity

Many hypotheses exist that could explain some or all of this observed heterogeneity in cell mechanics, although they have not been extensively explored. Underlying this discussion of single cell mechanical heterogeneity is the assumption that this variability is not an artifact of culture. While identical measurements cannot be made of cells in tissue, some evidence suggests that here, too, there is substantial variability. For example, Minshall et al. and others have shown that ASM contractile responsiveness in tissue is extremely variable [39, 93], which is reminiscent of *in vitro* studies of ASM cells showing log normal variability in contractile responses to histamine [83, 94]. Accordingly, although this discussion is by no means exhaustive, I will discuss several potential driving factors behind the observed heterogeneity of single cell mechanical measures.

First, and most well characterized, is the role of cell spread area and aspect ratio in determining cell stiffness and contractile force. Many studies have shown clear relationships between cell spread area, cell width, focal adhesion size, and cell tractions [94–97]. However, the correlation between these geometric factors and cell traction forces is not perfect; there are clearly other factors that contribute to this variability. This is not surprising, as cell area, width and length are normally distributed, whereas cell

traction force and cell stiffness are log normally distributed [83, 94]. Intriguingly, increases in traction force in human ASM cell stimulated with histamine are distributed log normally, however these force increases do not correlate with cell area or shape parameters [94]. Most importantly, none of these observed correlations demonstrate why this variability emerges, or whether cell area and traction force are both sequellae of some as-yet unidentified biological difference within the cell population.

Together with these observations on cell size and shape, come other hypotheses regarding the geometry and ordering of the cytoskeleton, which is known to be extremely dynamic and constantly remodeling. It has been well characterized that cell division causes substantial shifts in the magnitude and localization of cell traction forces [98, 99], although cell stiffness and traction force show log normal heterogeneity in serum-starved ASM cells which are not dividing [25, 83]. Similarly, migrating cells also show temporal and spatial heterogeneity in traction force [86], although the causes of this are still unclear. It was recently demonstrated that durotaxis, or migration towards stiffer extracellular matrix, is guided by small-scale force fluctuations in individual focal adhesions [100]. However, as with observations of cell size and traction force magnitude, it is unclear what is the direct causative factor that drives the cell to exert more traction force.

Another interesting hypothesis emerges from the field of single cell analysis. Several studies over the past decade have shown that single cell gene expression is also very heterogeneous [101–104], and in many cases gene expression varies according to a log normal distribution [103–107]. Recent work has shown that this log normal gene expression can be caused by the stochastic on-off switching of transcription, often

referred to as "transcriptional bursts," where random differences in the amount of time that transcription is activated result in large differences in gene expression (Figure 2.6) [101, 108–111]. Interestingly, some recent studies have found that in certain pathways, the stochastic expression of an individual protein can actually generate a diversity of phenotypes [105, 106, 111]. One such study done by Feinerman et al., found that stochastic variation in the expression of CD8 co-receptor and soluble hematopoietic phosphatase 1 led to a substantial range of activation within a clonal population of T cells [106]. Another study by Chang et al. showed that the expression of Sca-1, a stem cell marker, was log normally distributed in a clonal hematopoietic cell population and that the relative expression of this marker actually impacted a cell's likelihood of differentiating into a myeloid or erythroid lineage [105]. In these cases, examining only the mean expression of a gene in the cell population obscures the contribution of single cell expression levels to a diversity of phenotypes. It is possible that in the case of cell contractility, we could also learn by examining single cell gene expression. Many proteins are potentially of interest including myosin, myosin light chain kinase, α-actinin, lamin, filamin, actin binding and severing proteins such as cofilin and gelsolin [112, 113], and proteins in the LIM family [114, 115]. While the expression of these proteins in single cells has not yet been examined in connection with cell mechanics, the field of single cell analysis has given rise to several tools that could aid in this exploration.

2.2.3 Novel tools have emerged from the field of single cell analysis

New tools for single cell gene expression analysis have been reviewed previously [109, 116], but I will highlight some key techniques in mRNA and protein analysis. The development of mRNA-Seq for use in single cells by Kurimoto el al. revealed the single cell transcriptome [117]. RNA-Seq is a deep-sequencing technique where RNA

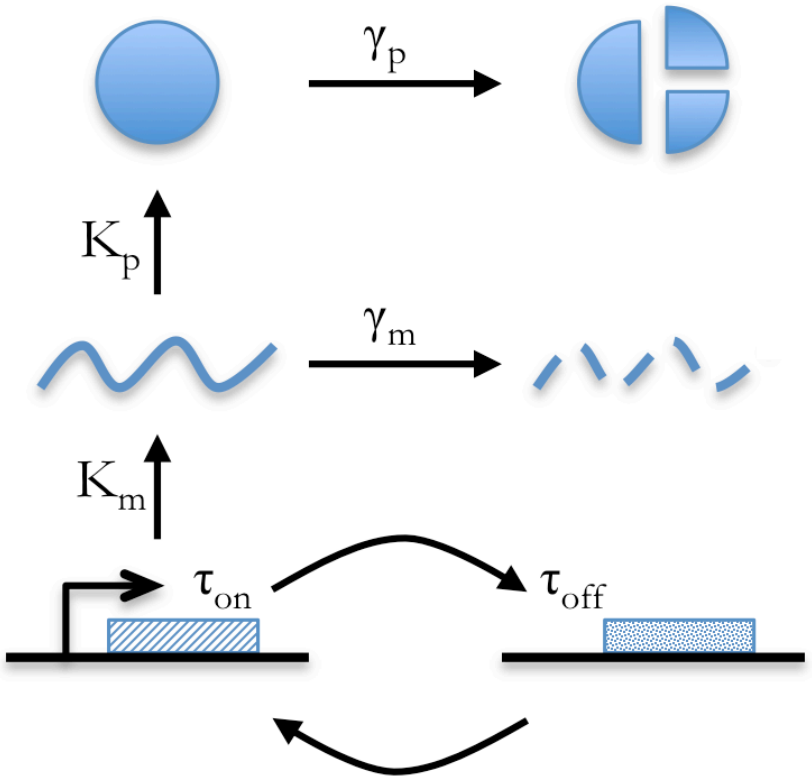

Figure 2.6: Rapid on-off switching of transcription drives the stochastic expression of genes. The gene promoter switches between on and off states with characteristic time scales τ_{on} and τ_{off}. While the promoter is "on," transcription usually occurs at a constant rate, K_m. Protein translation occurs at a rate K_p. mRNA and protein degradation are described by a Poisson process with rates of γ_m and γ_p. All of these rates can potentially be shifted with gene activation. The "bursting" hypothesis proposes that the stochastic activation of transcription is the key driver of the observed heterogeneity in gene expression. Adapted from Molina et al., 2013 [111].

fragments are first converted to cDNA and then adaptors are added to both ends of the molecule. These short fragments are read using high-throughput sequencing techniques and the resulting reads are aligned with the reference genome or transcriptome [118]. This technique has since been developed further, providing a more complete view of gene expression in the single cell [118, 119]. Another method of single cell mRNA analysis is single-cell PCR. This was first described in Zhang et al, where they demonstrated that polymerase clones or "plones" could be amplified from the DNA of single cells with good coverage and high accuracy [120]. This technique was further refined for single cell mRNA analysis by Taniguchi et al., where they used a single-cell cDNA library immobilized on beads to measure the expression of multiple genes in a single cell [121]. Another recently developed technique to quantify mRNA is RNA FISH (florescence in situ hybridization), developed by Raj et al. to measure gene expression in fixed cells using fluorophore moieties fused to oligonucleotide probes that hybridize with specific mRNA targets [122]. This method can resolve gene expression down to individual mRNA transcripts and could be a good tool to examine gene expression in parallel with cell traction forces, as it measures endogenous protein and can be used to measure multiple genes simultaneously through the use of different fluorophores [109, 122].

In addition to measuring gene transcripts, one can also measure protein expression in single cells. Individual proteins can be labeled with fluorescent molecules using either transfected fluorescently tagged protein reporters or single-protein antibody labeling. The primary advantage of using fluorescently tagged proteins is the ability to do real time imaging, but this comes at the cost of being able to measure endogenously expressed proteins. Conversely, labeling with antibodies allows for the measuring of endogenous protein expression, but cannot be done in real time. Because of this, combinations of

these techniques are often used to compensate for their individual weaknesses [109].

Additionally, new technologies are continually being developed for single cell analysis. Recently, RNA-Seq has been further improved for increased sensitivity and accuracy as well as allowing for full-length coverage of the genome [119]. Lee et al. recently described a technique called fluorescent in situ RNA sequencing (FISSEQ), where stably cross-linked cDNA amplicons are sequenced within a cell or tissue [123]. Therefore, FISSEQ allows for parallel detection of many transcripts *in situ* instead of only a few genes at a time, as with RNA FISH [123]. Using recently developed tools for detecting single-cell mRNA transcripts, such as RNA-Seq and RNA FISH, as well as techniques for single-cell protein detection, we could begin to find an answer for the question of what drives single cell heterogeneity in cell mechanics.

2.2.4 A novel approach to study the molecular roots of heterogeneity in cell mechanics

Recent advances in the field of single cell analysis have shed light on the possibility that key insights into how cells function are missed by focusing on population means and overlooking the role of cells in the tails of the distribution. This idea can be immediately applied to the field of cell mechanics, where we already have excellent tools to examine the mechanical properties of single cells [25, 36, 89]. Using these tools and those from the field of single cell gene expression analysis discussed above, we could begin to study the genetic diversity that underlies the substantial heterogeneity we observe in cell stiffness and contractility. By searching for patterns between cell mechanical properties and gene expression in single cells, we may discover new insights as to the key drivers that regulate cell contractility. New correlations emerging from this line of inquiry could be

further studied to determine the causal nature of the relationship. It remains unclear to what extent gene expression variability drives the variability in we observe in cell mechanics and conversely, to what extent cell mechanical variability drives variability in gene expression. Pursuing an investigation of these relationships at the single cell level could help us to better understand the relationship between complex biochemical processes within the cell and emergent cell mechanical properties.

3

Methodology

While the previous chapter explored the scientific background supporting the ideas developed in this thesis, this chapter turns to the unique methodology employed to pursue the central question of the thesis: what is the role of zyxin in airway dynamics? I will lay out the reasoning behind the multi-scale approach chosen to explore this question, and also provide context for the methods used in this work.

3.1 Introduction: Working Across Scales in a Systems Approach

In developing this thesis, I saw the problem of bronchospasm as being driven by phenomena that scaled from molecular events in individual cells to changes in the airway and lung tissue. As such, I sought to study bronchospasm as an emergent phenomenon at multiple scales, in the hope that such an approach would be synergistic and reveal more insight than a study of bronchospasm at only one scale. At the subcellular level, I was motivated to explore the molecular events that give rise to the "frozen" cytoskeleton observed in asthmatic airway smooth muscle [23]. I sought to better understand the role of cytoskeletal regulatory proteins, with a central focus on zyxin, in promoting a "frozen" versus a fluidized cytoskeleton. At the cellular level, I was motivated to characterize how these molecular events give rise to the cell mechanical phenotype, with a particular focus on cell responses to physiologic stretch. In particular, I sought to identify molecular drivers behind resolidification of the cytoskeleton following stretch-induced fluidization [5, 25]. At the tissue level, I looked to expand these findings to the integrated airway *ex vivo*. I was motivated to explore how the multicellular nature and specific geometry of the integrated airway impacted cellular responses to stretch, especially in the regulation of the actin contractile apparatus by zyxin. The consistencies and inconsistencies observed across these levels revealed zyxin as a nuanced regulator of ASM contractility in the dynamic environment of the lung.

3.2 Subcellular Measurements

3.2.1 High-resolution microscopy of protein dynamics

Working with collaborators in Dr. Mary Beckerle's lab at the University of Utah, especially Dr. Mark Smith, and with Dr. Rama Krishnan, at the Center for Vascular

Biology Research, we developed a system to image zyxin and actin dynamics immediately following stretch. This system allowed us to track zyxin, actin, and cellular tractions simultaneously immediately following the application of mechanical stretch. Using GFP-zyxin and LifeAct transient transfections of zyxin$^{-/-}$ MEFs, we were able to visualize real-time changes in zyxin localization and actin SFs. Imaging was performed on an inverted Nikon Ti*e* (Nikon Instruments) equipped with either a Nikon 20X Plan Apo NA .75 dry, or a Nikon 40X Apo LWD NA 1.15 water immersion lens. This system also utilized an Andor spinning disk confocal (Andor Technology) and an Andor Ixon 885 EMCCD camera. Automation and image capture utilized Andor IQ software running on a Hewlett Packard workstation. Time-lapse image sequences were collected with 10-second time resolution of GFP-zyxin and LifeAct. We adapted this system to apply mechanical stretches by designing a small annular punch indenter that fit on the condenser and could be lowered to the surface of the gel. The final positioning and application of stretch were guided by precise movement of the stage in Z with a Piezo stage insert. The punch used was a small bore stainless steel cylinder with inner and outer diameters of 100 and 150 μm, respectively. This allowe us to apply measured stretches across a physiologically relevant range (2.5-20%). This method comprised the first attempt to observe zyxin dynamics within a cell immediately following a transient physiologic stretch.

3.2.2 Measurements of spontaneous bead motion to approximate cytoskeletal reorganization rate

To measure the dynamic reorganization of the cytoskeleton quantitatively, cells were first plated on collagen I-coated 96-well plastic plates at a density of 20,000 cells per well to form a confluent monolayer. After 24-72 hours to spread, the cells were serum-starved

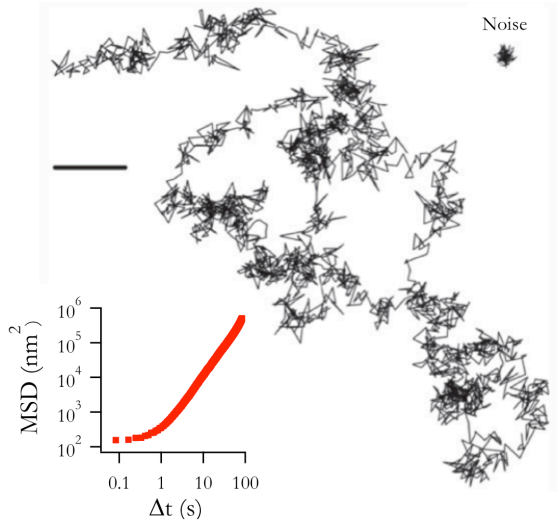

Figure 3.1: Spontaneous bead motions as a proxy for cytoskeletal remodeling rates. Spontaneous motions of a representative bead on a cell approximate cytoskeletal remodeling rates and are far larger than the measurement noise (Scale bar = 10 μm). Total MSD increases with time (inset). Adapted from Bursac et al. [35].

for another 24 hours and treated with RGD-coated 5 μm iron microbeads. Next, spontaneous bead motions were optically recorded on a light microscope. Because the RGD-coated beads are attached to the actin cytoskeleton itself via focal adhesions, these spontaneous bead motions correspond with the remodeling of the underlying actin cytoskeleton [35]. The overall rate of remodeling can be quantified by the mean square displacement (MSD) over changes in time (Figure 3.1). Beads attached to cells in which the cytoskeleton is remodeling rapidly exhibit more motions, leading to higher MSD values. Here we define MSD as

$$\langle r^2(\Delta t)\rangle = \langle (r(t+\Delta t) - r(t))^2\rangle \tag{3.1}$$

where $r(t)$ is the bead position at time t, Δt is the time lag, and brackets indicate an average over many starting times t and over all beads. The MSD value $\langle r^2(\Delta t)\rangle$, can be plotted on a log-log scale versus time lag. Over short time scales, the MSD value shows subdiffusive behaviors, while over longer time scales superdiffusive behaviors dominate [35]. This superdiffusive behavior can be fit to the power law $D^*(\Delta t)/t_o)^\beta$, with cells exhibiting higher rates of remodeling fitting curves with a higher D^* [35, 124]. This value is then used to compare remodeling rates between different cells and conditions. For a more complete discussion of MSD and cytoskeletal remodeling, refer to Lenormand and Fredberg, 2006 [124].

3.3 Cellular Measurements

3.3.1 Optical Magnetic Twisting Cytometry (OMTC) to measure cell stiffness

Cells were plated and left for 24-72 hours, depending on cell type and condition, to spread and form mature focal adhesions. The cells were then serum-starved for a further 24 hours. RGD-coated 5 μm iron microbeads were added and incubated for approximately 20 minutes to allow the cells to form focal adhesions on the beads (Figure 3.2A)[34, 89]. Both zyxin$^{-/-}$ MEFs and zyxin knockdown HASM cells bound the RGD beads similarly to cells with zyxin, likely due to the fact that integrin expression is not compromised in the zyxin$^{-/-}$ cell [81]. The RGD-coated beads were magnetized and subjected to torque from a 30G magnetic field across a range of frequencies to collect measures of cellular stiffness and elasticity. As with all OMTC experiments, lateral bead displacements were measured by optical tracking (Figure 3.2B) and used to calculate stiffness (an inverse relationship exists between lateral bead displacement and stiffness).

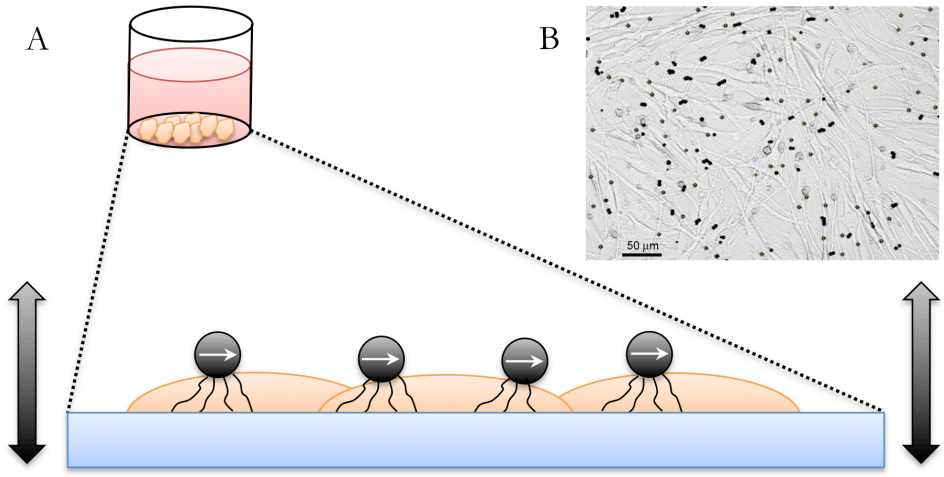

Figure 3.2: OMTC as a tool to measure cell stiffness. A) Cells plated in a 96-well are treated with ferromagnetic beads, which are then magnetized in one direction (white arrows) and subjected to a perpendicular alternating magnetic field (black arrows) to collect cell rheology measures. B) Image showing optical bead tracking. Scale bar is 50 µm.

Two values were collected for each bead and each pulse of the magnetic field. The first, G', or the in-phase constant, is a measure of the storage modulus of the cell, and represents the elastic portion. The second, G", or the out-of-phase constant, is a measure of the loss modulus of the cell, and represents the dissipative portion. In this study, I used G', or the elastic modulus, as the primary measure of cell stiffness. For a more detailed explanation of the calculation of G' and G", the best resources are Fabry et al, 2003 and Lenormand and Fredberg, 2006 [124, 125].

3.3.2 Using traction force microscopy to measure single cell contractility

In order to measure cell-exerted forces, cells were plated on collagen-coated polyacrylamide gel substrates (Young's modulus of 1.2-11 kPa) containing florescent marker beads and allowed to adhere and stabilize over 24-96 hours, depending on the cell

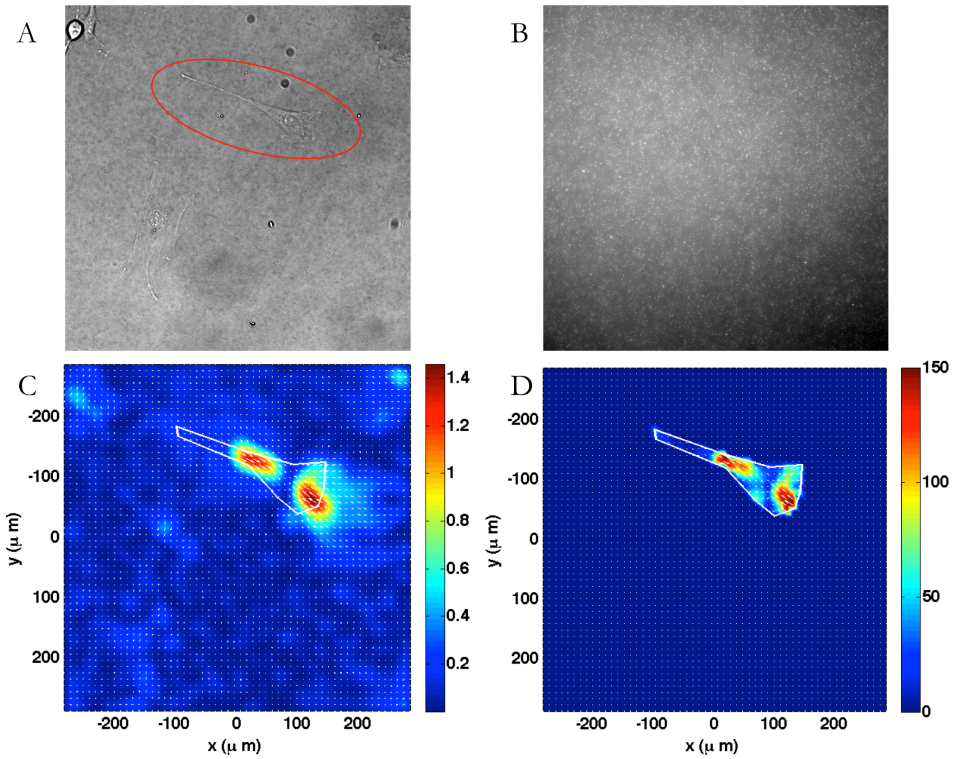

Figure 3.3: FTTC as a tool to measure cell contractility. A) MEF on polyacrylamide gel. The red ellipse indicates the cell of interest. B) Image of 200 nm fluorescent marker beads used to visualize gel displacements. C) Measured displacements of a single MEF (in μm). D) Constrained tractions of a single MEF (in Pa).

type (Figure 3.3A). Images of marker beads were taken for individual adherent cells, before and after the application of trypsin to gain a reference image of the gel (Figure 3.3B). By comparing the image of the beads with the cell still adherent to the gel and the reference image of the gel with no cell attached, the displacements of the beads could be calculated and then converted into a vector map of cell-induced displacements of the gel (Figure 3.3C). As described previously in Butler et al. [36], the traction field was then calculated from this displacement vector map using Fourier Transform Traction Cytometry (FTTC) (Figure 3.3D). This traction field was subsequently used to calculate

the net contractile moment of the cell, a scalar measure of the cell's contractility (expressed in picojoules-pJ).

3.4 Tissue Measurements

3.4.1 Using Precision Cut Lung Slices (PCLS) to measure airway hyper-responsiveness and responses to physiologic stretch

Many *in vivo* mouse models have been developed for the study of asthma; however, there is still no model that can reflect the severe airway hyper-responsiveness (AHR) response to challenge with contractile agonists seen in asthmatics [126, 127]. Here, instead of taking such an *in vivo* approach to examine bronchospasm, I examine the integrated airway *ex vivo* using a novel dynamic Precision Cut Lung Slice (PCLS) model system. PCLS has emerged as a promising method for observing individual airway responses to pharmacological or mechanical stimulation, and has been refined greatly by Michael Sanderson, who assisted in our development of the technique [38, 128–133]. Dassow et al. first demonstrated the feasibility of biaxial distension of PCLS [133]. However, their system, while functional, is extremely complex, and so our lab, in collaboration with Julian Solway at the University of Chicago, has developed a more straightforward approach to the problem of imposing mechanical stretch on PCLS [8]. The use of this system allows the observation and quantification of airway constriction and resolution in real-time and the application of quantified mechanical stretch to the tissue [8, 39].

3.4.2 Stretch of the integrated airway in murine PCLS

In order to stretch the lungs in a manner that mimics breathing, I used an approach similar to that used to stretch adherent cells. A vertical stainless steel annular "indenter" was attached to a micromanipulator and centered above the airway of interest. The

indenter was perforated above its edge in order to allow the free flow of solution in the tissue bath to the PCLS of interest. The indenter was then used to push a ring of parenchyma into the gel substrate periodically, stretching the encircled lung tissue uniformly over the underlying gel. In this approach, radial strain can be transmitted to the airway through its attachments to the lung parenchyma, closely approximating the mechanism through which force fluctuations are transmitted to the airway *in vivo*. A LabView-based program was used to control the micromanipulator. During periods of no imposed stretch, the indenter was positioned so as to touch the PCLS, but not displace the tissue. During periods of imposed stretch, the indenter started from this position, and then was pushed into and withdrawn from the PCLS/polyacrylamide gel in a triangle wave pattern. The system was calibrated such that a 250 μm displacement amplitude corresponded with a 10% stretch of the luminal diameter of the airway, which likely correlates with the stretch imposed upon airways during a deep inspiration.

3.4.3 Selection of PCLS as a model to study bronchospasm

Some might suggest that an *in vivo* model using ventilation of live mice would have been a stronger test of the role of zyxin in bronchospasm. However, there are several reasons why I chose to use a PCLS system to look at airway constriction. First, while there exist many models for inducing AHR in mice, there is no one perfect mouse model for asthma [126]. As such, choosing one amongst the many AHR models would invite speculation as to the importance of the chosen AHR induction in determining the experimental result. Second, in the live animal models, it is difficult to sort out the relative contribution of airway smooth muscle contraction from other possible changes that might occur in a given model including ASM proliferation, inflammation and mucus secretion [126]. By looking directly at airway responses to contractile agonists, much of the complication

created by the many additional variables present in the whole animal models is removed. Finally, the PCLS system allows far greater control over the airway being studied. I was able to apply measured stretches of varying magnitude and frequency to a specific airway far more precisely than possible in the living lung. I was also able to apply drugs directly to the airway of interest rapidly and with very tightly controlled concentration [128]. For these reasons, I believe that our dynamic PCLS system is superior in this case to an *in vivo* model to test ASM contractile responses and the ASM response to stretch in the living lung.

While the PCLS was an ideal model system to study integrated airway responses to contractile agonist stimulation and stretch, executing the experiments was hampered by the limited culture viability of the murine PCLS, which are best used within a few days [38]. Accordingly, to facilitate the PCLS studies in this thesis, I developed a method to cryopreserve the PCLS while maintaining cell viability and contractile agonist responsiveness [39]. In the next chapter, I will describe in detail this cryopreservation method.

4

Cryopreservation of the Precision Cut Lung Slice

 Cite: Sonia R. Rosner, Sumati Ram-Mohan, Jesus R. Paez-Cortez, Tera L. Lavoie, Maria L. Dowell, Lei Yuan, Xingbin Ai, Alan Fine, William C. Aird, Julian Solway, Jeffrey J. Fredberg, and Ramaswamy Krishnan. Airway contractility in the precision cut lung slice following cryopreservation. Am J Respir Cell Mol Biol, May 2014 (published online December 2013). Volume 50, Number 5. Official Journal of the American Thoracic Society.

An emerging tool in airway biology is the precision cut lung slice (PCLS). Adoption of the PCLS as a model for assessing airway reactivity has been hampered, however, by the limited time window within which tissues remain viable. Here I demonstrate that the PCLS can be frozen, stored long-term, and then thawed for later experimental use. Compared to the never-frozen murine PCLS, the frozen-thawed PCLS shows metabolic activity that is decreased to an extent comparable to that observed in other cryopreserved tissues but no differences in cell viability or in airway caliber responses to the contractile agonist methacholine or the relaxing agonist chloroquine. These results indicate that freezing and long-term storage is a feasible solution to the problem of limited viability of the PCLS in culture.

4.1 Introduction

In preclinical models of airway reactivity, responses to constrictor or relaxant agonists are typically assessed using the intubated and ventilated living animal, the isolated airway smooth muscle (ASM) strip, or the isolated ASM cell. Assessment in the living animal offers the advantage of studying the airway in its native microenvironment [126], but because responses of individual airways are innately and dramatically heterogeneous [83, 93, 134, 135], inference of airway behavior is indirect, complex and often ambiguous [136, 137], as well as being costly in terms of time and money. The ASM strip [18, 20, 138] or ASM cell [5, 25, 83, 139] isolated from trachea or major bronchi provides a direct and unambiguous assessment of muscle contractility, but results so obtained may not be representative of responses of muscle from smaller airways. Moreover, such preparations lack the mechanical and humoral microenvironment provided by parenchymal tethering and other cellular components of the airway wall *in situ*. Accordingly, these preparations of isolated tissues and cells comprise an important

tool but are of equivocal physiological relevance [140].

An attractive new preparation for studying reactivity of the small airway is the precision cut lung slice (PCLS) [8, 38, 130, 133, 141–146]. Using the PCLS, airway narrowing can be assessed by direct microscopic observation of individual airways of any size. While there is no alveolar air-liquid interface and lung recoil is therefore not faithfully maintained, the muscle microenvironment roughly approximates *in situ* conditions [130]. Additional practical advantages of the PCLS include ease of preparation, widespread applicability to nearly every animal species including human [8, 147], and suitability for high-resolution imaging [38, 144]. In the PCLS even responses to neural stimulation [143, 145] and stretch [8, 133, 146] have been evaluated.

Use of the PCLS for assessment of airway responsiveness is presently limited by tissue viability in culture, however, which is only 3-6 days from time of tissue harvest [38]. This limitation imposes scheduling difficulties and severely constrains the number of slices that can be studied per lung. In addition to these limitations, my thesis work required that the PCLS be prepared from animals in the Beckerle lab at the Huntsman Cancer Institute in Utah and then shipped to Boston for my experiments, further complicating the use of PCLS in my study. To overcome these limitations, I describe here a new approach to collect, preserve, and then study airway contractility in the PCLS. Using the conventional cryopreservative DMSO [148, 149], I demonstrated that murine PCLS can be frozen, stored, and thawed for study at a later time.

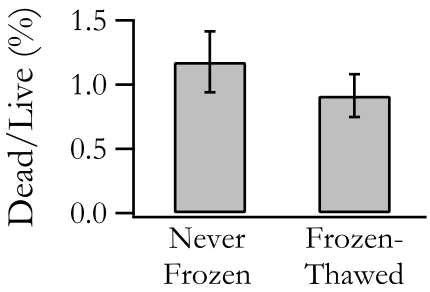

Figure 4.1: Viability is preserved in frozen-thawed PCLS. LDH assay shows no significant difference between frozen-thawed and never-frozen groups in the percentage of dead to live cell (n=22 PCLS in each group).

4.2 Results

After slow freezing in 10% DMSO and rapid thawing at 37°C, frozen-thawed PCLS were not statistically different from never-frozen PCLS in fractional cell death, integrity of the epithelial and smooth muscle layers, or contractile responsiveness to methacholine.

4.2.1 Freezing-thawing does not increase cell death or compromise tissue integrity

Ciliary beating in the airway epithelium was robust in the frozen-thawed PCLS (data not shown) and qualitatively similar between the never-frozen and the frozen-thawed groups. The LDH assay showed that cell death was slight (1%) and similar in both the never-frozen and the frozen-thawed PCLS (Figure 4.1). The MTT assay showed that cell enzymatic activity was reduced in the frozen-thawed group (Figure 4.2, $p<0.05$, unpaired two-tailed t-test), but these changes fell well within the range previously reported for other cryopreserved tissues [150–152]. Immunohistology of PCLS thin sections showed the airway epithelium and smooth muscle layers to be similarly intact in both never

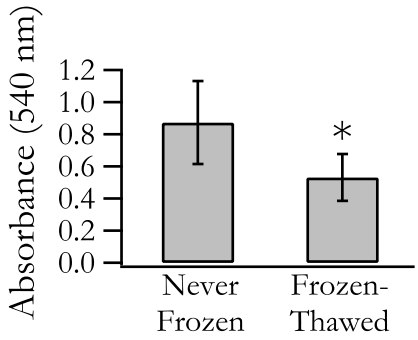

Figure 4.2: Cell metabolic function reduced but within acceptable range in frozen-thawed PCLS. MTT assay showed a significant reduction in cell metabolic activity after freeze-thaw (*, $p<0.05$) but well within the acceptable range previously reported for other tissues [150–152]. These data are reported as mean and standard deviation of formazan absorbance at 540 nm (n=18 PCLS in each group).

frozen and frozen-thawed PCLS (Figure 4.3). Microscopic observation showed that lung parenchyma, blood vessels and airways of both never-frozen and frozen-thawed PCLS were structurally intact (Figure 4.4A,B). Associated cell death was minimal and predominantly localized along the edges of the PCLS and in the airway epithelium, although even there the vast majority of cells were alive (Figure 4.4A,B).

4.2.2 Freezing-thawing does not alter contractile response to methacholine

In response to methacholine (MCh, 10^{-7} to 10^{-4} M), airway contractile responses in both the never-frozen and the frozen-thawed groups were highly variable. These responses varied slightly with initial airway size, with smaller airways (<200 μm) being more responsive (Figure 4.5C, D, Figure 4.6). Irrespective of initial airway size, however, contractile responses were not statistically different between the never-frozen and the frozen-thawed groups (p=0.1-0.5; Figure 4.5A, B, C, D). For example, at 10^{-4} MCh,

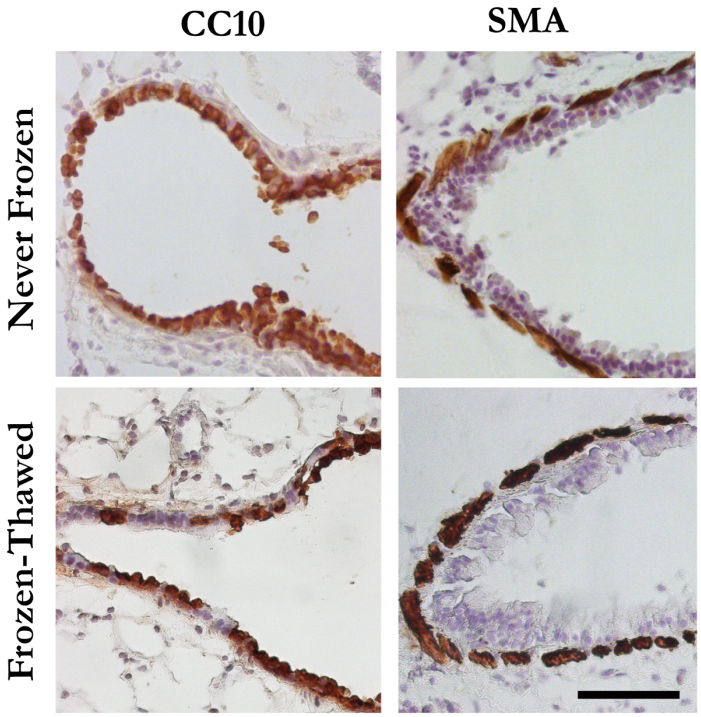

Figure 4.3: Airway epithelium and smooth muscle layers are similarly intact in never frozen and frozen-thawed PCLS. Sections of never frozen and frozen-thawed PCLSs were immunostained for CC10 expression in the lung epithelium and SMA expression by airway smooth muscle cells. Nuclei of the cells on sections were counterstained by hemotoxylin (Sigma). Scale bar, 50 μm.

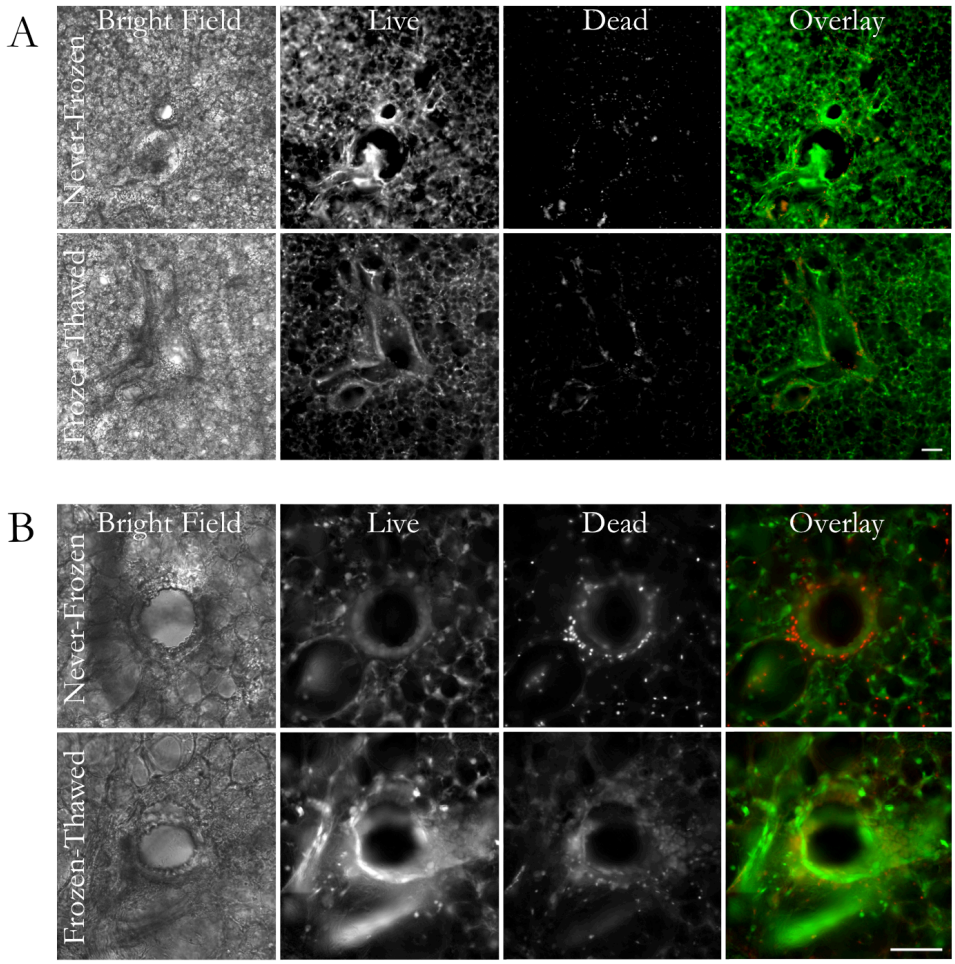

Figure 4.4: Cell death in PCLS is minimal and predominantly localized to airway epithelium. (A) Representative bright field and florescence images of live-dead stained never-frozen or frozen-thawed PCLS at 10X magnification (Scale bar = 200 μm). (B) Representative bright field and fluorescence images of live-dead stained never-frozen or frozen-thawed PCLS at 20X magnification (Scale bar = 200 μm).

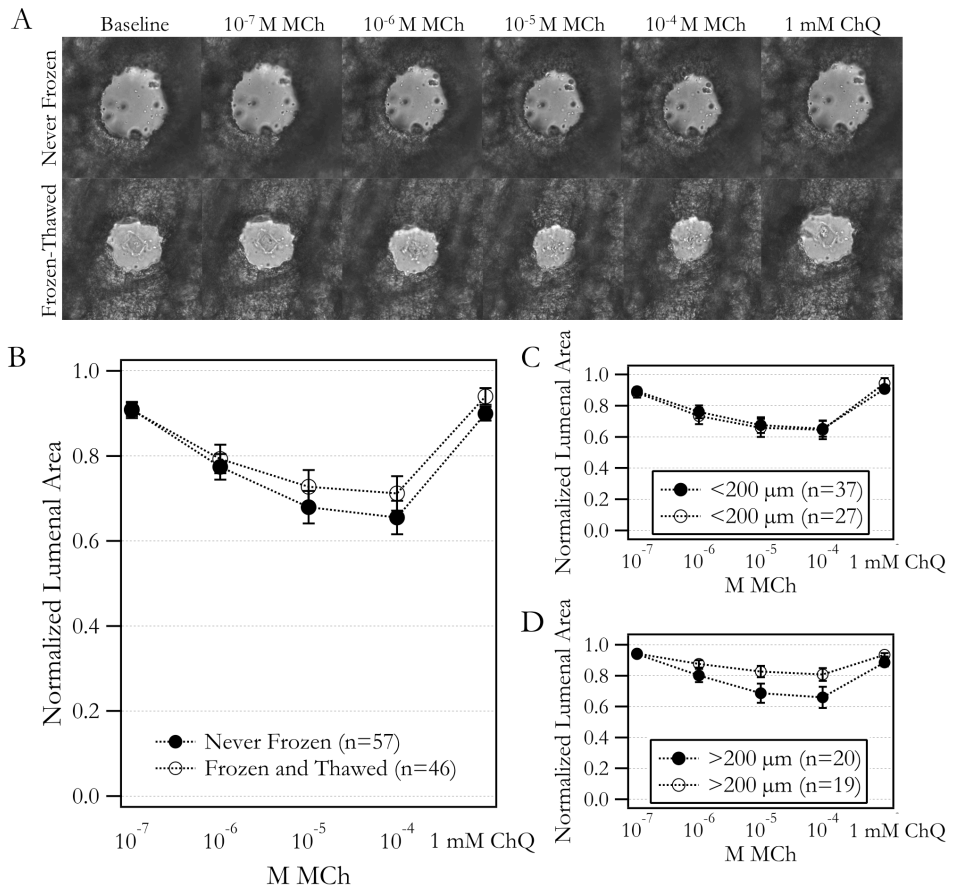

Figure 4.5: Airway contractility is preserved in frozen-thawed PCLS. In the never-frozen group the mean diameter was 151 μm and the range was 88-389 μm; in the frozen-thawed group the mean diameter was 175 μm and the range was 77-415 μm. (A) Representative images of airway contraction to MCh (10^{-7}-10^{-4} M) and airway relaxation to ChQ (1mM) in never-frozen and frozen-thawed groups (Scale bar = 50 μm). (B) When pooled, airway contraction and relaxation in never-frozen (n = 57 airways) and frozen-thawed (n=46 airways) PCLS were not statistically different with MCh or ChQ (p=0.2-0.4). Plotted are mean and SEM. (C, D) In both groups, individual airways contracted heterogeneously. To assess the role of initial airway size, I grouped airways into two bins: smaller than 200 μm (C) and larger than 200 μm (D). Within each airway size bin, never-frozen and frozen-thawed airways did not show significant differences in their responses to MCh and to ChQ (p=0.1-0.5).

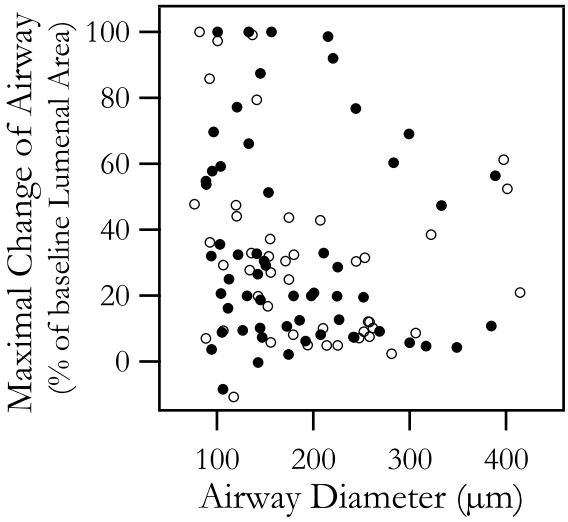

Figure 4.6: Airway contractility is weakly dependent on airway size. Change in luminal area versus initial airway diameter for never-frozen (closed circles, n= 57 airways) and frozen-thawed (open circles, n=46 airways).

airway luminal area contracted to a mean value of 64% ± 9% (SEM) of the baseline in the never-frozen group (n=57 airways) compared with a mean value of 69% ± 5% of baseline in the frozen-thawed group (n=46 airways; p=0.2). At a time resolution of one minute, we observed no differences in the rate of contraction with MCh between never-frozen and frozen-thawed airways (Figure 4.7). Additionally, there was no significant difference in the values for EC50 between the never-frozen and frozen-thawed groups (Table 4.1, p = 0.24).

Condition	EC50 for MCh
Never Frozen	3.99×10^{-7} M
Frozen-Thawed	2.97×10^{-7} M

Table 4.1: EC50 values are not significantly different for MCh in never-frozen and frozen-thawed PCLS.

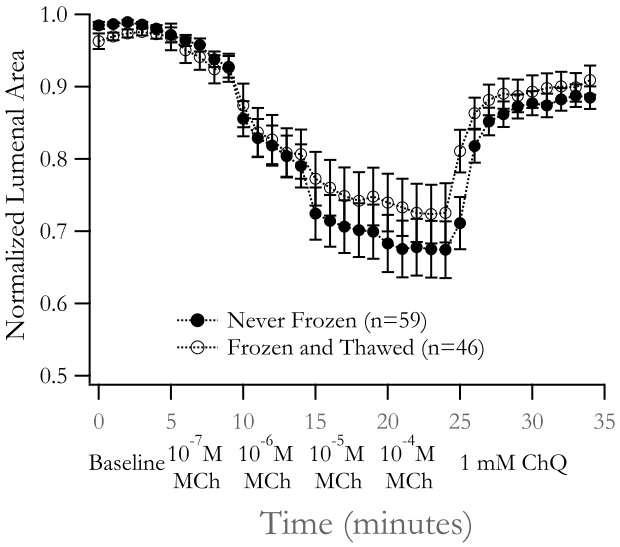

Figure 4.7: Dynamics of airway closure are similar in never frozen and frozen-thawed PCLS. Time series of airway responses to methacholine and chloroquine at a resolution of one minute. Increasing doses of methacholine were added at 5, 10, 15, and 20 minutes and 1 mM chloroquine was added at 25 minutes.

4.2.3 Freezing-thawing does not alter relaxant response to chloroquine

To airways that were pre-constricted with MCh, as described above, I administered the relaxant agonist chloroquine (1 mM) [153]. Relaxation responses were not statistically different between never-frozen and frozen-thawed groups (p=0.21; Figure 4.5A-C, 4.8). Airways relaxed to a mean of 90% ± 2% of the baseline in the never-frozen group (n=57 airways) and 94% ± 2% of the baseline in the frozen-thawed group (n=46 airways). We also observed significant dilation in response to the relaxing agonist formoterol in airways from frozen-thawed PCLS (Figure 4.9), which in pilot experiments was of a similar magnitude as observed in never-frozen PCLS (data not shown).

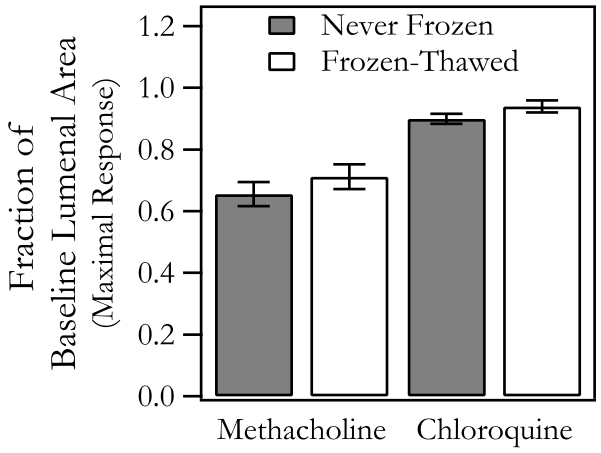

Figure 4.8: Airway responses to chloroquine are unchanged in frozen-thawed PCLS.

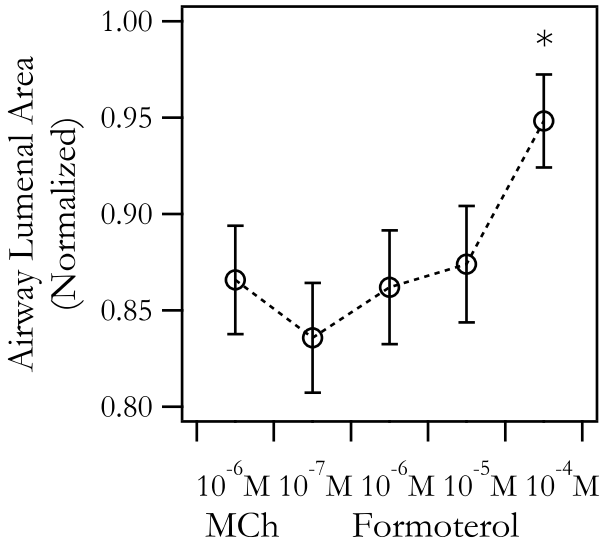

Figure 4.9: Frozen-thawed airways dilate in response to formoterol, a relaxing agonist. As expect, the frozen-thawed airways contracted approximately 15% with 10^{-6} M MCh. The airways subsequently dilated to approximately 95% of their original baseline area. This response is similar to that observed in never frozen airways.

4.3 Discussion

Here I demonstrate for the first time that it is possible to freeze and thaw the murine PCLS while maintaining unaltered responses to contractile and relaxant agonists. Although cellular metabolic activity was somewhat reduced, cell death, ciliary beating, and airway narrowing were not appreciably affected. It remains unclear, however, if this methodology might be useful to preserve nerve fiber endings, mast cells, or other receptor targets on airway smooth muscle. These findings are of practical importance because the time window for measurement of airway responses in the never-frozen PCLS is limited to a few days [38, 141] whereas the time window for measurement in the frozen PCLS is demonstrated here to extend as long as two weeks.

4.3.1 Development of the cryopreservation method

Storage times substantially longer than two weeks are plausible, as cryopreservation studies in other tissues typically find that the duration of storage does not appreciably affect viability [154–157], and in pilot studies I found no changes in airway contractility after 3 months. In slices of other organs, a variety of cryopreservation techniques have been used [148, 149, 158, 159], although airway contractile responses in the PCLS have never before been studied after cryopreservation. I used the conventional cryoprotectant, DMSO, and obtained satisfactory results using a high concentration. At this concentration, DMSO readily infiltrates the cell membrane, remains water-soluble even at low temperatures, and has low cytotoxicity [148]. I chose a slow freezing rate of 1°C/minute to prevent the formation of ice crystals inside cells. I chose a rapid thawing rate because pilot experiments showed less ciliary beating and more cell death in PCLS thawed more slowly. These measurements were limited to 37°C, however, and do not preclude other conditions including lower thaw temperatures. Ultimately, our method

resulted in an average of 1% cell death in both never frozen and frozen-thawed PCLS. The cell metabolic activity was significantly reduced in the frozen-thawed PCLS but well within the acceptable range previously reported for other tissues [150–152].

4.3.2 Innate heterogeneity of airway responsiveness

Innate biological variability of airway responsiveness across airways even within the same animal is quite large and does not follow a normal distribution [93, 134, 145]. For example, Minshall et al. showed at the level of human lung slices that airway responses are remarkably heterogeneous even in the same lung donors [93]. Even at the level of the underlying smooth muscle cell, cellular contractility and other cellular mechanical properties are known to be innately heterogeneous and distributed non-normally with geometric standard deviations of about 3 [83, 85, 125, 160]. No factor of airway geometry can account for these non-Gaussian heterogeneities, which seem to be innate to the contractile units themselves. Accordingly, for statistical analysis of airway narrowing I used the Mann-Whitney-Wilcoxon rank-sum test.

I found large variation in airway contractile response to MCh even for airways from the same animal, the same experimental condition, and the same initial size (Figure 4.5B, C, D), consistent with earlier studies demonstrating innate biological heterogeneity of ASM contractility in tracheal smooth muscle strips, isolated ASM cells and the human PCLS [8, 83, 93, 129, 134, 135, 161, 162]. Smaller airways were systematically more responsive, however (Figure 4.5C, D, Figure 4.6). The airway narrowing that I observed was comparable in extent with other recently published literature in the C57BL/6 mouse showing airway narrowing of approximately 40% with 10^{-4} M MCh, as compared to the 36% mean narrowing reported in our control at the same dose [163, 164].

4.3.3 Contractile and relaxing agonists

To test the effects of cryopreservation on airway responsiveness I used the contractile cholinergic agonist, MCh, and the dilating bitter tastant agonist, chloroquine. I chose chloroquine because it causes a substantially greater bronchodilation in murine airways compared with β-agonists [153] and, as such, I reasoned that any differences in bronchodilation caused by cryopreservation would be made more apparent.

4.3.4 A novel method of cryopreservation that could enable broader use of the PCLS

Together, the data reported here establish the frozen-thawed PCLS as a useful preparation for study of airway responsiveness. By freezing and storing the PCLS, timing of experiments becomes uncoupled from that of harvesting, and utilization of precious samples is maximized. It seems likely that similar results could be obtained using human tissues or genetically engineered laboratory animals, but this remains to be tested directly. Freezing and thawing thus makes feasible the notion of a PCLS bank and enables expanded use of this emerging *ex vivo* preparation.

4.4 Materials and Methods

4.4.1 Animals

Lungs were obtained from seven 20-week-old C57/BL6 mice (Jackson Laboratory, Bar Harbor, ME). The Boston University Institutional Animal Care and Use Committee approved all animal procedures.

4.4.2 Preparation and culture of PCLS

Each PCLS was prepared as described previously [142]. Following tracheotomy, excised mouse lungs were insufflated with 1% low-melting point agarose in HBSS, followed by air. The insufflated lungs were then placed in cold HBSS (Corning Life Sciences, MA, USA). After the agarose gelled, the left lower lobe was separated and then sectioned into slices 250 μm thick using a tissue slicer (Precisionary Instruments VF-300). Lung slices were incubated at 37°C in 1:1 DMEM/F-12 supplemented with penicillin, streptomycin, kanamycin, and amphotericin B (Invitrogen, MA, USA). Culture medium was changed once an hour for the first 4 hours and once a day thereafter.

4.4.3 Freezing and thawing of PCLS

For cryopreservation, I used 10% DMSO diluted in DMEM/F-12 medium. Each single PCLS was placed in cryopreservation medium in individual cryovials and frozen at -80°C (Nalgene Mr. Frosty Freezing Container, Thermo Scientific, MA, USA). Following overnight freezing, each cryovial was transferred to liquid nitrogen for long-term storage up to two weeks. On the day of the experiment, each cryovial was thawed rapidly in a 37°C water bath. The PCLS was then carefully removed and washed once in fresh culture medium. (Figure 4.10)

4.4.4 Measurement of cytotoxicity using the lactate dehydrogenase (LDH)-releasing assay

LDH releasing assay was performed using the CytoTox 96 non-Radioactive Cytotoxicity Assay kit (Promega) according to the manufacturer's instructions. Briefly, PCLS were incubated for 18 hours in culture medium at 37°C. The amount of LDH released into the

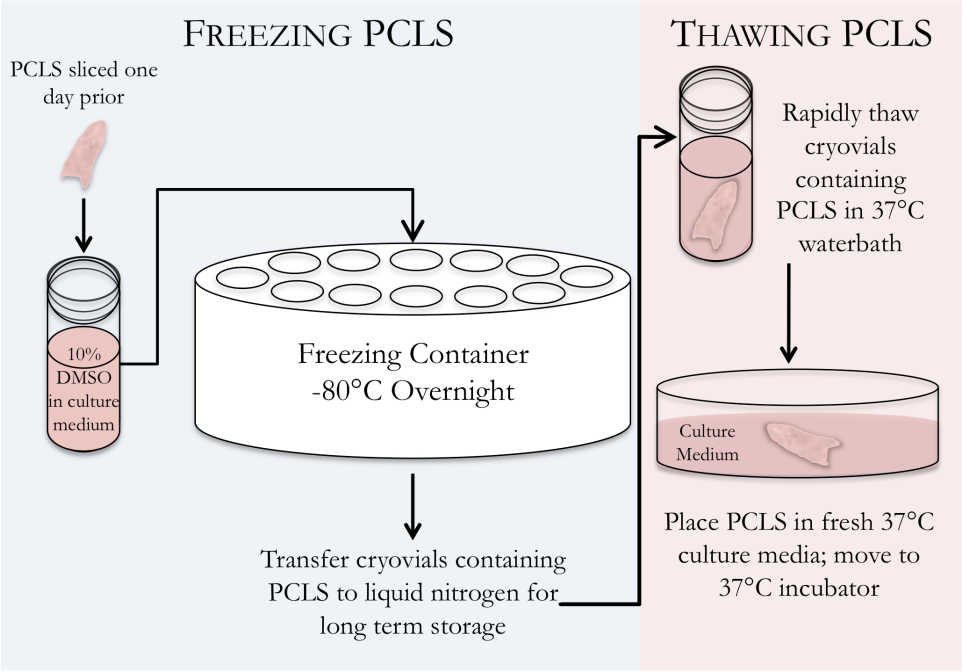

Figure 4.10: Schematic of freezing and thawing protocol for PCLS.

culture supernatant was used to determine the number of dead cells. Using the culture supernatant, cell death was quantified using a standard enzyme-linked immunosorbent assay (ELISA) for LDH implemented at an optical density of 490 nm (SpectraMax M5, Molecular Devices). These measurements were normalized to total number of cells in the PCLS that were obtained in a representative set through standard procedures of lysis and sonication.

4.4.5 Measurement of cell enzymatic activity

An MTT assay was performed using a Vybrant MTT Cell Proliferation Assay Kit (Life Technologies, CA, USA). Briefly, PCLS were incubated for 3 hours in culture medium containing 500 ng/mL MTT. The culture medium was then replaced with 100% DMSO and the amount of dissolved formazan was quantified by examining the supernatant at an

absorbance of 540 nm.

4.4.6 Preparation and immunohistology of PCLS thin sections

Never frozen and frozen-thawed PCLSs were fixed in 4% paraformaldehyde/PBS for 20 minutes. After washes with PBS, fixed PCLS were cryoprotected by immersion in 30% sucrose/PBS overnight. PCLSs were then embedded in OCT and sections 10 microns thick were collected. Sections of PCLSs were immunostained with antibodies against the lung epithelium marker CC10 (1:500, T-18, Santa Cruz) and alpha-smooth muscle actin (SMA) (1:500, MS-113, Thermo Scientific) using an established protocol [165]. Antigen-antibody complexes were detected by chromogenic substrates.

4.4.7 Live/dead staining and imaging of PCLS

The viability of the PCLS was tested using a commercially available kit (LIVE/DEAD kit L-3224, Molecular Probes, OR, USA). Briefly, the PCLS was stained with 4 mM calcein-AM and 2 mM ethidium homodimer-1 in HBSS with calcium and magnesium, incubated at 37°C for 30-45 min, and imaged on an inverted microscope, using a GFP filter (BP 470/40) for calcein-AM and a Cy3 filter (BP 545/30) for ethidium homodimer-1 (DMI6000B, Leica Microsystems, IL, USA).

4.4.8 Measurements of airway contraction and relaxation

Using a ring of nylon mesh and a stainless steel washer, each PCLS was secured in place within a 12-well plate. The multi-well plate was mounted on a computer controlled translation stage and imaged using an inverted microscope (Leica Microsystems, DMI6000B, IL, USA). Intact airways were selected for imaging, and PCLS were incubated sequentially with increasing doses of methacholine (MCh) 10^{-7} M, 10^{-6} M,

10^{-5} M, and 10^{-4} M (Sigma Aldrich, St. Louis, MO) for 5 minutes each, followed by 1mM chloroquine (ChQ, Sigma Aldrich) for 10 minutes. Each airway was maintained in the same plane of focus and imaged every minute for a total duration of 35 minutes. From the acquired images, I quantified airway luminal area (Image J, NIH), and normalized its magnitude to the pre-treatment baseline value. From the normalized data, I picked those values corresponding to maximum constriction with each dose of MCh and maximum dilation with ChQ.

4.4.9 Statistics

For reasons addressed in the discussion, fractional changes of airway lumenal area of never-frozen PCLS (n=57 airways) versus frozen-thawed PCLS (n=46 airways) were compared using a Mann-Whitney-Wilcoxon rank-sum (MWW) test [134]. Differences were considered significant when $p<0.05$. All data are reported as mean and SEM.

5

Zyxin in Static Cell Mechanics and Cell Responses to Stretch

In response to a spontaneous deep inspiration, contracted airway smooth muscle (ASM) fluidizes rapidly and then resolidifies slowly, but molecular mechanisms accounting for these salutary bronchodilatory responses –and their dramatic breakdown in asthma– are unknown. I will show here that both the baseline contractile force and the fluidization response of ASM are independent of the cytoskeletal protein zyxin, but the

resolidification response is zyxin-dependent.

5.1 Introduction

Cells in tissues as diverse as the lung, gut, bladder, great vessels, and kidneys experience a repeating sequence of transient mechanical stretches [5, 166–169]. Despite differences in structure and function, various cell types within these tissues show the very same physical response to stretch. Specifically, previous work has established that all cell types exhibit: 1) a rapid fluidization of the cytoskeleton marked by the disappearance of actin stress fibers and traction forces exerted by the cell upon its substrate, followed by 2) a gradual and ATP-dependent resolidification of the cytoskeleton marked by recovery of both actin fibers and traction forces to baseline levels [5, 25, 170]. Prior work to determine mechanism has shown that F-actin stabilization or depolymerization, myosin inhibition, and calcium depletion all act to change actin stress fibers and traction forces at baseline as expected, but fail to fundamentally alter responses to stretch [5]. Molecular mechanisms underlying this phenomenon remain poorly characterized.

The cytoskeletal protein zyxin is a key player in the repair and maintenance of actin stress fibers [32, 115]. Zyxin relocalizes from the focal adhesions to actin stress fibers, particularly in the presence of an external mechanical stress on the cell [31, 32]. Zyxin is also necessary for the cytoskeletal reinforcement that follows mechanical stress, which further suggests that zyxin may also play a role in the rapid recovery of actin stress fibers following stretch [31]. Intriguingly, both the observed repair of stress fibers by zyxin and the resolidification of the cytoskeleton following stretch occur on the timescale of a few minutes [5, 25, 32]. This empirical evidence led to the hypothesis that zyxin may have a critical role in cytoskeletal resolidification following stretch-induced fluidization.

While fluidization and resolidification are universal responses, I focus here on the airway smooth muscle cell, as regulation of the stiffness and contractility of airway smooth muscle (ASM) in the presence of stretch is of key importance in the pathophysiology of asthma [5, 11, 25, 171, 172]. Wherever possible, I used primary ASM cells, both from wild type and zyxin$^{-/-}$ mice as well as a siRNA-mediated knockdown of zyxin in human ASM cells. In some cases where sufficient quantities of primary airway smooth muscle cells could not obtained, I used instead the murine embryonic fibroblast (MEF), a mesenchymal cell type which has a similar contractile apparatus composed of actin stress fibers. With these model systems, I measured baseline stiffness and cell contractile force, cytoskeletal remodeling rates and responses to stretch. From these studies, I found that while under isometric conditions, zyxin played little role in determining cell mechanical properties, under dynamic conditions, zyxin acted to stabilize the cell contractile apparatus.

5.2 Results

5.2.1 Following a single isotropic cell stretch, zyxin recruits to sites of actin SF fragmentation

Although changes in zyxin localization in response to high-frequency cyclic stretches have been reported previously [31], physiologic responses such as net cellular contractile force and responses to a single transient stretch of physiological magnitude and duration have not yet been reported. In order to measure protein dynamics immediately following a single stretch, in collaboration with Rama Krishnan and Mark Smith, we adapted the system of Krishnan et al. [25] to work with high-resolution confocal microscopy. Zyxin$^{-/-}$ MEFs rescued with GFP-zyxin were transfected with LifeAct [115] and subjected to a single transient isotropic stretch and unstretch of 10% strain amplitude and

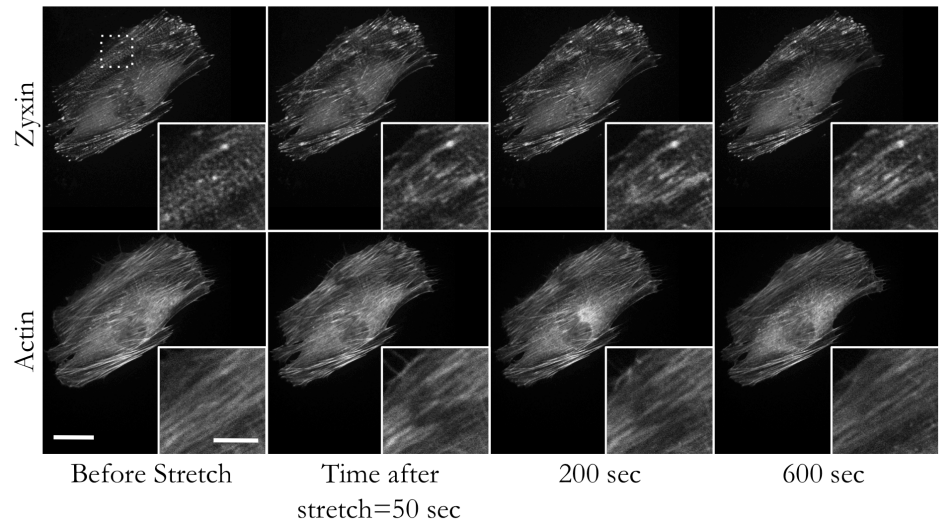

Figure 5.1: Zyxin is widely recruited to sites of actin SF fragmentation following single isotropic stretch. Representative images showing localization of actin and zyxin before, and 50, 200, and 600 seconds after a single isotropic stretch. Scale bar for large images is 30 μm, and for insets is 5 μm.

4 second duration, as in a DI. At baseline, zyxin was predominantly localized at focal adhesions (Figure 5.1). Within 50 seconds after completion of this maneuver, however, zyxin began to localize predominantly along actin SFs (Figure 5.1) and persisted on SFs for more than five minutes, which is a timescale reminiscent of ASM resolidification after stretch-induced fluidization [5, 25]. Punctate bands of zyxin corresponded with local decreases in LifeAct-actin intensity (Figure 5.2), thus establishing that even a single transient stretch of physiological magnitude is sufficient to cause zyxin to recruit rapidly to sites of imminent SF failure [32].

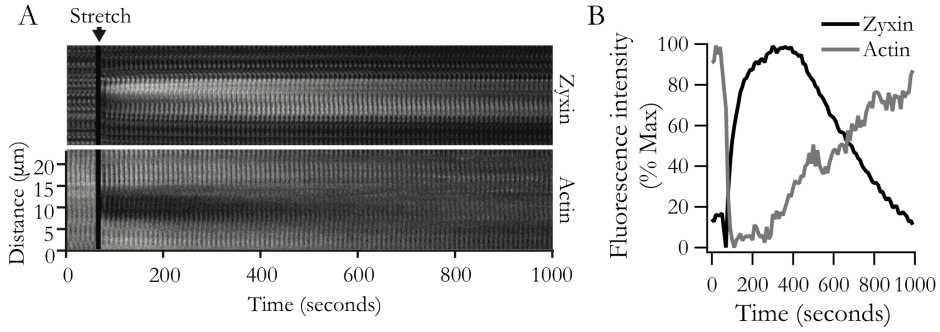

Figure 5.2: Zyxin localizes to and stabilizes actin stress fibers following stretch. (A) Kymograph of actin and zyxin on a representative stress fiber following a single isotropic stretch. (B) Quantification of actin and zyxin intensity on a representative stress fiber following a single isotropic stretch.

5.2.2 In the zyxin$^{-/-}$ MEF, baseline stiffness and net contractile force are similar to that of rescued MEFs, but the rate of cytoskeletal remodeling increases

To what extent does zyxin influence cellular mechanical properties, either statically or dynamically? To answer this question I first assessed the rate of remodeling within the stress fiber. To do this I quantified the spontaneous nano-scale motions of a microbead to which the stress fiber is firmly attached; because the microbead can barely move unless the associated stress fiber remodels, such motions can be taken as a reporter of the rate of internal stress fiber reorganization [5, 35]. Microbeads (5 μm) were coated with the peptide sequence RGD, which binds avidly to integrins [35]. These beads were added to cultured adherent MEFs, which bound the beads and formed focal adhesions with associated stress fibers. The measured nano-scale motions of these beads were 45% larger in the beads attached to zyxin$^{-/-}$ MEFs than those attached to the GFP-zyxin rescued MEFs (Figure 5.3), thus indicating that zyxin caused a modest but systematic slowing in the rate of cytoskeletal remodeling (Figure 5.3), as if stabilizing cytoskeletal structures.

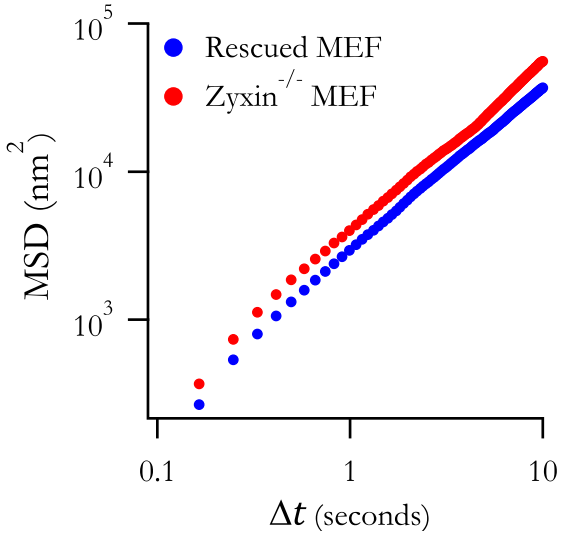

Figure 5.3: Zyxin-/- MEFs show an increased cytoskeletal remodeling rate. MSDs of microbeads adherent to the cytoskeleton in zyxin$^{-/-}$ (n=739) and GFP-zyxin-rescued (n=844) MEFs show that zyxin$^{-/-}$ cells have a somewhat increased rate of remodeling, as evidenced by the upward shift of the MSD curve.

But when I examined isometric cell stiffness using optical magnetic twisting cytometry probed through these same beads [160] in zyxin$^{-/-}$ versus GFP-zyxin rescued MEFs, I found no difference in stiffness (Figure 5.4). Similarly, when I measured net contractile force generated by each cell using traction force microscopy [36], I found no difference in baseline net contractile moment (Figure 5.5). For the zyxin$^{-/-}$ compared with the zyxin-rescued MEF, peak tractions corresponding to the highest quartile of local tractions become systematically attenuated, but with no change in whole-cell net contractile moment, thus suggesting a change in intracellular spatial distribution [32]. Here I found, further, that while zyxin contributed appreciably to slowing and stabilizing the rate of cytoskeletal remodeling, zyxin contributed little to isometric stiffness or isometric contractile force, suggesting either that zyxin played at most only a slight role in these static mechanical properties of the MEF or that other proteins somehow

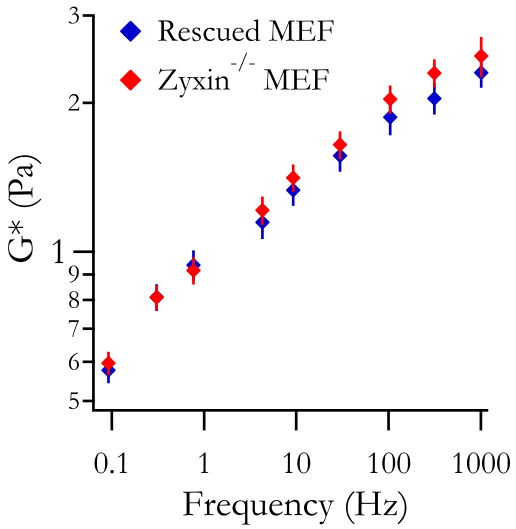

Figure 5.4: Zyxin does not contribute to isometric stiffness of the MEF. Across a wide range of bead twisting frequencies, GFP-zyxin-rescued (n=261) and zyxin$^{-/-}$ (n=273) MEFs show no difference in isometric stiffness.

compensated for zyxin's absence.

5.2.3 The absence of zyxin alters cell mechanical responses to changes in the stiffness of the microenvironment

It is well known that cells respond to the mechanical properties of their microenvironment, and that changes in the stiffness of a cell's microenvironment can result in that cell changing its stiffness or contractile force [173–175]. I sought to determine whether zyxin plays a role in determining a cell's mechanical response to changes in substrate stiffness using the zyxin$^{-/-}$ MEF. I found that zyxin appears to blunt the change in cell contractile force in response to changes in substrate stiffness. Over an order of magnitude increase in substrate stiffness, wild type MEFs show on average a fifteen-fold increase in cell contractile force, while zyxin$^{-/-}$ MEFs show only a

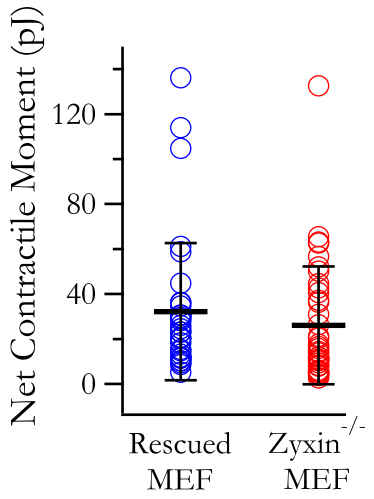

Figure 5.5: Zyxin$^{-/-}$ and zyxin-rescued MEFs show no difference in baseline contractile force. Net contractile moment is unchanged between the GFP-zyxin-rescued and zyxin$^{-/-}$ MEFs. Circles are individual cellular net contractile moment, black bars are means, and error bars are standard deviation (n=34 zyxin-rescued, n=38 zyxin$^{-/-}$; p=0.4).

four-fold increase in cell contractile force (Figure 5.6). Additionally, on the softest substrates I tested with a Young's modulus of only 1.2 kPa, zyxin$^{-/-}$ MEFs exert significantly more force than wild type MEFs (Figure 5.6). These results suggest that zyxin may play a key role in transducing mechanical cues from a cell's microenvironment and guiding accompanying shifts in cell contractile force.

5.2.4 Mechanical responses of zyxin$^{-/-}$ and zyxin-rescued MEFs to contractile agonist stimulation are incongruent

As zyxin is known to be an actin regulatory protein, I sought to determine whether zyxin contributed to the cell mechanical response to contractile agonist stimulation. To test this in the MEF, I chose fetal bovine serum (FBS) as an agonist as it is known to be a potent inducer of cell contractility in the fibroblast [176–178]. When I examined

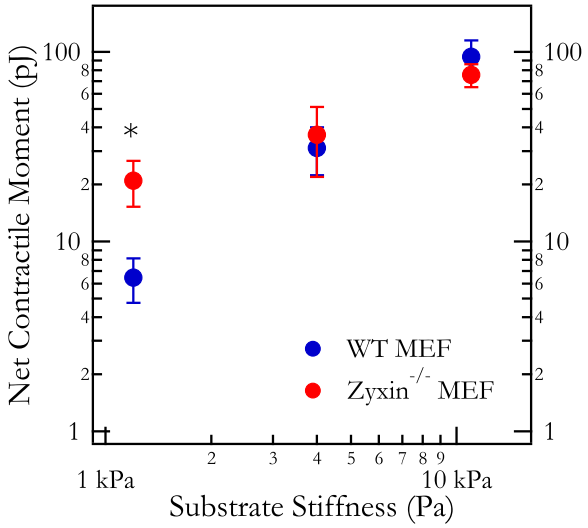

Figure 5.6: The relationship between cell net contractile moment and substrate stiffness is blunted in zyxin$^{-/-}$ MEFs. Baseline cell net contractile moment versus substrate stiffness in wild type and zyxin$^{-/-}$ MEFs. When plated on 1.2 kPa gels, zyxin$^{-/-}$ MEFs have significantly higher average net contractile moment than wild type MEFs ($p<0.05$).

changes in cell stiffness following treatment of serum-starved zyxin-rescued and zyxin$^{-/-}$ MEFs with FBS, I found that while both types of cell plateaued at an approximately 50% increase in stiffness, the initial spike in stiffness following FBs addition was much higher in zyxin-rescued MEFs (Figure 5.7). Zyxin-rescued MEFs showed a maximum increase in stiffness of over 150%, while zyxin$^{-/-}$ MEFs showed a maximum increase in stiffness of only about 80% (Figure 5.7).

As changes in cell stiffness generally correlate with changes in cell traction force [34], I sought to confirm this result by measuring changes in contractile force following contractile agonist stimulation with FBS. In contrast, here I found a paradoxical result. In the zyxin-rescued MEFs, by 300 seconds following FBS addition, net contractile moment increased by 36% ± 11% (n=25; Figure 5.8). However, in zyxin$^{-/-}$ MEFs, net

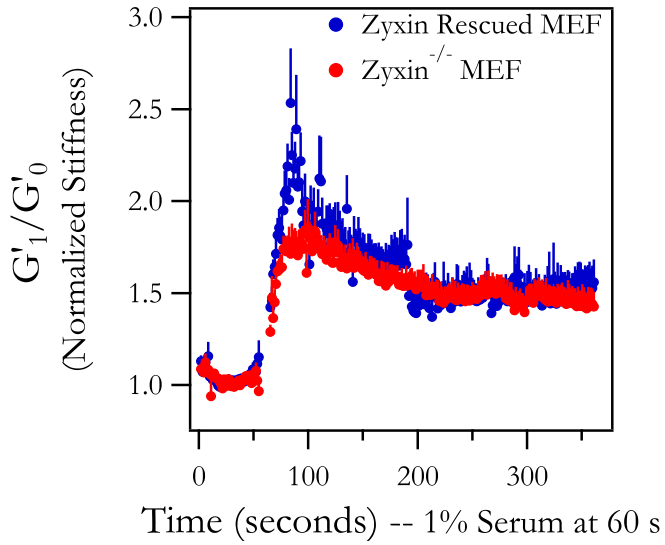

Figure 5.7: Zyxin-rescued and zyxin$^{-/-}$ MEFs show a similar increase in cell stiffness in response to serum stimulation. While zyxin-rescued MEFs show a higher initial spike in stiffness in response to serum stimulation, both zyxin-rescued (n=277) and zyxin$^{-/-}$ (n=284) MEFs plateau to the same 50% increase in cell stiffness.

contractile force increased by 78% ± 22% over this time period (n=34; Figure 5.8), and the increase was significantly more than that of zyxin-rescued MEFs at 100 and 200 seconds following serum addition ($p<0.5$; Figure 5.8) and trended significant at 300 seconds ($p=0.1$; Figure 5.8). This represents an unresolved paradox, as one would normally expect that traction force findings would correlate with cell stiffness findings. A possible hypothesis explain these findings is that, in the MEF following FBS addition, the changes driving increases in stiffness and those driving increases in contractility are acting through different pathways that involve zyxin in different capacities. The clarification and testing of this hypothesis is a subject for future work in the field.

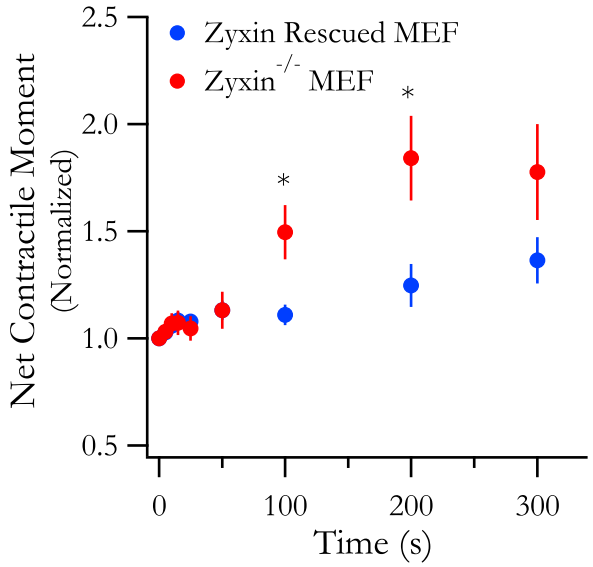

Figure 5.8: Zyxin$^{-/-}$ MEFs (n=34) show a larger and faster increase in cell contractile moment than zyxin-rescued MEFs (n=25) in response to serum stimulation.

5.2.5 In the MEF, resolidification responses to stretch show less dependence on substrate stiffness in the absence of zyxin

In order to look at the relationship between substrate compliance and responses to stretch, I measured the contractile response to stretch in wild type and zyxin$^{-/-}$ MEFs on substrates spanning an order of magnitude of stiffness, from 1.2 to 11 kPa. In these experiments, I tested the hypothesis that zyxin drives mechanosensing of substrate stiffness in a dynamic environment, rather than the static measures examined in the above experiments. When MEFs were plated on substrates with Young's modulus of 11 kPa and stretched with 5% strain, I found that wild type MEFs trend towards greater resolidification than zyxin$^{-/-}$ MEFs, although this finding fell short of statistical significance (Figure 5.9). Additionally, I found that both wild type and zyxin$^{-/-}$ MEFs fail to resolidify following larger physiologic stretches of approximately 10% strain

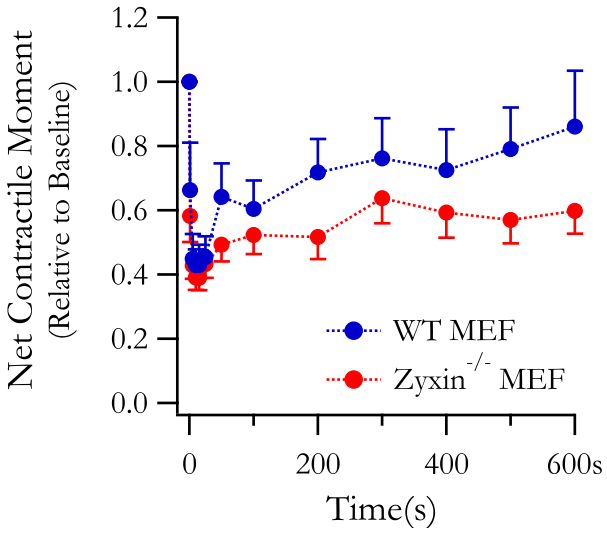

Figure 5.9: While shy of statistical significance, zyxin$^{-/-}$ MEFs trend towards less complete resolidification following transient stretch. Wild type (n=16) and zyxin$^{-/-}$ (n=22) MEFs plated on 11 kPa gels were subjected to stretches of approximately 5% strain. Measures of contractile moment before and after showed that zyxin$^{-/-}$ MEFs trended towards a less complete resolidification, although this finding was not significant (p=0.1).

(Figure 5.10). It is possible that this cell type is not as robust to large strains as other cell types previously studied [5], and ultimately this finding limited the stretch experiments in MEFs to lower strain amplitudes. When I tested cell responses to 5% stretch across a range of substrate stiffnesses, I found that wild type MEFs resolidify fully in locally stiffer environments, while they fail to resolidify to baseline levels of traction in softer environments (Figures 5.9, 5.11, 5.12). Zyxin$^{-/-}$ MEFs showed the same diminished resolidification across a tenfold range of substrate stiffness(Figures 5.9, 5.11, 5.12), suggesting a role for zyxin in dynamic mechanosensing. These findings indicate that there may be a relationship between substrate stiffness and resolidification following stretch in MEFs that is dependent on zyxin.

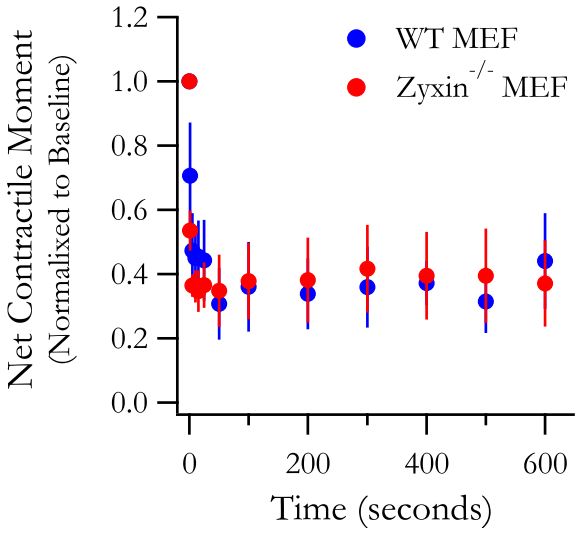

Figure 5.10: MEFs are unable to recover traction forces following transient stretches of 10% magnitude. wild type (n=9) and zyxin$^{-/-}$ (n=9) MEFs fluidize but do not resolidify with higher strains.

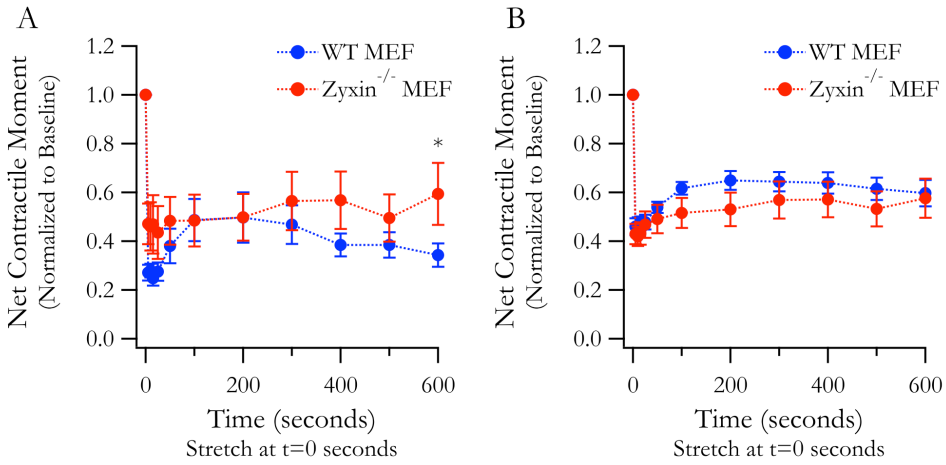

Figure 5.11: On softer substrates, both wild type and zyxin$^{-/-}$ MEFs fail to reach their baseline net contractile moment following transient stretch. Following a single transient isotropic stretch, wild type (n=11) and zyxin$^{-/-}$ (n=8) MEFs plated on 1.2kPa (A) or 4 kPa (B) polyacrylamide gels plateaued at net contractile moments well below their baseline.

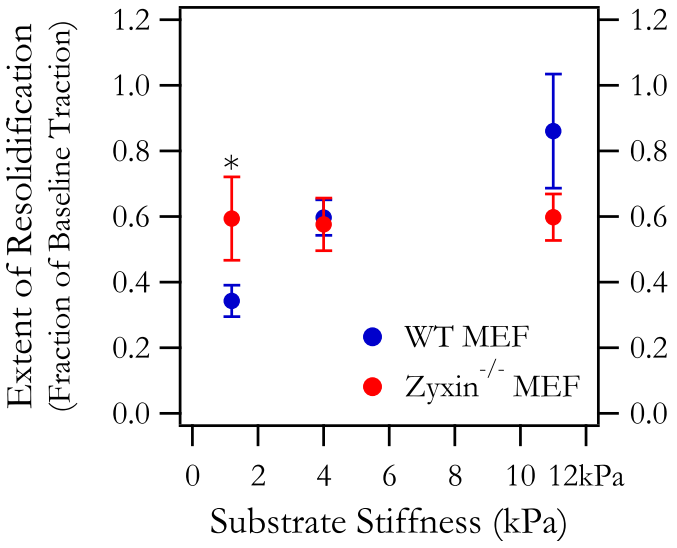

Figure 5.12: The extent of resolidification after transient stretch is dependent upon substrate stiffness in wild type but not zyxin$^{-/-}$ MEFs Across an order of magnitude of substrate stiffness, the degree of resolidification after stretch-induced fluidization in wild type MEFs ranged from 34% ± 5% on the softest substrate to 86% ± 17% on the stiffest substrate. Zyxin$^{-/-}$ MEFs showed the same degree of resolidification of approximately 60% across the tested range of substrate stiffness.

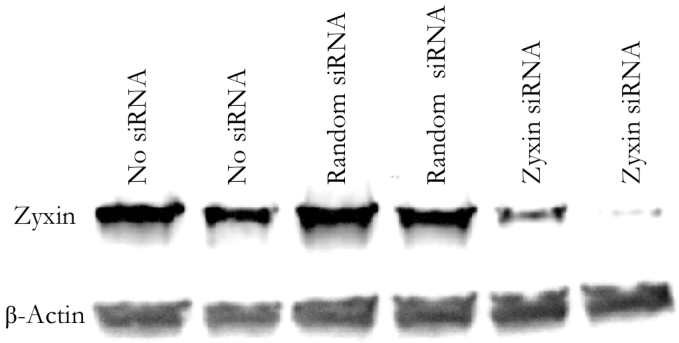

Figure 5.13: Knockdown of zyxin in primary human ASM cells results in greatly decreased protein expression. Western blot of zyxin and actin at 72 hours shows an 88% ± 10% decrease in protein expression.

5.2.6 In the human ASM cell after zyxin knockdown, baseline stiffness and responsiveness to histamine are unchanged, but the rate of cytoskeletal remodeling increases

In the adherent primary human ASM cell in culture I used siRNA to achieve 91% ± 2% reduction in zyxin mRNA at 48 hours (Figure 5.13), and noted 88% ± 10% reduced protein expression at 72 hours (Figure 5.14). Using nano-scale bead motions as a metric of remodeling rate, as above, I found that the zyxin-knockdown human ASM cells had a similarly increased rate of remodeling (Figure 5.15). When I treated these cells with the contractile agonist histamine [10 μM], cell stiffness [71] increased 26-28% in both zyxin-depleted and control cells with no significant differences between them (Figure 5.16). Baseline stiffness before contractile stimulation similarly showed no difference (Figure 5.17). In primary human ASM cells as in MEFs, zyxin influenced remodeling rates but not isometric cell stiffness.

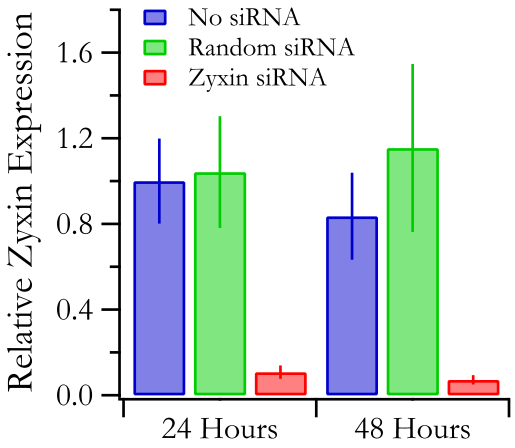

Figure 5.14: Knockdown of zyxin in primary human ASM cells results in greatly decreased zyxin mRNA. qPCR of zyxin at 48 hours post-transfection shows a 91% ± 2% reduction in zyxin mRNA.

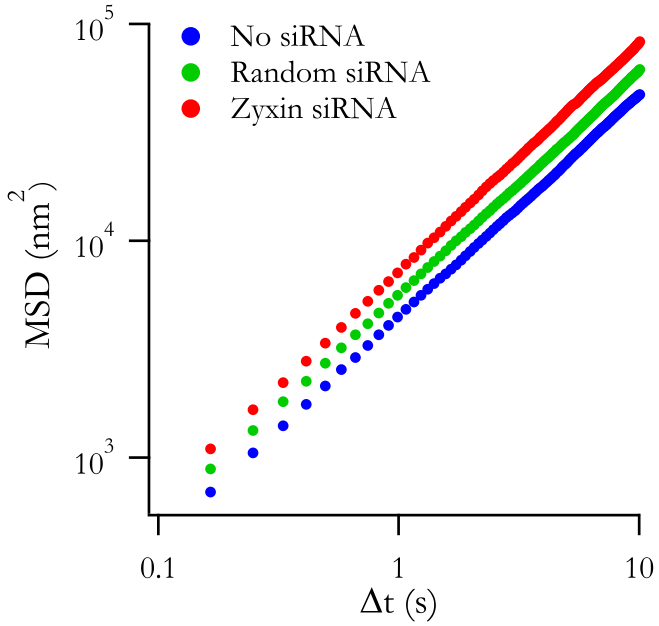

Figure 5.15: Knockdown of zyxin results in an increase in cytoskeletal remodeling rate in primary human ASM cells. The cytoskeletal remodeling rate is increased after zyxin knockdown as indicated by the upward shift of the MSD curve (n=1054 with no siRNA, 1019 with scrambled siRNA and 1095 with zyxin siRNA).

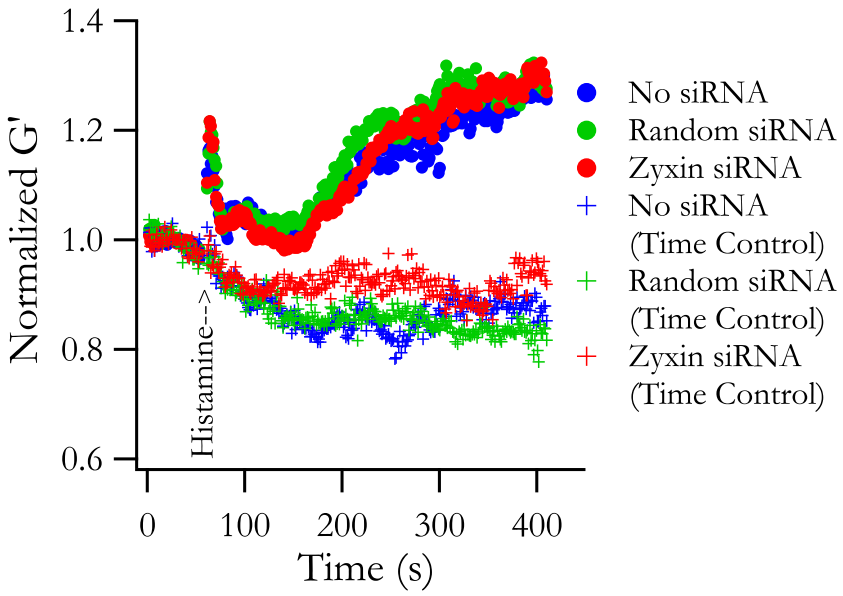

Figure 5.16: Zyxin does not affect the cell stiffening response to histamine in the primary human ASM cell. Primary human ASM cell stiffening responses to histamine (added at 60 seconds) are unchanged by zyxin knockdown (n=547 with no siRNA, 736 with scrambled siRNA and 761 with zyxin siRNA). Time controls with HASM media added at 60 seconds show no increase in stiffness (n=239 with no siRNA, 347 with scrambled siRNA and 356 with zyxin siRNA.

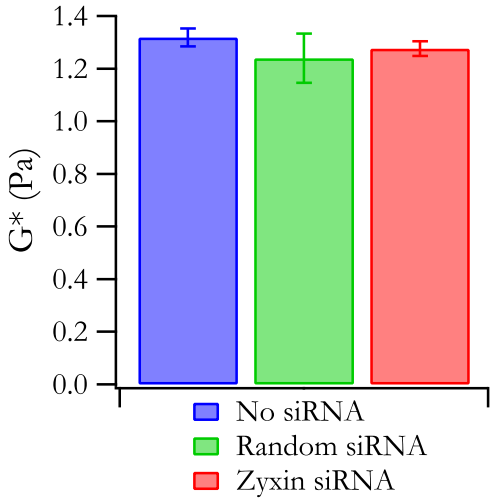

Figure 5.17: Zyxin does not affect isometric cell stiffness in the primary human ASM cell. Baseline isometric stiffness is similar in control and zyxin knockdown HASMs (n=547 with no siRNA, 736 with scrambled siRNA and 761 with zyxin siRNA).

5.2.7 In the isolated airway smooth muscle cell, resolidification –but not fluidization– is zyxin-dependent

In the ASM cell experiments above, conditions were purely static and isometric. In the lung, by contrast, the microenvironment is highly dynamic; the ASM cell strains by about 4% of its length with each tidal breath and as much as 10-25% of its length with each spontaneous DI or sigh [2, 24]. While studies of zyxin$^{-/-}$ mice have shown no obvious physiologic defect [78], the role of zyxin in actin remodeling [31], repair [32] and stabilization –as presented here– suggest that zyxin might play an important role in the response to stretch-induced cytoskeletal fluidization or subsequent resolidification [25]. Accordingly, working with Mark Smith at the Huntsman Cancer Institute, I examined the role of zyxin in maneuvers approximating those dynamic events. In isolated primary ASM cells from zyxin$^{-/-}$ versus wild type (wild type) mice, western

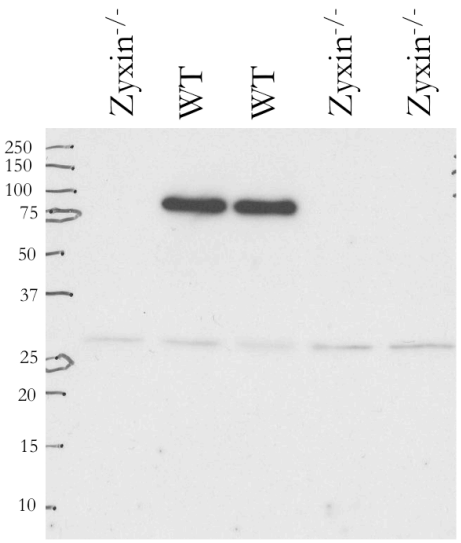

Figure 5.18: Western blotting confirms the knockout of zyxin in primary ASM cells from the zyxin$^{-/-}$ mouse.

blot confirmed the absence of zyxin (Figure 5.18). After culturing these ASM cells on gels of physiologic stiffness for 4 days without further passaging, we used traction microscopy [36] to measure contractile forces before and after a single transient isotropic stretch (Figure 5.19). In zyxin$^{-/-}$ versus wild type primary ASM cells, there was no difference in the net contractile moment prior to the stretch (Figure 5.20). Immediately following a single transient stretch (5-10% strain), wild type ASM cells fluidized rapidly and the net contractile moment [36] decreased dramatically, by 65% ± 6% (Figures 5.19 and 5.21). The contractile moment then gradually recovered completely over the next 300 seconds to 101% ± 7% of baseline (Figure 5.21). In response to imposed stretch, zyxin$^{-/-}$ cells showed a similar fluidization response (Figure 5.21). However, compared with wild type cells, zyxin$^{-/-}$ cells failed to resolidify to the same extent (Figure 5.21, $p<0.01$). While the fluidization response and the early part of the resolidification

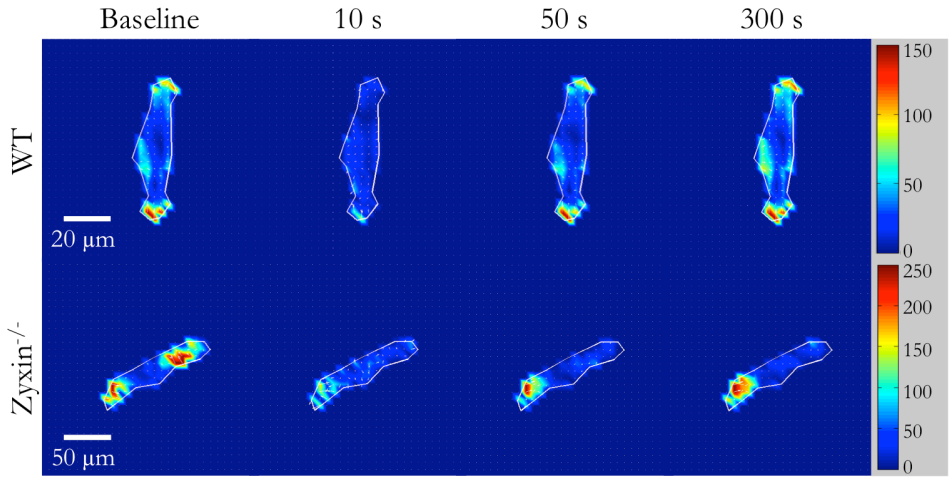

Figure 5.19: Zyxin mediates post-fluidization resolidification in primary ASM cells. Representative traction maps of wild type and zyxin$^{-/-}$ primary ASM cells at baseline and 10, 50 and 300 seconds after a single transient isotropic stretch.

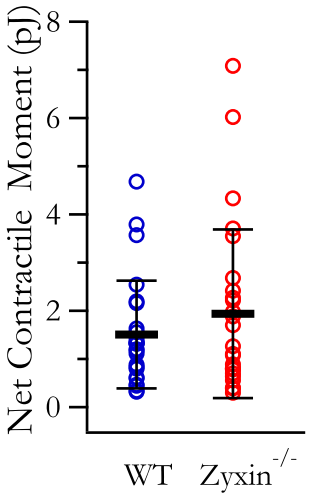

Figure 5.20: Baseline net contractile moment is similar in both zyxin$^{-/-}$ and wild type primary ASM cells. Circles are individual cellular net contractile moment, black bars are means, and error bars are standard deviation (n=25 wild type, n=26 zyxin$^{-/-}$; p=0.3).

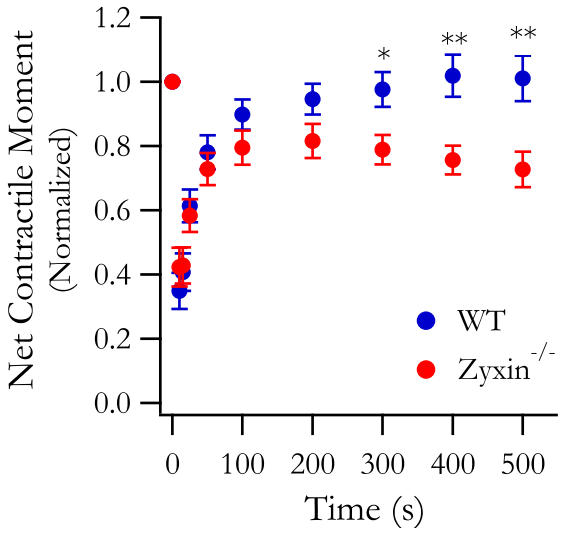

Figure 5.21: Resolidification following transient stretch is dependent on zyxin in primary ASM cells. Normalized changes in net contractile moment in wild type (n=25) and zyxin$^{-/-}$ (n=26) primary ASM cells following a transient 5-10% stretch at time = 0 seconds. By 5 minutes post-stretch it is clear that the zyxin$^{-/-}$ ASM cells are not recovering their contractile force to the same extent as the wild type ASM cells.

response tracked similarly, by 500 seconds this resolidification in zyxin$^{-/-}$ cells stalled and was only 73% ± 6% of baseline (Figure 5.21).

To simulate physiologic conditions even more closely, we stacked DIs at a frequency approximating that observed during spontaneous breathing [2]. Within the 300 seconds following each stretch, wild type ASM cells recovered to 81-97% of their baseline initial contractile force whereas zyxin$^{-/-}$ ASM cells recovered to only 63-70% (Figure 5.22, $p<0.05$). At the level of the primary ASM cell, both the rate and the extent of resolidification following transient stretch were clearly zyxin-dependent.

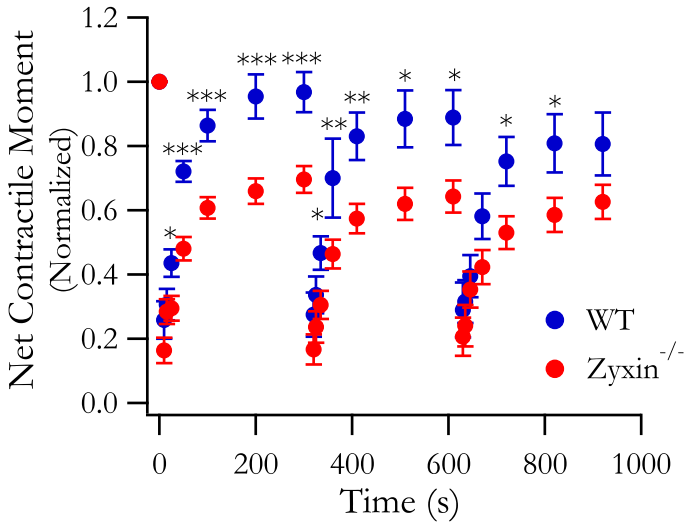

Figure 5.22: Zyxin-dependence of resolidification holds through a series of transient stretches. Normalized changes in net contractile moment in wild type (n=22) and zyxin$^{-/-}$ (n=23) primary ASM cells following a series of three transient 5-10% stretches at 0, 310 and 620 seconds. Incomplete resolidification of the zyxin$^{-/-}$ ASM cells persists across the three stretches.

5.2.8 Zyxin expression levels are similar in asthmatic and normal human ASM cells

Based on the results I found in murine and human ASM cells showing the role of zyxin in regulating dynamic cell mechanical properties, I sought to examine whether ASM from normal and asthmatic humans had similar levels of zyxin expression. Accordingly, I cultured ASM cells from three normal and three asthmatic donors and used western blotting to detect zyxin protein expression. While there was significant variation of zyxin expression in ASM cells between the different donors, there were no systematic differences in expression of zyxin between the normal and asthmatic human ASM cells (Figure 5.23A, B). Based on this, and the lack of evidence from genome-wide association studies on asthma for any SNPs on or near the zyxin gene locus [179–181], it seems likely that there are not systematic differences in zyxin expression between normals and

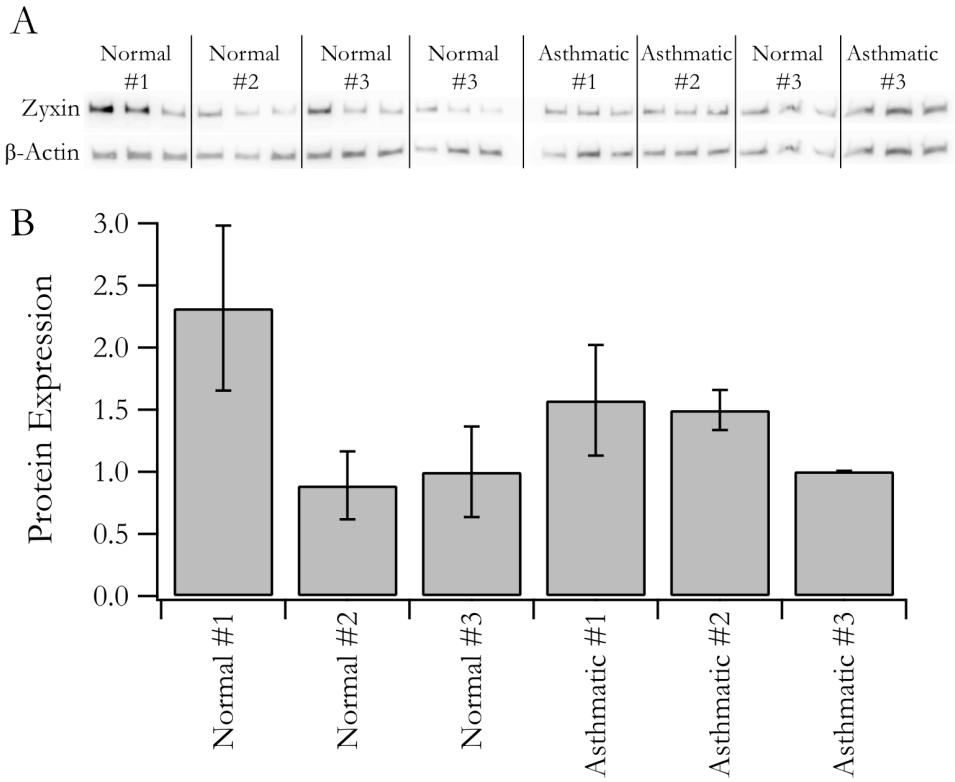

Figure 5.23: There is no systematic variation in zyxin protein expression between normal and asthmatic ASM. Western blot of zyxin and actin in primary human ASM cells from normal and asthmatic donors.

asthmatics.

5.3 Discussion

From these experiments, I concluded that zyxin plays only a small role in determining the mechanical nature of the isolated ASM or MEF cell under isometric conditions, but plays a substantial role in determining the mechanical nature of the isolated ASM or MEF cell under dynamic conditions. This is most apparent in the case of isotropic stretch of the isolated cell, where the absence of zyxin results in the failure of the ASM cell to resolidify

fully.

5.3.1 The contribution of zyxin to cytoskeletal remodeling rates

Recent work on ASM mechanics has established the hypothesis that the material properties of ASM are reminiscent of those of soft glassy material [23, 160, 182, 183]. The kinetics of actomyosin interactions cannot fully explain the dynamics of ASM [23, 183], but instead several properties of ASM can only be adequately explained by treating the ASM as a soft glassy material. One of these properties is the nature of the microscale rearrangement of the cytoskeleton in the ASM cell [35]. In the ASM cell, rearrangements of the cytoskeleton are subdiffusive over short time scales and superdiffusive over longer time scales; over short time scales the molecules are trapped or caged in the crowed intracellular space, while over longer time scales these molecules are actively rearranged in an ATP-dependent manner [35]. However, depending on the circumstances of the cell, these superdiffusive behaviors can exhibit faster or slower rates [5, 35], which are indicative of the cell being in a more fluid-like or more solid-like (jammed) state. Here I measured these cytoskeletal remodeling rates in the isolated MEF and the human ASM cell and found that cells lacking zyxin exhibit faster remodeling rates (Figures 5.3, 5.15). This indicates that zyxin decreases the fluidity of the cells, likely by stabilizing existing stress fibers and thereby inhibiting microscale cytoskeletal rearrangements [32]. Based on the previously discussed soft glassy material hypothesis of ASM and bronchospasm, this suggests that zyxin could, in fact, contribute to the frozen ASM state that precipitates bronchospasm [23].

5.3.2 Possible downstream effects of zyxin in response to stretch

As zyxin is known to localize to the nucleus and appears to influence protein transcription, these studies were limited to immediate responses following mechanical stimuli [184–188]. In this way, any influence of further downstream effects in response to stretch caused by the absence of zyxin acting to affect transcription are not at issue, as these changes occur on a timescale of several minutes to hours [189]. Instead, by focusing on the first few minutes following stretch, I was able to examine primarily the impact of zyxin on the actin cytoskeleton, to which it localizes rapidly following mechanical perturbation [32]. However, should zyxin be shown to instigate further changes in protein expression in response to stretch, it is possible that zyxin may play a role in the ASM cell's long term adaptation to its dynamic mechanical environment. This would then merit further study in the zyxin$^{-/-}$ mouse *in vivo*.

5.3.3 As airway smooth muscle resolidification after stretch is zyxin-dependent, there may be a role for zyxin in the integrated airway

This work demonstrates that zyxin only plays a small role in regulating cell mechanics under isometric conditions. While previous studies have shown that the absence of zyxin alters the distribution of traction forces within the isolated cell [32], the absence of zyxin has not been found to alter the baseline net contractile moment or isometric stiffness of the isolated cell. However, zyxin does contribute substantially to the control of cellular contractility under dynamic conditions, as resolidification of the ASM following stretch is dependent on zyxin. This presents the question as to whether these observations exist only in the isolated cell or whether they scale across levels. To answer this question requires an exploration of the role of zyxin in the integrated airway, which is the subject of the next chapter.

5.4 Materials and Methods

5.4.1 Cell lines and cell culture

Derivation and immortalization of embryonic fibroblasts from zyxin$^{-/-}$ mice was described previously [81]. These zyxin$^{-/-}$ fibroblasts were stably rescued with N-terminally tagged zyxin by viral infection followed by FACS sorting to select cells expressing GFP-tagged zyxin [78]. Primary airway smooth muscle cells were isolated from the tracheas of wild type and zyxin$^{-/-}$ mice as described previously [71, 190] and cultured on soft polyacrylamide gels without further passaging. Human ASM cells were obtained from R. Panettiere (University of Pennsylvania) and cultured in Ham's Nutrient Mixture F-12 medium supplemented with 10% fetal bovine serum (FBS), 100 U ml-1 penicillin, 100 μg ml-1 streptomycin, 200 μg ml-1 amphotericin B, 12 mM NaOH, 1.6 mM $CaCl_2$, 2 mM l-glutamine and 25 mM HEPES.

5.4.2 Live-cell imaging for protein dynamics studies and analysis

Imaging of MEFs was performed on PDMS gels coupled to 200 nm fluorescent beads and fibronectin. Images were collected every 10 seconds on an inverted Nikon Ti*e* (Nikon Instruments) equipped with either a Nikon 20X Plan Apo NA .75 dry, or a Nikon 40X Apo LWD NA 1.15 water immersion lens. This system also utilized an Andor spinning disk confocal (Andor Technology) and an Andor Ixon 885 EMCCD camera. Automation and image capture utilized Andor IQ software running on a Hewlett Packard workstation. [115]. Working with my collaborators, Mark Smith and Rama Krishnan, we adapted this system to apply mechanical stretches by designing a small annular punch indenter that fits on the condenser and could be lowered to the surface of the gel [25]. Stretch was applied using a condenser mounted annular indenter. The final positioning

and application of stretch were done by precise movement of the stage in Z with a Piezo stage insert. Following each experiment, an additional stretch was applied to verify the magnitude of stretch applied.

5.4.3 Optical magnetic twisting cytometry, bead tracking and analysis

Cells were plated for 24 hours to spread and form mature focal adhesions and then were serum starved for a further 24-48 hours. RGD-coated 5 μm iron microbeads were added and incubated for 20 minutes to allow the cells to form focal adhesions on the beads. The RGD-coated beads were magnetized and subjected to torque from a 30G magnetic field across a range of frequencies to collect measures of cellular stiffness. Lateral bead displacements were collected and used to calculate stiffness as previously described [124, 182]. To measure cytoskeletal remodeling, spontaneous bead motions were recorded. The overall rate of remodeling was quantified by the mean square displacement (MSD) over changes in time as described previously [35, 124].

5.4.4 RNA interference

HASM cells were plated overnight and then transfected with either a pool of 4 non-coding siRNAs (ON-TARGETplus Non-targeting Pool Catalogue #D-001810-10-05, Dharmacon, PA, USA) or 4 zyxin-targeted siRNAs (ON-TARGETplus SMARTpool - Human ZYX Catalogue #L-016734-00-0005, Dharmacon) at a concentration of 25 nM using a transfection reagent at a concentration of 0.2% by volume (DhamaFECT 1 siRNA Transfection Reagent Catalogue #T-2001-02, Dharmacon). Q-PCR assay of transfection efficiency was performed at 48 hours and protein knockdown confirmed by western blot at 72 hours. All experiments were performed at 72 hours to ensure adequate protein knockdown.

5.4.5 Single-cell traction force microscopy and stretch

Primary ASM (and MEF) cells were plated on 4 kPa polyacrylamide gels with 200 nm fluorescent beads and allowed to adhere and stabilize over 96 hours (48 hours for MEFs). As described previously in Butler et al. [36], the traction field was calculated from a displacement vector map of changes in bead positions using Fourier transform traction microscopy (FTTM). This field was used to calculate the net contractile moment of the cell. Stretch experiments were conducted as follows: baseline images of the cell and beads were recorded and then homogeneous isotropic stretch of between 5% and 10% strain was applied. Bead images were collected every 10 seconds for 10 minutes following stretch (or for 15 minutes in the case of the multiple stretch experiment), followed by a final reference image of the gel after the cell's removal by trypsin. Stretch was applied with an annular indenter as described in Krishnan et al. [25].

6

Zyxin in the Integrated Airway

In the previous chapter, I demonstrated at the level of the isolated airway smooth muscle (ASM) cell that zyxin does not alter isometric contractile force but does alter the pace and the extent of force recovery after a dynamic stretch that mimics a deep inspiration (DI). In this chapter, I will show at the level of the integrated airway in the murine precision cut lung slice (PCLS) that, similarly to findings at the cellular level, zyxin does not alter airway narrowing in response to methacholine in the absence of DIs. Similarly, I will also show that in response to DIs, the pace of the bronchodilation is

strongly dependent on zyxin. However, in contrast to results at the cellular level, the overall magnitude of that integrative response is not dependent on zyxin. These data thus reveal a remarkable incongruence between cellular and integrated airway responses to stretch that remains unexplained. Compensatory developmental events in the zyxin$^{-/-}$ airway cannot be ruled out.

6.1 Introduction

As previously discussed in Chapter 1, the most effective of all known bronchodilators is the stretch of airway smooth muscle (ASM) that results from a simple deep inspiration (DI) [1, 3, 3, 191, 191]. During an asthmatic attack, however, this important mechanism fails [10–12, 192]. Related hallmarks of asthma include not only increased contractile stimulus of ASM but also increased ASM mass [14, 15], increased airway wall thickness [13, 193], and decreased lung recoil [16, 194]. Acting alone or in concert, these factors cause ASM to stretch less with each breath [12, 17], which allows it to become stiffer still, until eventually a tipping point is reached beyond which the ASM can become so stiff that it is virtually frozen [20] and therefore no longer stretches with each breath [19, 27, 195]. ASM would thereafter remain refractory to the beneficial effects of deep inspirations, stuck in a shortened state until the contractile stimulus is removed or bronchodilator drugs take effect. This mechanistic framework provides a plausible biophysical basis to explain why the effects of deep breathing are so effective in the normal lung but become blunted in the asthmatic lung. However, the molecular mechanism responsible for this difference remains less clear.

The work described in Chapter 5 of this thesis indicated a candidate molecule for the dynamic regulation of ASM contractility: zyxin. Zyxin is a focal adhesion protein known

to be involved in the regulation of the actin cytoskeleton, primarily through the stabilization and repair of actin stress fibers [32]. Zyxin is also known to be mechanoresponsive, localizing to actin stress fibers in response to cylic uniaxial stretch or local mechanical stimulation [31, 32, 82]. In the previous chapter of this thesis, zyxin was shown to be necessary for the normal resolidification response to stretch; zyxin$^{-/-}$ ASM cells did not return to their baseline contractile force within the same timeframe as wild type ASM cells, but instead plateaued at around 75% of baseline force. Importantly, I also found that zyxin affected only cellular contractile force in response to stretch, and not baseline contractile force or responsiveness to contractile stimuli. I therefore proposed that zyxin works dynamically, but not statically, to stabilize the contractile apparatus in ASM.

Based on these interesting results, I sought to test whether these observations at the level of the isolated ASM cells translated to the level of the integrated airway. To address this issue, I chose the murine precision cut lung slice (PCLS) as a model system because it preserves the multicellular composition and much of the structural organization of the lung [37, 38, 142]. As described in the pioneering work of Sanderson, the PCLS also allows for direct microscopic observation of individual airway responses to various stimuli including contractile agonists and mechanical stretch [37, 38, 129, 142]. Using PCLS from wild type and zyxin$^{-/-}$ mice, I measured contractile responses to methacholine and subsequent airway dilation during a series of imposed stretches. I found that while the magnitude of airway dilation with cyclic stretch was zyxin-independent, the dynamics of airway dilation were strongly zyxin-dependent, with airways from zyxin$^{-/-}$ mice dilating more rapidly than airways from wild type mice.

6.2 Results

6.2.1 Using PCLS to probe airway responses to stretch

To compare responses at the level of the SF and the isolated cell, as described in Chapter 5, to responses at the level of the integrated murine airway, we used the precision cut lung slices (PCLS) [8, 37] obtained from wild type and zyxin$^{-/-}$ mice. In brief, the freshly excised lung is filled with agarose, cooled, allowed to gel, and then sliced to a uniform thickness of 250 μm. When re-warmed and placed upon a polyacrylamide gel, small airways embedded within the lung parenchyma are readily visualized, remain highly contractile in response to agonist, and can be stretched in a simple manner (Figure 6.1) so as to simulate the tidal action of breathing and DIs [8, 37]. Another important advantage of the PCLS is as follows. In the isolated cell, as described above, the extent and timing of cell stretch is imposed and controlled in a manner that is insensitive to the mechanical properties of the ASM cell itself, and, as a result, the positive mechanical feedbacks described above are rendered inoperative. But in the PCLS the extent and timing of lung parenchymal expansion is imposed and controlled in a manner intended to mimic a spontaneous DI *in vivo*. Much as conditions *in vivo*, were the ASM relaxed and limp, airway strain would follow closely that of surrounding lung parenchyma, but were the ASM contracted and stiff, as the surrounding lung parenchyma expands the airway might become so stiff as to strain hardly at all. Consequently, the resultant stretch of the embedded and integrated airway smooth muscle cell is set in large part by the airway smooth muscle itself, its stiffness, and the dynamic load against which that muscle is contracting. When these factors dictate that ASM become fluidized and soft [4, 5], it follows that stretch induces stretch. In this preparation –as in the living, breathing lung– positive mechanical feedbacks are therefore enabled. In this study, airways in PCLS were

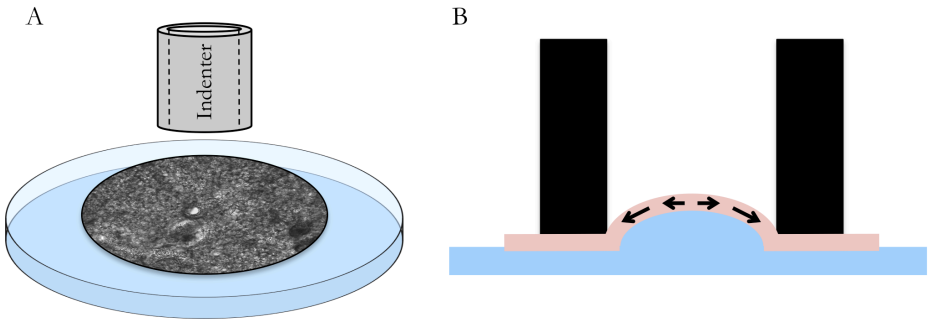

Figure 6.1: Applying stretch to the murine PCLS. (A) Schematic of the annular indenter used to stretch PCLS (not to scale). (B) Cut-through view of the indenter causing the confined gel to bulge and stretch the PCLS (not to scale). Arrows indicate stretch of PCLS.

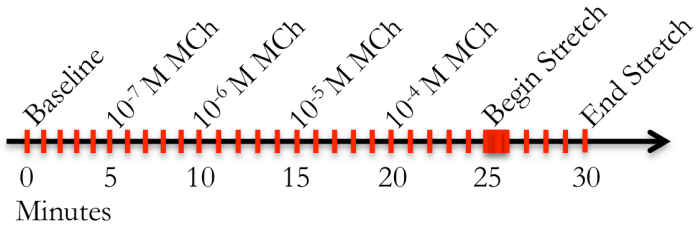

Figure 6.2: Experimental design to contract and stretch airways in PCLS. Experimental timeline of MCh dose-response and stretch, red bars indicate image acquisition.

first contracted using increasing doses of methacholine. Once airways were maximally contracted, cyclic isometric stretch was applied to a subset of the airways and dilation responses were recorded (Figure 6.2).

6.2.2 Airway contractile responses to methacholine are zyxin-independent

In the absence of parenchymal strains, as methacholine concentration increased, airway lumenal area decreased in both wild type and zyxin$^{-/-}$ airways (Figure 6.3). In line with previously reported studies in C57BL/6 animals [164], wild type airways showed a mean decrease in airway lumenal area of 37% ± 3% with 10^{-4} M MCh, which was not

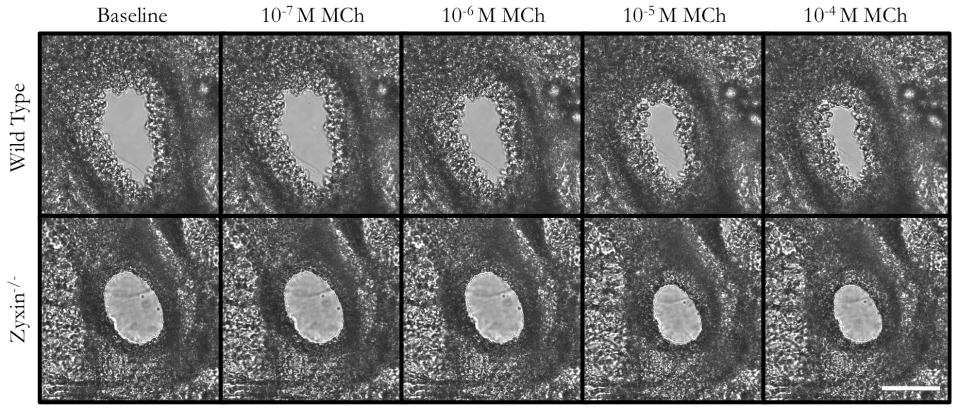

Figure 6.3: MCh responses are similar in both wild type and zyxin$^{-/-}$ airways. Representative airways from wild type and zyxin$^{-/-}$ animals, scale bar is 200 µm.

significantly different from the decrease in lumenal area observed in zyxin$^{-/-}$ airways (Figure 6.4, p=0.12). This finding is in line with my finding in the previous chapter that ASM responses to histamine are unchanged with zyxin siRNA knockdown. Previous work has shown that the responsiveness of murine airways is size-dependent [39, 132]. While only small airways were used in this study, I examined the data for a possible effect of airway size, but did not find one. Controlling for the size of the airways did not affect the finding that responses to MCh are zyxin-independent (Figure 6.5).

6.2.3 Fluctuation-induced relengthening in the constricted airway in the murine PCLS

In the presence of physiological parenchymal strains, the caliber of a constricted airway increases and smooth muscle relengthens; this phenomenon is called fluctuation-induced relengthening (FIR) [8, 196]. To measure FIR in the PCLS we used the method of Krishnan et al. [25] and Lavoie et al. [8] to apply cyclic isotropic

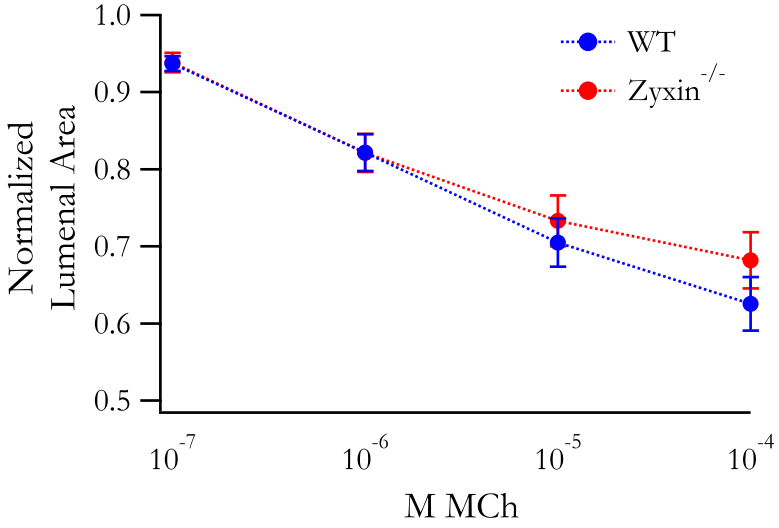

Figure 6.4: MCh responses are not significantly different between wild type and zyxin$^{-/-}$ airways. Normalized changes in lumenal area of airways from wild type (n=114) and zyxin$^{-/-}$ (n=75) animals in response to increasing doses of methacholine.

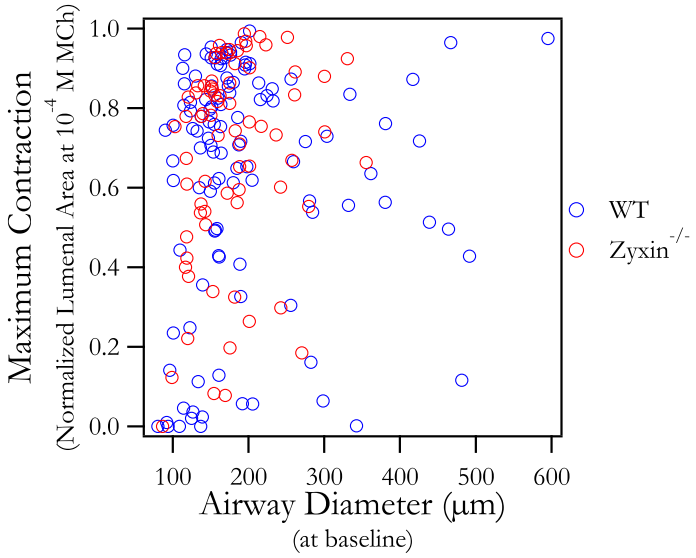

Figure 6.5: No strong relationship was observed between airway size and MCh responsiveness. Airways ranging 500 μm in diameter show similar distributions of maximum contraction. No differences were observed between wild type (n=114) and zyxin$^{-/-}$ (n=75), other than a somewhat higher number of very large airways in the wild type group. However, both wild type and zyxin$^{-/-}$ airways had similar median and IQR of airway size.

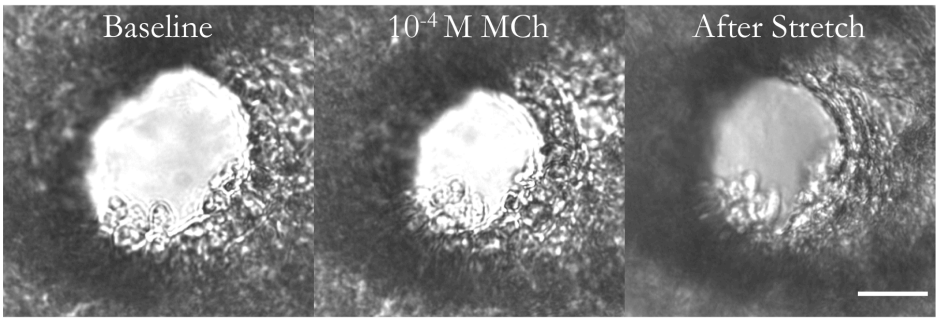

Figure 6.6: Airways in murine PCLS dilate with cyclic isometric stretch of the surrounding parenchyma. Scale bar is 100 μm.

parenchymal strains targeting 10% linear amplitude once every 6 seconds for 5 minutes (Figures 6.1, 6.2, 6.6). This applied parenchymal strain was transmitted effectively to airways on average, although, as expected from Lavoie et al [8], this degree of strain was highly variable from airway to airway (Figure 6.7). In accordance with the findings of Lavoie et al. [8], we also found a positive trend but not a significant relationship between the local amplitude of airway tidal strain and the local FIR in the same airway in wild type, but not in zyxin$^{-/-}$, although this could be an effect of small sample size (Figure 6.8). We found no relationship between the degree of initial constriction of the airway and the subsequent magnitude of FIR in that same airway, however (Figure 6.9).

6.2.4 In the integrated murine airway, the rate of airway dilation in response to a DI --but not the final airway caliber-- is zyxin-dependent

In response to these cyclic strains, reversal of bronchospasm by DIs varied greatly from airway to airway, as expected based on previous studies [39, 164], with an average

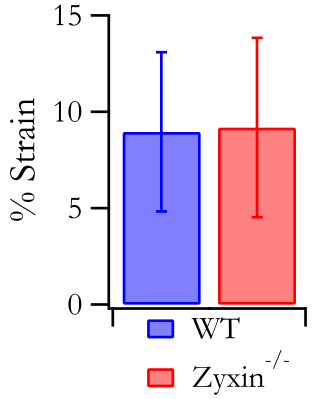

Figure 6.7: Applied strain to the lung parenchyma was transferred effectively to the airways. Mean strain transferred to airways with stretch indenter, bars are SEM (n=20 wild type, 14 zyxin$^{-/-}$ airways).

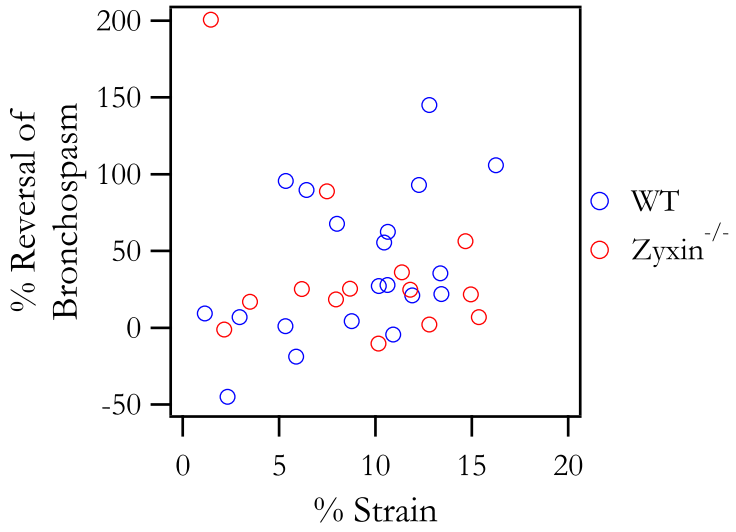

Figure 6.8: Reversal of bronchospasm versus strain transferred to the airway.

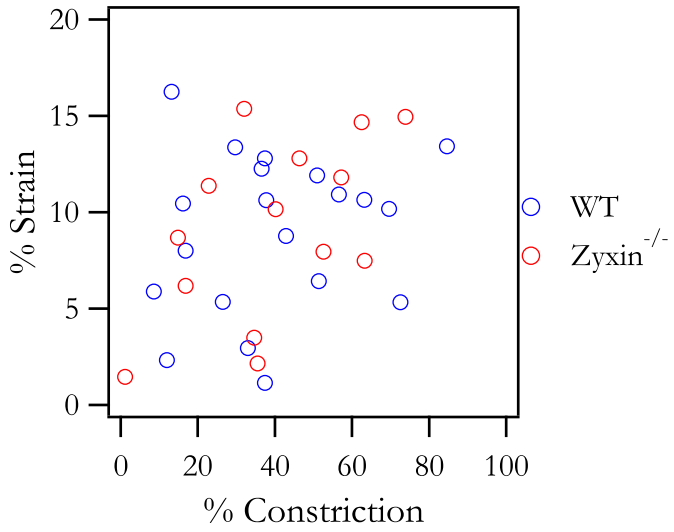

Figure 6.9: Strain transferred to the airway versus airway constriction.

reversal of lumenal area of 40% ± 11% in wild type airways (Figures 6.6, 6.10). Surprisingly, the magnitude of this reversal in the zyxin$^{-/-}$ airway was 37% ± 14% and was not different than that observed in wild type (Figure 6.10, p=0.3). However, zyxin$^{-/-}$ airways achieved this relengthening much more rapidly. For example, in both wild type and zyxin$^{-/-}$ slices many airways dilated to more than 75% of their final steady state airway with the first stretch, but a larger fraction of these were from zyxin$^{-/-}$ airways (Figure 6.11). Indeed, 79% of the zyxin$^{-/-}$ airways dilated with the first stretch to 75% of the final steady state area, whereas only 45% of wild type airways did so (Figure 6.11). Over the course of many stretches, the strong response to the first stretch together with other innate heterogeneities caused these data to be distributed in time in a strongly non-exponential, non-Gaussian, and noisy fashion (Figures 6.12, 6.13). This is not entirely unexpected, as previous work has shown substantial heterogeneities in airway

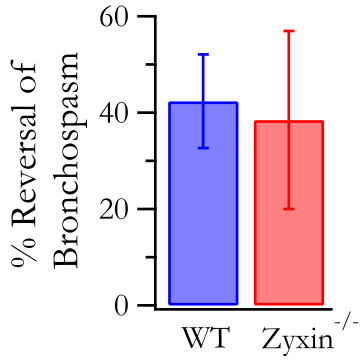

Figure 6.10: Reversal of bronchospasm with cyclic stretch was similar in wild type and zyxin$^{-/-}$ airways. No significant differences in the magnitude of reversal of bronchospasm were observed between airways from wild type (n=20) and zyxin$^{-/-}$ (n=14) animals.

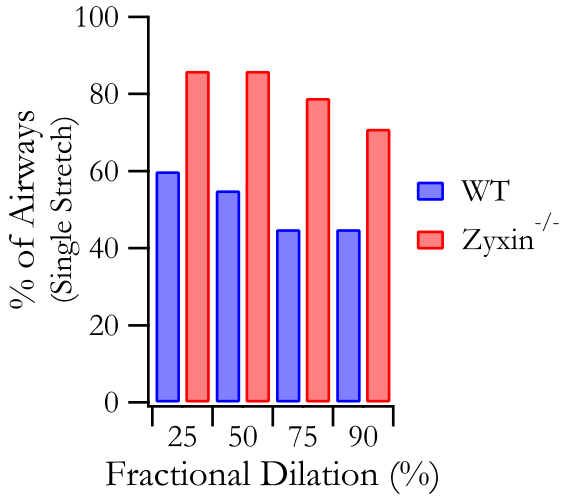

Figure 6.11: Percentage of airways reaching a given fraction of their ultimate steady state dilation with a single stretch. A higher percentage of airways from zyxin$^{-/-}$ animals (as compared to airways from wild type animals) reach 25, 50, 75, and 90% of the final steady state dilation in a single stretch.

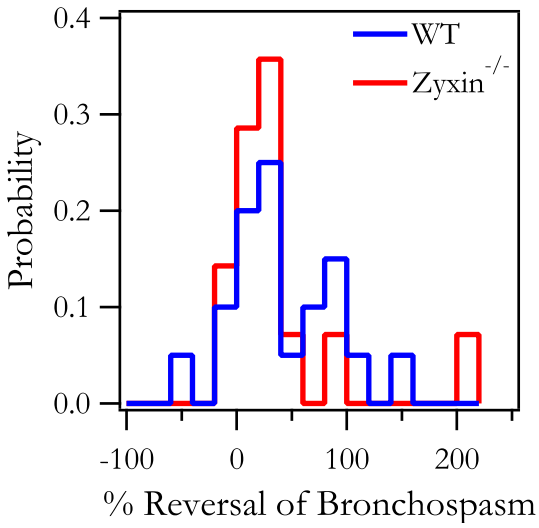

Figure 6.12: Histogram of reversal of bronchospasm observed in wild type and zyxin$^{-/-}$ airways.
Y-axis indicates probability, 14 bins of 20% width.

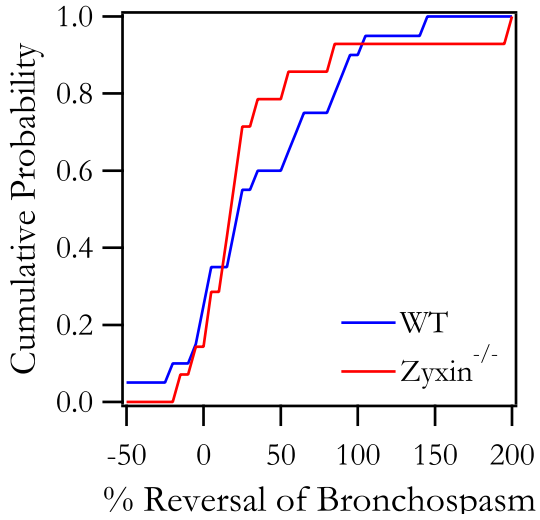

Figure 6.13: Cumulative probability function of percent reversal of bronchospasm in wild type and zyxin$^{-/-}$ airways.

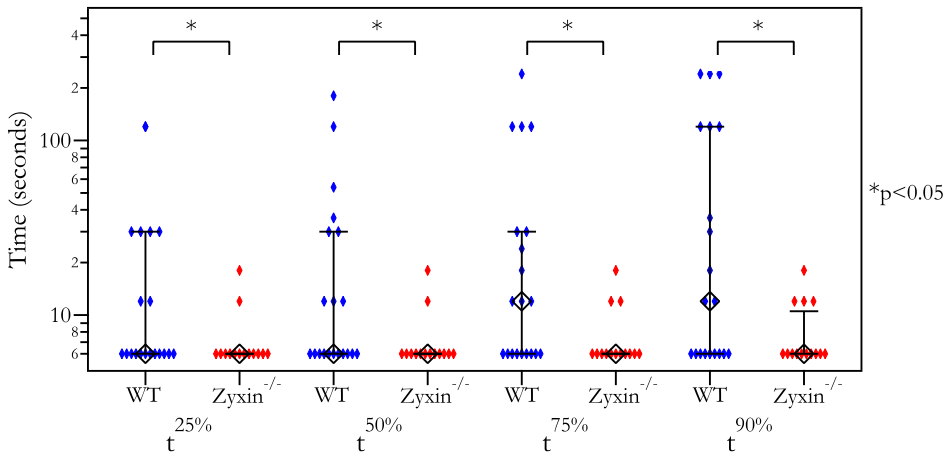

Figure 6.14: Airways in zyxin$^{-/-}$ PCLS exhibit more rapid dilation following stretch. Times to achieve 25%, 50%, 75%, and 90% of final steady state dilation (black diamonds are median values, whiskers are IQR). Airways from zyxin$^{-/-}$ (n=14) animals have significantly lower time constants to reach each of these fractions than airways from wild type (n=20) animals (*p<0.05).

responses to contractile agonist stimulation and stretch [8, 93]. Nonetheless, the Mann-Whitney rank sum test showed that the median time required for each airway to dilate to 90% of its final steady state area ($t^{90\%}$) was smaller by half in zyxin$^{-/-}$ versus wild type airways (Figure 6.14; $p<0.05$), and that times were also significantly shorter in zyxin$^{-/-}$ airways to reach $t^{25\%}$, $t^{50\%}$, and $t^{75\%}$ (Figure 6.14; $p<0.05$). At the level of the intact airway embedded within the PCLS, zyxin did not change the extent of airway lumen recovery following a sequence of DIs but did substantially slow the rate of that recovery.

6.3 Discussion

6.3.1 Mechanical stretch, deep inspirations and zyxin

In Chapter 5, I showed that resolidification of the ASM cell following stretch is dependent on zyxin. However, I found the role of zyxin at the level of the integrated airway to be paradoxical, with no difference observed in the magnitude of reversal of bronchospasm. I did, however, observe that the dynamics of this reversal were strongly zyxin-dependent, with airways from zyxin$^{-/-}$ mice dilating more rapidly with cyclic stretch. It remains unclear what accounts for these observed differences in response to stretch between isolated ASM cells and ASM in the intact airway, although it is possible that compensatory changes occur in the airway during development in the zyxin$^{-/-}$ mouse.

6.3.2 Do compensatory events occur during development in the zyxin$^{-/-}$ airway?

The preceding work reveals a paradox: in the isolated ASM cell, resolidification after stretch was strongly dependent on zyxin, while in the integrated airway, the magnitude of airway dilation with stretch was similar in both wild type and zyxin$^{-/-}$ airways. One hypothesis to explain this observation could be that the zyxin$^{-/-}$ airway experiences compensatory remodeling during the animals development. Previous work characterizing the zyxin$^{-/-}$ mouse examined primarily development of the nervous system and skin architecture, where no differences were observed [33]. A detailed study of airway structure has never been done in these animals.

However, it is quite possible that compensatory events occur during the development of

the lung based on the evidence presented here that zyxin is a mechanoresponsive regulator of dynamic contractility. Earlier work has shown that in many mammalian species, including mice, mechanical stretch is implicated in normal lung development both pre- and post-natally [197–201]. Several studies have shown that mechanical stretch of the developing lung stimulates growth [197, 199, 201]. Additionally, previous work looking at bronchial myogenesis in both mouse and human cells demonstrated that stretch induces alternative splicing of the serum response factor protein, which is know to trigger muscle-specific gene expression [200]. As zyxin is known to be involved in transducing external mechanical stimuli to the cell [32, 78–80, 82, 202–204], I suggest the hypothesis that the absence of zyxin during development alters these cues in the developing airway, resulting in structural differences in the zyxin$^{-/-}$ airway. If true, then compensatory changes in the extracellular matrix composition of the airway basement membrane or lung parenchyma, or in the size, number or organization of the ASM cells, might resolve the paradox.

6.3.3 A phenotypic role for zyxin in the murine airway

At the level of the stress fiber and the isolated cell, both the pace and the overall magnitude of the response were dependent upon zyxin. I show here that at the level of the integrated PCLS the pace but not the overall magnitude of the dilation response is dependent upon zyxin. Despite the paradoxical findings in the isolated cell versus the integrated airway, this work nonetheless shows for the first time a phenotypic role for zyxin in the murine airway. These findings demonstrate a clear role for zyxin in ASM responses to dynamic mechanical strains as occur during spontaneous deep inspiration, indicating that in the dynamic mechanical environment characteristic of the lung, zyxin is a potential target to drive down contractility in ASM and attenuate bronchospasm.

6.4 Materials and Methods

6.4.1 Animals

Lungs were obtained from four 16-week-old wild type and three 16-week-old zyxin$^{-/-}$ C57BL/6 mice. All mice used in this study were housed in a specific-pathogen-free barrier facility and cared for, handled, and euthanized following guidelines approved by the Institutional Animal Care and Use Committee of the University of Utah.

6.4.2 Precision cut lung slice (PCLS) preparation and culture

PCLS were prepared as described previously [37, 38]. Following tracheotomy, the mouse lungs were insufflated with 1% low-melting point agarose in HBSS. The insufflated lungs were then placed in cold HBSS (Corning Life Sciences, MA, USA). After the agarose had formed a gel, the two largest lobes were separated and then sectioned into 250 μm thick slices using a Precisionary Instruments VF-300 tissue slicer. Lung slices were cultured in 1:1 DMEM/F-12 supplemented with penicillin, streptomycin, kanamycin, and amphotericin B (Invitrogen, MA, USA). Media was changed once an hour for the first 4 hours. The PCLS were then frozen in the culture media supplemented with 10% DMSO as described in Rosner et al. [39] and shipped on dry ice from Utah to Boston where they were rapidly thawed and cultured in fresh culture media for at least 2 hours before experiments were performed.

6.4.3 Methacholine dose-response and stretch of airways in murine PCLS

Using a ring of nylon mesh embedded in a PDMS ring, each PCLS was secured in place on a 4 kPa polyacrylamide gel in a standard 6 well culture plate. The multi-well plate was

mounted on a computer controlled translation stage and imaged using an inverted microscope (Leica Microsystems, DMI6000B, with adaptive focus, motorized stage, and stage incubator, IL, USA). Airways with an intact smooth muscle layer and a diameter between 100 and 400 μm were selected for study. These airways were treated with 10^{-7} M, 10^{-6} M, 10^{-5} M, and 10^{-4} M methacholine (MCh, Sigma Aldrich, St. Louis, MO). A subset of the airways was used to test responses to DI. The airways used in the stretch experiments had to meet three conditions: first, the airways had to have visibly contracted in response to MCh treatment (by approximately 80%); second, the airways had to be far enough away from the edge of the lung slice that all of the annular indenter would be in contact with the tissue when centered around the airway of interest; and lastly, only one airway from each slice could be used as the stretching of one airway would confound any results from the subsequent stretch of another airway in the same slice. Each of these airways was stretched for 5 minutes with an annular indenter as described in Lavoie et al. [8]. Briefly, an annular indenter was lowered until it compressed the gel on which the PCLS lies, causing the confined gel to bulge and apply a radial stretch to the lung tissue within the indenter (Figure 6.1). Each airway was imaged every minute during the dose-response and stretch, except the first minute of stretch where the airways were imaged every second (Figure 6.2). From the acquired images, we quantified airway lumenal area (Image J, NIH), and normalized its magnitude to the pre-treatment baseline value.

6.4.4 Statistics for airway responses

Where not otherwise noted, standard two-sided t-tests were used. The normalized changes in lumenal area in airways in PCLS from wild type and zyxin$^{-/-}$ animals were compared using the Mann-Whitney-Wilcoxon rank-sum (MWW) test. We chose the

MWW test instead of the more common t-test for this comparison because distributions of airway lumenal area do not follow a normal distribution [134]. Differences with $p<0.05$ were considered significant.

7

Conclusions and Implications

7.1 The Role of Zyxin in Airway Smooth Muscle Dynamics

Here we examined the role of zyxin during dynamic loading and across multiple scales –stress fiber, isolated cell, and precision cut lung slice. The multi-scale approach is important, because it is only when comparing across scales that certain consistencies, as well as informative inconsistencies, become evident. At the level of the stress fiber within the isometric zyxin$^{-/-}$ versus GFP-zyxin-rescued MEF, there were differences in the rate of remodeling (Figure 5.3) and in the rate of spontaneous stress fiber ruptures [32]

but no appreciable differences in static cytoskeletal structure. Peak tractions under particular focal adhesions depend upon zyxin [32], but the integrated whole-cell net contractile moment under isometric conditions was not dependent on zyxin (Figures 5.5, 5.20). At the integrative level, similarly, the minimum airway caliber after exposure to contractile agonist but before exposure to DIs was not dependent on zyxin (Figure 6.4). At each of these levels results were mutually consistent in the absence of DIs; in the measures reported here zyxin played no role in the absence of a DI except in the case of the rate of cytoskeletal remodeling.

In the presence of DIs, still other consistencies across scale became readily apparent. At the cellular level the extent of fluidization of the ASM by a DI did not depend upon zyxin (Figure 5.21) and, similarly, at the tissue level the extent of airway dilation, and associated fluctuation-induced ASM relengthening, did not depend upon zyxin (Figure 6.10). Moreover, at both these levels, it was only the remodeling dynamics (Figures 5.3, 5.15) and the rate of recovery of contractile force, and not the isometric mechanical properties, that were zyxin dependent (Figures 5.21, 5.22, 6.14). The data presented here show that at the level of the stress fiber, the isolated cell, and the integrated airway, zyxin stabilizes the contractile response during resolidification (Figure 7.1). These results extend previous studies showing that zyxin exhibits rapid, force dependent recruitment to actin structures, where it is essential for normal reinforcement, remodeling [31] and repair [32] of cellular actin structure (Figure 7.2).

Consistencies across scale notwithstanding, certain inconsistencies across scale were striking. In particular, at the level of the isolated cell the absence of zyxin prevented full

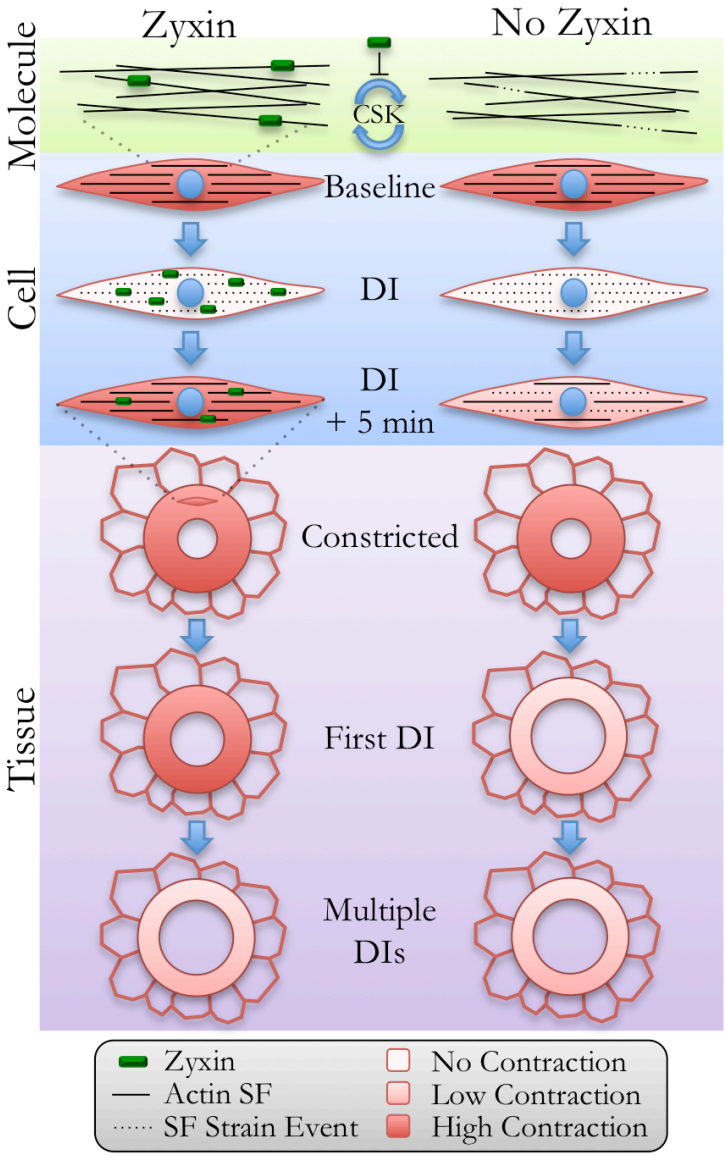

Figure 7.1: Across multiple length scales, zyxin dynamically stabilizes the contractile apparatus. In response to a transient stretch mimicking the effect of a deep inspiration (DI), contracted airway smooth muscle (ASM) fluidizes rapidly and then resolidifies slowly. Zyxin acts dynamically during the resolidification response to stabilize the contractile apparatus and its actin scaffolding at the levels of the stress fiber, the isolated cell, and the integrated airway. At the molecular level (top panels), zyxin acts to stabilize actin stress fibers (SFs), thereby inhibiting cytoskeletal (CSK) remodeling. At the cellular level (middle panels), net contractile force under isometric conditions and the rapid fluidization in response to a DI are independent of the cytoskeletal protein zyxin, whereas the slow resolidification response is dependent upon zyxin. At the integrated tissue level (bottom panels), zyxin similarly stabilizes the contractile apparatus in ASM, slowing airway dilation from DI. Across these multiple scales of length, zyxin acts dynamically to promote cytoskeletal stabilization and resolidification.

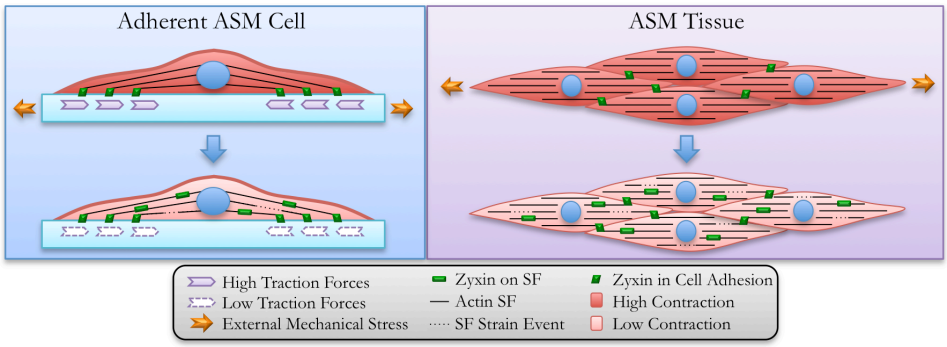

Figure 7.2: Zyxin acts dynamically during the resolidification response to stabilize the contractile apparatus and its actin scaffolding. At the cellular level (left panel), under isometric conditions zyxin is largely localized to cell adhesions. In response to an external mechanical stress, the cell fluidizes and zyxin localizes to sites of SF strain to facilitate their repair, stabilizing the contractile apparatus to again support high traction force. At the integrated tissue level (right panel), in response to mechanical stress, zyxin similarly stabilizes the contractile apparatus in ASM, slowing airway dilation from DI.

recovery of contractile forces in response to a DI (Figures 5.21, 5.22), whereas at the level of the integrated airway the extent of reversal of airway narrowing by DIs did not depend upon zyxin (Figure 6.4). Moreover, in the absence of zyxin the rate of airway dilation was substantially faster (Figure 6.14). Slower recovery in the presence of zyxin is consistent with the role of zyxin in stabilizing the contractile apparatus, however. Nonetheless, in the integrated airway zyxin influenced the rate of recovery but did not influence the extent of that recovery.

Taken together, these findings reveal important gaps of understanding. As regards the prompt fluidization response, the question remains as to whether fluidization is driven primarily by a passive breaking of acto-myosin bonds as well as other weak molecular bonds [5, 25] or rather is driven primarily by active molecular disassembly through the agency of actin-severing proteins. As regards the slow resolidification response, both the striking inconsistencies across scales in the extent of recovery (Figures 5.21, 5.22, 6.10) and in the rate of that recovery (Figures 5.21, 5.22, 6.14) I take to be important clues. It is

not at all surprising that other cytoskeletal proteins besides zyxin might contribute to the resolidification response, play a compensatory role, and thus account for these inconsistencies. However, the specific molecular players, their roles, and their interactions within the ASM cell are unknown and might include other LIM-domain proteins, such as paxillin [115, 205], or others. Besides such specific compensatory molecular events transpiring within the ASM cell, might other compensatory events transpire without? For example, both prenatally and postnatally the developing airway is subjected to an unending sequence of large tidal stretches [206]. In response, might the airway of the zyxin$^{-/-}$ mouse undergo compensatory developmental changes in muscle mass, connective tissue structure, or tethering forces exerted between the airway and surrounding lung parenchyma? Both within the ASM cell and without, our molecular picture of airway dynamics remains at best fragmentary, and thus suggest that still other unidentified events at a variety of levels might come into play. These possibilities comprise interesting new questions.

I establish here a multi-scale approach that reveals a plausible phenotypic role for zyxin. At the levels of the stress fiber, the isolated cell, and the integrated airway, these findings support the idea that zyxin plays little or no role in the static isometric mechanical properties of ASM but in response to physiological stretch zyxin acts dynamically to stabilize the contractile apparatus and its scaffolding and promote resolidification. More than just the motor of contraction, ASM is thus viewed in the broader context of a self-healing active material wherein resolidification and its molecular determinants are revealed as being important factors in the biology of bronchospasm.

7.2 The Value of a Deeper Understanding of the Cytoskeletal Changes in Airway Smooth Muscle that Promote Bronchospasm

With these findings showing that zyxin regulates the dynamic contractility of ASM, our understanding of the cytoskeletal changes that underlie bronchospasm is deepened. This understanding could prove useful in the treatment of asthma. Existing asthma treatments fall in three main categories: β2 adrenergic receptor (β2AR) agonists, corticosteroids and leukotriene antagonists [207, 208]. In patients with infrequent and mild asthma symptoms, short-acting β2AR agonists, which are highly efficacious in reversing acute bronchospasm, can be used alone to manage the disease [207, 208]. However, if patients experience more severe and frequent symptoms, long-term medications must be used to prevent symptoms [207, 208]. However, long-term treatments are not equally efficacious for all patients. Long-term use of β2AR agonists often leads to a decline in their effectiveness due to β2AR desensitization [209, 210]. In rare cases, this can even render short-acting β2AR agonists less effective [211]. In the case of corticosteroids, 5-10% of patients are refractory to this treatment [47, 48]). Leukotriene antagonists, while effective for many patients and generally perceived to be safe, do not generally provide as good control of asthma symptoms as corticosteroids, and are often a second choice treatment [207, 208, 212, 213]. Long-term treatments to control bronchoconstriction are especially important in light of recent research showing that bronchoconstriction in the absence of airway inflammation can induce airway remodeling in asthmatics [214, 215]. Accordingly, there exists a need for novel asthma treatments.

One potential target for the treatment of asthma is the ASM cell contractile apparatus. Existing drugs that target the cell contractile apparatus (such as myosin inhibitors and

actin disruptors) are too non-specific to safely or effectively use in asthma treatment, and so current asthma treatments do not yet directly target the cytoskeleton. However, if zyxin, as indicated in this thesis, or other actin regulatory proteins promote the frozen cytoskeletal state associated with bronchospasm, than they could possibly be safely inhibited in order to promote a more fluid cytoskeleton and less contractile ASM.

7.3 Implications for Future Work

Several directions for future work emerged from this thesis; I will discuss here some of the most promising future directions. The first possible line of work indicated by this thesis comprises an exploration of the role of zyxin in the mouse lung *in vivo*. This could include both a study of the differences in lung function and airway responsiveness in the live animal, as well as a comparative exploration of airway structure in wild type and zyxin$^{-/-}$ mice. Based on the intriguing findings in this thesis from the *ex vivo* airway in PCLS, further study of airway resistance and airway hyperresponsiveness, as well as responses to DI are indicated *in vivo*. The finding that zyxin slows rates of airway dilation in the *ex vivo* airway could be followed up in the zyxin$^{-/-}$ mouse *in vivo*, and possibly elaborated upon through the use of an AHR mouse model. Further, as mentioned in the previous chapter, it appears plausible that key variables in airway structure such as ASM mass and basement membrane thickness could be different between the wild type and zyxin$^{-/-}$ mouse, owing to zyxin's indicated role in response to mechanical stretch and the known mechanical strains imposed during lung development *in vivo* [206].

A second possible line of inquiry stemming from this work would be an examination of other mechano-responsive actin regulatory proteins in the cell mechanical response to stretch. Of these other potential regulators, paxillin stands outs as being of particular

interest. Paxillin, like zyxin, is a LIM protein; it has four LIM domains near the C-terminus of the protein [216]. These LIM domains target paxillin primarily to focal adhesions [217], although recent work has indicated that, like zyxin, paxillin also localizes to actin SFs [115]. Of particular interest, paxillin has been shown to localize to sites of SF strain, where it stabilizes SFs independently of zyxin [115, 205]. It remains unclear whether zyxin and paxillin-directed SF repair are parallel mechanisms, with each serving as a backup for the other, or whether they are synergistic, working together via different mechanisms to promote SF stabilization. However, based on this evidence, paxillin would be a particularly interesting candidate for further study in ASM and bronchospasm. Other LIM proteins may also be good candidates for further study, including the LIM kinases (LIMK1 and LIMK2), which are known to regulate actin dynamics via the phosphorylation and inactivation of ADF/cofillin [114, 218]. Of course, other actin regulatory proteins could be involved in the cell mechanical response as well, including α-actinin and VASP, which are known to be involved in zyxin-mediated stress fiber repair, or others [32].

Lastly, as discussed at length in Chapter 2 of this thesis, another possible direction for future work would consist of a study of the molecular cause(s) of heterogeneity in cell mechanics. To summarize here, it has been observed that cell mechanical measures, including cellular contractility and stiffness, are log normally distributed [25, 83], however, the causes of this apparent heterogeneity remain unclear. While some hypotheses have been proposed, including focal adhesion size, cell spread area, and aspect ratio [94–97], these are not able to fully account for the large variability observed in mechanical measures of the cell. I propose that looking to the field of single cell analysis could bring new insights to this problem. Single cell analysis has shown that gene

expression in single cell is also highly heterogeneous [101–104] and often varies according to a log normal distribution [103–107]. Accordingly, scientists in this field have developed new techniques, including RNA FISH [122] and single-cell RNA-Seq [117], to measure gene expression in single cells, which could be used in conjunction with cell mechanical measures to study potential molecular determinants of mechanical heterogeneity. This could inform our understanding of the molecular contribution behind emergent cell mechanical phenotypes, and in turn identify new mechanisms underlying cellular contractility.

References

[1] J. A. Nadel and D. F. Tierney, "Effect of a previous deep inspiration on airway resistance in man," *J Appl Physiol*, vol. 16, pp. 717–9, Jul 1961.

[2] H. H. Bendixen, G. M. Smith, and J. Mead, "Pattern of ventilation in young adults," *J Appl Physiol*, vol. 19, pp. 195–8, Mar 1964.

[3] A. Gump, L. Haughney, and J. Fredberg, "Relaxation of activated airway smooth muscle: relative potency of isoproterenol vs. tidal stretch," *J Appl Physiol (1985)*, vol. 90, pp. 2306–10, Jun 2001.

[4] M. N. Oliver, B. Fabry, A. Marinkovic, S. M. Mijailovich, J. P. Butler, and J. J. Fredberg, "Airway hyperresponsiveness, remodeling, and smooth muscle mass: right answer, wrong reason?," *Am J Respir Cell Mol Biol*, vol. 37, pp. 264–72, Sep 2007.

[5] X. Trepat, L. Deng, S. S. An, D. Navajas, D. J. Tschumperlin, W. T. Gerthoffer, J. P. Butler, and J. J. Fredberg, "Universal physical responses to stretch in the living cell," *Nature*, vol. 447, pp. 592–5, May 2007.

[6] D. R. Stirling, D. J. Cotton, B. L. Graham, W. C. Hodgson, D. W. Cockcroft, and J. A. Dosman, "Characteristics of airway tone during exercise in patients with asthma," *J Appl Physiol Respir Environ Exerc Physiol*, vol. 54, pp. 934–42, Apr 1983.

[7] A. Jensen, H. Atileh, B. Suki, E. P. Ingenito, and K. R. Lutchen, "Selected contribution: airway caliber in healthy and asthmatic subjects: effects of bronchial challenge and deep inspirations," *J Appl Physiol (1985)*, vol. 91, pp. 506–15; discussion 504–5, Jul 2001.

[8] T. L. Lavoie, R. Krishnan, H. R. Siegel, E. D. Maston, J. J. Fredberg, J. Solway, and M. L. Dowell, "Dilatation of the constricted human airway by tidal expansion of lung parenchyma," *Am J Respir Crit Care Med*, vol. 186, pp. 225–32, Aug 2012.

[9] J. J. Fredberg, "Airway smooth muscle in asthma: flirting with disaster," *Eur Respir J*, vol. 12, pp. 1252–6, Dec 1998.

[10] H. H. Salter, *On asthma: its pathology and treatment*. Philadelphia: Blanchard and Lea, 1864.

[11] T. K. Lim, N. B. Pride, and R. H. Ingram, Jr, "Effects of volume history during spontaneous and acutely induced air-flow obstruction in asthma," *Am Rev Respir Dis*, vol. 135, pp. 591–6, Mar 1987.

[12] G. Skloot, S. Permutt, and A. Togias, "Airway hyperresponsiveness in asthma: a problem of limited smooth muscle relaxation with inspiration," *J Clin Invest*, vol. 96, pp. 2393–403, Nov 1995.

[13] A. L. James, P. D. Paré, and J. C. Hogg, "The mechanics of airway narrowing in asthma," *Am Rev Respir Dis*, vol. 139, pp. 242–6, Jan 1989.

[14] B. R. Wiggs, C. Bosken, P. D. Paré, A. James, and J. C. Hogg, "A model of airway narrowing in asthma and in chronic obstructive pulmonary disease," *Am Rev Respir Dis*, vol. 145, pp. 1251–8, Jun 1992.

[15] P. T. Macklem, "Relationship between airway smooth muscle dysfunction and airway inflammation in asthma," *Can Respir J*, vol. 5, no. 1, p. 40, 1998.

[16] A. F. Gelb, J. Licuanan, C. M. Shinar, and N. Zamel, "Unsuspected loss of lung elastic recoil in chronic persistent asthma," *Chest*, vol. 121, pp. 715–21, Mar 2002.

[17] R. H. Brown and W. Mitzner, "Effect of lung inflation and airway muscle tone on airway diameter in vivo," *J Appl Physiol (1985)*, vol. 80, pp. 1581–8, May 1996.

[18] J. J. Fredberg, K. A. Jones, M. Nathan, S. Raboudi, Y. S. Prakash, S. A. Shore, J. P. Butler, and G. C. Sieck, "Friction in airway smooth muscle: mechanism, latch, and implications in asthma," *J Appl Physiol (1985)*, vol. 81, pp. 2703–12, Dec 1996.

[19] J. J. Fredberg, D. S. Inouye, S. M. Mijailovich, and J. P. Butler, "Perturbed equilibrium of myosin binding in airway smooth muscle and its implications in bronchospasm," *Am J Respir Crit Care Med*, vol. 159, pp. 959–67, Mar 1999.

[20] J. J. Fredberg, "Airway smooth muscle in asthma. perturbed equilibria of myosin binding," *Am J Respir Crit Care Med*, vol. 161, pp. S158–60, Mar 2000.

[21] M. Oliver, T. Kováts, S. M. Mijailovich, J. P. Butler, J. J. Fredberg, and G. Lenormand, "Remodeling of integrated contractile tissues and its dependence on strain-rate amplitude," *Phys Rev Lett*, vol. 105, p. 158102, Oct 2010.

[22] J. J. Fredberg, "Bronchospasm and its biophysical basis in airway smooth muscle," *Respir Res*, vol. 5, p. 2, 2004.

[23] R. Krishnan, X. Trepat, T. T. B. Nguyen, G. Lenormand, M. Oliver, and J. J. Fredberg, "Airway smooth muscle and bronchospasm: fluctuating, fluidizing, freezing," *Respir Physiol Neurobiol*, vol. 163, pp. 17–24, Nov 2008.

[24] J. J. Fredberg, D. Inouye, B. Miller, M. Nathan, S. Jafari, S. H. Raboudi, J. P. Butler, and S. A. Shore, "Airway smooth muscle, tidal stretches, and dynamically determined contractile states," *Am J Respir Crit Care Med*, vol. 156, pp. 1752–9, Dec 1997.

[25] R. Krishnan, C. Y. Park, Y.-C. Lin, J. Mead, R. T. Jaspers, X. Trepat, G. Lenormand, D. Tambe, A. V. Smolensky, A. H. Knoll, J. P. Butler, and J. J. Fredberg, "Reinforcement versus fluidization in cytoskeletal mechanoresponsiveness," *PLoS One*, vol. 4, no. 5, p. e5486, 2009.

[26] S. J. Gunst and J. J. Fredberg, "The first three minutes: smooth muscle contraction, cytoskeletal events, and soft glasses," *J Appl Physiol (1985)*, vol. 95, pp. 413–25, Jul 2003.

[27] S. J. Gunst, R. A. Meiss, M. F. Wu, and M. Rowe, "Mechanisms for the mechanical plasticity of tracheal smooth muscle," *Am J Physiol*, vol. 268, pp. C1267–76, May 1995.

[28] S. J. Gunst, D. D. Tang, and A. Opazo Saez, "Cytoskeletal remodeling of the airway smooth muscle cell: a mechanism for adaptation to mechanical forces in the lung," *Respir Physiol Neurobiol*, vol. 137, pp. 151–68, Sep 2003.

[29] T. L. Lavoie, M. L. Dowell, O. J. Lakser, W. T. Gerthoffer, J. J. Fredberg, C. Y. Seow, R. W. Mitchell, and J. Solway, "Disrupting actin-myosin-actin connectivity in airway smooth muscle as a treatment for asthma?," *Proc Am Thorac Soc*, vol. 6, pp. 295–300, May 2009.

[30] A. W. Crawford and M. C. Beckerle, "Purification and characterization of zyxin, an 82,000-dalton component of adherens junctions," *J Biol Chem*, vol. 266, pp. 5847–53, Mar 1991.

[31] M. Yoshigi, L. M. Hoffman, C. C. Jensen, H. J. Yost, and M. C. Beckerle, "Mechanical force mobilizes zyxin from focal adhesions to actin filaments and regulates cytoskeletal reinforcement," *J Cell Biol*, vol. 171, pp. 209–15, Oct 2005.

[32] M. A. Smith, E. Blankman, M. L. Gardel, L. Luettjohann, C. M. Waterman, and M. C. Beckerle, "A zyxin-mediated mechanism for actin stress fiber maintenance and repair," *Dev Cell*, vol. 19, pp. 365–76, Sep 2010.

[33] L. M. Hoffman, D. A. Nix, B. Benson, R. Boot-Hanford, E. Gustafsson, C. Jamora, A. S. Menzies, K. L. Goh, C. C. Jensen, F. B. Gertler, E. Fuchs, R. Fässler, and M. C. Beckerle, "Targeted disruption of the murine zyxin gene," *Mol Cell Biol*, vol. 23, pp. 70–9, Jan 2003.

[34] N. Wang, I. M. Tolić-Nørrelykke, J. Chen, S. M. Mijailovich, J. P. Butler, J. J. Fredberg, and D. Stamenović, "Cell prestress. i. stiffness and prestress are closely associated in adherent contractile cells," *Am J Physiol Cell Physiol*, vol. 282, pp. C606–16, Mar 2002.

[35] P. Bursac, G. Lenormand, B. Fabry, M. Oliver, D. A. Weitz, V. Viasnoff, J. P. Butler, and J. J. Fredberg, "Cytoskeletal remodelling and slow dynamics in the living cell," *Nat Mater*, vol. 4, pp. 557–61, Jul 2005.

[36] J. P. Butler, I. M. Tolić-Nørrelykke, B. Fabry, and J. J. Fredberg, "Traction fields, moments, and strain energy that cells exert on their surroundings," *Am J Physiol Cell Physiol*, vol. 282, pp. C595–605, Mar 2002.

[37] A. Bergner and M. J. Sanderson, "Acetylcholine-induced calcium signaling and contraction of airway smooth muscle cells in lung slices," *J Gen Physiol*, vol. 119, pp. 187–98, Feb 2002.

[38] M. J. Sanderson, "Exploring lung physiology in health and disease with lung slices," *Pulm Pharmacol Ther*, vol. 24, pp. 452–65, Oct 2011.

[39] S. R. Rosner, S. Ram-Mohan, J. R. Paez-Cortez, T. L. Lavoie, M. L. Dowell, L. Yuan, X. Ai, A. Fine, W. C. Aird, J. Solway, J. J. Fredberg, and R. Krishnan, "Airway contractility in the precision cut lung slice following cryopreservation," *Am J Respir Cell Mol Biol*, vol. 50, pp. 876–881, May 2014.

[40] M. Masoli, D. Fabian, S. Holt, R. Beasley, and Global Initiative for Asthma (GINA) Program, "The global burden of asthma: executive summary of the gina dissemination committee report," *Allergy*, vol. 59, pp. 469–78, May 2004.

[41] C. Mathers, D. M. Fat, and J. T. Boerma, *The global burden of disease: 2004 update*. Geneva, Switzerland: World Health Organization, 2008.

[42] C. for Disease Control, "Asthma in the us: Growing every year." Vital Signs, 1600 Clifton Road NE, Atlanta, GA, May 2011.

[43] L. P. Chung, G. Waterer, and P. J. Thompson, "Pharmacogenetics of β2 adrenergic receptor gene polymorphisms, long-acting β-agonists and asthma," *Clin Exp Allergy*, vol. 41, pp. 312–26, Mar 2011.

[44] D. Cheung, M. C. Timmers, A. H. Zwinderman, E. H. Bel, J. H. Dijkman, and P. J. Sterk, "Long-term effects of a long-acting beta 2-adrenoceptor agonist, salmeterol, on airway hyperresponsiveness in patients with mild asthma," *N Engl J Med*, vol. 327, pp. 1198–203, Oct 1992.

[45] R. J. Hancox, R. E. Aldridge, J. O. Cowan, E. M. Flannery, G. P. Herbison, C. R. McLachlan, G. I. Town, and D. R. Taylor, "Tolerance to beta-agonists during acute bronchoconstriction," *Eur Respir J*, vol. 14, pp. 283–7, Aug 1999.

[46] D. W. McGraw and S. B. Liggett, "Molecular mechanisms of beta2-adrenergic receptor function and regulation," *Proc Am Thorac Soc*, vol. 2, no. 4, pp. 292–6; discussion 311–2, 2005.

[47] A. J. Ammit, "Glucocorticoid insensitivity as a source of drug targets for respiratory disease," *Curr Opin Pharmacol*, vol. 13, pp. 370–6, Jun 2013.

[48] D. Reddy and F. F. Little, "Glucocorticoid-resistant asthma: more than meets the eye," *J Asthma*, vol. 50, pp. 1036–44, Dec 2013.

[49] R. Pellegrino, P. J. Sterk, J. K. Sont, and V. Brusasco, "Assessing the effect of deep inhalation on airway calibre: a novel approach to lung function in bronchial asthma and copd," *Eur Respir J*, vol. 12, pp. 1219–27, Nov 1998.

[50] A. S. LaPrad, T. L. Szabo, B. Suki, and K. R. Lutchen, "Tidal stretches do not modulate responsiveness of intact airways in vitro," *J Appl Physiol (1985)*, vol. 109, pp. 295–304, Aug 2010.

[51] P. B. Noble, R. L. Jones, A. Cairncross, J. G. Elliot, H. W. Mitchell, A. L. James, and P. K. McFawn, "Airway narrowing and bronchodilation to deep inspiration in bronchial segments from subjects with and without reported asthma," *J Appl Physiol (1985)*, vol. 114, pp. 1460–71, May 2013.

[52] O. J. Lakser, R. P. Lindeman, and J. J. Fredberg, "Inhibition of the p38 map kinase pathway destabilizes smooth muscle length during physiological loading," *Am J Physiol Lung Cell Mol Physiol*, vol. 282, pp. L1117–21, May 2002.

[53] R. V. Rice, J. A. Moses, G. M. McManus, A. C. Brady, and L. M. Blasik, "The organization of contractile filaments in a mammalian smooth muscle," *J Cell Biol*, vol. 47, pp. 183–96, Oct 1970.

[54] M. Bárány, "Atpase activity of myosin correlated with speed of muscle shortening," *J Gen Physiol*, vol. 50, pp. Suppl:197–218, Jul 1967.

[55] C. Y. Seow and N. L. Stephens, "Force-velocity curves for smooth muscle: analysis of internal factors reducing velocity," *Am J Physiol*, vol. 251, pp. C362–8, Sep 1986.

[56] P. F. Dillon and R. A. Murphy, "Tonic force maintenance with reduced shortening velocity in arterial smooth muscle," *Am J Physiol*, vol. 242, pp. C102–8, Jan 1982.

[57] P. F. Dillon, M. O. Aksoy, S. P. Driska, and R. A. Murphy, "Myosin phosphorylation and the cross-bridge cycle in arterial smooth muscle," *Science*, vol. 211, pp. 495–7, Jan 1981.

[58] H. E. Huxley, "The double array of filaments in cross-striated muscle," *J Biophys Biochem Cytol*, vol. 3, pp. 631–48, Sep 1957.

[59] H. E. Huxley, "Recent x-ray diffraction and electron microscope studies of striated muscle," *J Gen Physiol*, vol. 50, pp. Suppl:71–83, Jul 1967.

[60] S. M. Mijailovich, J. P. Butler, and J. J. Fredberg, "Perturbed equilibria of myosin binding in airway smooth muscle: bond-length distributions, mechanics, and atp metabolism," *Biophys J*, vol. 79, pp. 2667–81, Nov 2000.

[61] V. R. Pratusevich, C. Y. Seow, and L. E. Ford, "Plasticity in canine airway smooth muscle," *J Gen Physiol*, vol. 105, pp. 73–94, Jan 1995.

[62] L. Wang, P. D. Paré, and C. Y. Seow, "Selected contribution: effect of chronic passive length change on airway smooth muscle length-tension relationship," *J Appl Physiol (1985)*, vol. 90, pp. 734–40, Feb 2001.

[63] C. Y. Seow, V. R. Pratusevich, and L. E. Ford, "Series-to-parallel transition in the filament lattice of airway smooth muscle," *J Appl Physiol (1985)*, vol. 89, pp. 869–76, Sep 2000.

[64] H. E. Huxley and M. Kress, "Crossbridge behaviour during muscle contraction," *J Muscle Res Cell Motil*, vol. 6, pp. 153–61, Apr 1985.

[65] J. A. Cooper, "Effects of cytochalasin and phalloidin on actin," *J Cell Biol*, vol. 105, pp. 1473–8, Oct 1987.

[66] S. Y. Saito, M. Hori, H. Ozaki, and H. Karaki, "Cytochalasin d inhibits smooth muscle contraction by directly inhibiting contractile apparatus," *J Smooth Muscle Res*, vol. 32, pp. 51–60, Apr 1996.

[67] D. Mehta and S. J. Gunst, "Actin polymerization stimulated by contractile activation regulates force development in canine tracheal smooth muscle," *J Physiol*, vol. 519 Pt 3, pp. 829–40, Sep 1999.

[68] P. Kanchanawong, G. Shtengel, A. M. Pasapera, E. B. Ramko, M. W. Davidson, H. F. Hess, and C. M. Waterman, "Nanoscale architecture of integrin-based cell adhesions," *Nature*, vol. 468, pp. 580–4, Nov 2010.

[69] H. B. Schiller and R. Fässler, "Mechanosensitivity and compositional dynamics of cell-matrix adhesions," *EMBO Rep*, vol. 14, pp. 509–19, Jun 2013.

[70] W. Zhang, Y. Wu, L. Du, D. D. Tang, and S. J. Gunst, "Activation of the arp2/3 complex by n-wasp is required for actin polymerization and contraction in smooth muscle," *Am J Physiol Cell Physiol*, vol. 288, pp. C1145–60, May 2005.

[71] S. S. An, R. E. Laudadio, J. Lai, R. A. Rogers, and J. J. Fredberg, "Stiffness changes in cultured airway smooth muscle cells," *Am J Physiol Cell Physiol*, vol. 283, pp. C792–801, Sep 2002.

[72] A. W. Crawford, J. W. Michelsen, and M. C. Beckerle, "An interaction between zyxin and alpha-actinin," *J Cell Biol*, vol. 116, pp. 1381–93, Mar 1992.

[73] I. Sadler, A. W. Crawford, J. W. Michelsen, and M. C. Beckerle, "Zyxin and ccrp: two interactive lim domain proteins associated with the cytoskeleton," *J Cell Biol*, vol. 119, pp. 1573–87, Dec 1992.

[74] T. Macalma, J. Otte, M. E. Hensler, S. M. Bockholt, H. A. Louis, M. Kalff-Suske, K. H. Grzeschik, D. von der Ahe, and M. C. Beckerle, "Molecular characterization of human zyxin," *J Biol Chem*, vol. 271, pp. 31470–8, Dec 1996.

[75] B. Drees, E. Friederich, J. Fradelizi, D. Louvard, M. C. Beckerle, and R. M. Golsteyn, "Characterization of the interaction between zyxin and members of the ena/vasodilator-stimulated phosphoprotein family of proteins," *J Biol Chem*, vol. 275, pp. 22503–11, Jul 2000.

[76] J. Fradelizi, V. Noireaux, J. Plastino, B. Menichi, D. Louvard, C. Sykes, R. M. Golsteyn, and E. Friederich, "Acta and human zyxin harbour arp2/3-independent actin-polymerization activity," *Nat Cell Biol*, vol. 3, pp. 699–707, Aug 2001.

[77] E. J. van der Gaag, M.-T. Leccia, S. K. Dekker, N. L. Jalbert, D. M. Amodeo, and H. R. Byers, "Role of zyxin in differential cell spreading and proliferation of melanoma cells and melanocytes," *J Invest Dermatol*, vol. 118, pp. 246–54, Feb 2002.

[78] L. M. Hoffman, C. C. Jensen, A. Chaturvedi, M. Yoshigi, and M. C. Beckerle, "Stretch-induced actin remodeling requires targeting of zyxin to stress fibers and recruitment of actin regulators," *Mol Biol Cell*, vol. 23, pp. 1846–59, May 2012.

[79] T. P. Lele, J. Pendse, S. Kumar, M. Salanga, J. Karavitis, and D. E. Ingber, "Mechanical forces alter zyxin unbinding kinetics within focal adhesions of living cells," *J Cell Physiol*, vol. 207, pp. 187–94, Apr 2006.

[80] H. Wolfenson, A. Bershadsky, Y. I. Henis, and B. Geiger, "Actomyosin-generated tension controls the molecular kinetics of focal adhesions," *J Cell Sci*, vol. 124, pp. 1425–32, May 2011.

[81] L. M. Hoffman, C. C. Jensen, S. Kloeker, C.-L. A. Wang, M. Yoshigi, and M. C. Beckerle, "Genetic ablation of zyxin causes mena/vasp mislocalization, increased motility, and deficits in actin remodeling," *J Cell Biol*, vol. 172, pp. 771–82, Feb 2006.

[82] J. Colombelli, A. Besser, H. Kress, E. G. Reynaud, P. Girard, E. Caussinus, U. Haselmann, J. V. Small, U. S. Schwarz, and E. H. K. Stelzer, "Mechanosensing in actin stress fibers revealed by a close correlation between force and protein localization," *J Cell Sci*, vol. 122, pp. 1665–79, May 2009.

[83] B. Fabry, G. N. Maksym, S. A. Shore, P. E. Moore, R. A. Panettieri, Jr, J. P. Butler, and J. J. Fredberg, "Selected contribution: time course and heterogeneity of contractile responses in cultured human airway smooth muscle cells," *J Appl Physiol (1985)*, vol. 91, pp. 986–94, Aug 2001.

[84] L. Deng, X. Trepat, J. P. Butler, E. Millet, K. G. Morgan, D. A. Weitz, and J. J. Fredberg, "Fast and slow dynamics of the cytoskeleton," *Nat Mater*, vol. 5, pp. 636–40, Aug 2006.

[85] M. Balland, N. Desprat, D. Icard, S. Féréol, A. Asnacios, J. Browaeys, S. Hénon, and F. Gallet, "Power laws in microrheology experiments on living cells: Comparative analysis and modeling," *Phys Rev E Stat Nonlin Soft Matter Phys*, vol. 74, p. 021911, Aug 2006.

[86] X. Trepat, M. R. Wasserman, T. E. Angelini, E. Millet, D. A. Weitz, J. P. Butler, and J. J. Fredberg, "Physical forces during collective cell migration," *Nature Physics*, vol. 5, no. 6, pp. 426–430, 2009.

[87] A. K. Harris, P. Wild, and D. Stopak, "Silicone rubber substrata: a new wrinkle in the study of cell locomotion," *Science*, vol. 208, pp. 177–9, Apr 1980.

[88] L. K. Wrobel, T. R. Fray, J. E. Molloy, J. J. Adams, M. P. Armitage, and J. C. Sparrow, "Contractility of single human dermal myofibroblasts and fibroblasts," *Cell Motil Cytoskeleton*, vol. 52, pp. 82–90, Jun 2002.

[89] N. Wang, E. Planus, M. Pouchelet, J. J. Fredberg, and G. Barlovatz-Meimon, "Urokinase receptor mediates mechanical force transfer across the cell surface," *Am J Physiol*, vol. 268, pp. C1062–6, Apr 1995.

[90] L. Schnipper, "Clinical implications of tumor-cell heterogeneity," *N Engl J Med*, vol. 314, pp. 1423–31, May 1986.

[91] D. F. Hayes and C. Paoletti, "Circulating tumour cells: insights into tumour heterogeneity," *J Intern Med*, vol. 274, pp. 137–43, Aug 2013.

[92] T. Bongiorno, J. Kazlow, R. Mezencev, S. Griffiths, R. Olivares-Navarrete, J. F. McDonald, Z. Schwartz, B. D. Boyan, T. C. McDevitt, and T. Sulchek, "Mechanical stiffness as an improved single-cell indicator of osteoblastic human mesenchymal stem cell differentiation," *J Biomech*, Nov 2013.

[93] E. Minshall, C. G. Wang, R. Dandurand, and D. Eidelman, "Heterogeneity of responsiveness of individual airways in cultured lung explants," *Can J Physiol Pharmacol*, vol. 75, pp. 911–6, Jul 1997.

[94] I. M. Tolić-Nørrelykke and N. Wang, "Traction in smooth muscle cells varies with cell spreading," *J Biomech*, vol. 38, pp. 1405–12, Jul 2005.

[95] N. Q. Balaban, U. S. Schwarz, D. Riveline, P. Goichberg, G. Tzur, I. Sabanay, D. Mahalu, S. Safran, A. Bershadsky, L. Addadi, and B. Geiger, "Force and focal adhesion assembly: a close relationship studied using elastic micropatterned substrates," *Nat Cell Biol*, vol. 3, pp. 466–72, May 2001.

[96] N. Wang, E. Ostuni, G. M. Whitesides, and D. E. Ingber, "Micropatterning tractional forces in living cells," *Cell Motil Cytoskeleton*, vol. 52, pp. 97–106, Jun 2002.

[97] J. L. Tan, J. Tien, D. M. Pirone, D. S. Gray, K. Bhadriraju, and C. S. Chen, "Cells lying on a bed of microneedles: an approach to isolate mechanical force," *Proc Natl Acad Sci U S A*, vol. 100, pp. 1484–9, Feb 2003.

[98] K. Burton and D. L. Taylor, "Traction forces of cytokinesis measured with optically modified elastic substrata," *Nature*, vol. 385, pp. 450–4, Jan 1997.

[99] H. Tanimoto and M. Sano, "Dynamics of traction stress field during cell division," *Phys Rev Lett*, vol. 109, p. 248110, Dec 2012.

[100] S. V. Plotnikov, A. M. Pasapera, B. Sabass, and C. M. Waterman, "Force fluctuations within focal adhesions mediate ecm-rigidity sensing to guide directed cell migration," *Cell*, vol. 151, pp. 1513–27, Dec 2012.

[101] M. B. Elowitz, A. J. Levine, E. D. Siggia, and P. S. Swain, "Stochastic gene expression in a single cell," *Science*, vol. 297, pp. 1183–6, Aug 2002.

[102] M. Bengtsson, A. Ståhlberg, P. Rorsman, and M. Kubista, "Gene expression profiling in single cells from the pancreatic islets of langerhans reveals lognormal distribution of mrna levels," *Genome Res*, vol. 15, pp. 1388–92, Oct 2005.

[103] J. R. S. Newman, S. Ghaemmaghami, J. Ihmels, D. K. Breslow, M. Noble, J. L. DeRisi, and J. S. Weissman, "Single-cell proteomic analysis of s. cerevisiae reveals the architecture of biological noise," *Nature*, vol. 441, pp. 840–6, Jun 2006.

[104] A. Sigal, R. Milo, A. Cohen, N. Geva-Zatorsky, Y. Klein, Y. Liron, N. Rosenfeld, T. Danon, N. Perzov, and U. Alon, "Variability and memory of protein levels in human cells," *Nature*, vol. 444, pp. 643–6, Nov 2006.

[105] H. H. Chang, M. Hemberg, M. Barahona, D. E. Ingber, and S. Huang, "Transcriptome-wide noise controls lineage choice in mammalian progenitor cells," *Nature*, vol. 453, pp. 544–7, May 2008.

[106] O. Feinerman, J. Veiga, J. R. Dorfman, R. N. Germain, and G. Altan-Bonnet, "Variability and robustness in t cell activation from regulated heterogeneity in protein levels," *Science*, vol. 321, pp. 1081–4, Aug 2008.

[107] A. Raj and A. van Oudenaarden, "Nature, nurture, or chance: stochastic gene expression and its consequences," *Cell*, vol. 135, pp. 216–26, Oct 2008.

[108] N. Rosenfeld, J. W. Young, U. Alon, P. S. Swain, and M. B. Elowitz, "Gene regulation at the single-cell level," *Science*, vol. 307, pp. 1962–5, Mar 2005.

[109] A. Raj and A. van Oudenaarden, "Single-molecule approaches to stochastic gene expression," *Annu Rev Biophys*, vol. 38, pp. 255–70, 2009.

[110] B. Munsky, G. Neuert, and A. van Oudenaarden, "Using gene expression noise to understand gene regulation," *Science*, vol. 336, pp. 183–7, Apr 2012.

[111] N. Molina, D. M. Suter, R. Cannavo, B. Zoller, I. Gotic, and F. Naef, "Stimulus-induced modulation of transcriptional bursting in a single mammalian gene," *Proc Natl Acad Sci U S A*, vol. 110, pp. 20563–8, Dec 2013.

[112] Y. Bossé, A. Sobieszek, P. D. Paré, and C. Y. Seow, "Length adaptation of airway smooth muscle," *Proc Am Thorac Soc*, vol. 5, pp. 62–7, Jan 2008.

[113] W. Zhang and S. J. Gunst, "Interactions of airway smooth muscle cells with their tissue matrix: implications for contraction," *Proc Am Thorac Soc*, vol. 5, pp. 32–9, Jan 2008.

[114] K. Acevedo, R. Li, P. Soo, R. Suryadinata, B. Sarcevic, V. A. Valova, M. E. Graham, P. J. Robinson, and O. Bernard, "The phosphorylation of p25/tppp by lim kinase 1 inhibits its ability to assemble microtubules," *Exp Cell Res*, vol. 313, pp. 4091–106, Dec 2007.

[115] M. A. Smith, E. Blankman, N. O. Deakin, L. M. Hoffman, C. C. Jensen, C. E. Turner, and M. C. Beckerle, "Lim domains target actin regulators paxillin and zyxin to sites of stress fiber strain," *PLoS One*, vol. 8, no. 8, p. e69378, 2013.

[116] D. Wang and S. Bodovitz, "Single cell analysis: the new frontier in 'omics'," *Trends Biotechnol*, vol. 28, pp. 281–90, Jun 2010.

[117] K. Kurimoto, Y. Yabuta, Y. Ohinata, and M. Saitou, "Global single-cell cdna amplification to provide a template for representative high-density oligonucleotide microarray analysis," *Nat Protoc*, vol. 2, no. 3, pp. 739–52, 2007.

[118] Z. Wang, M. Gerstein, and M. Snyder, "Rna-seq: a revolutionary tool for transcriptomics," *Nat Rev Genet*, vol. 10, pp. 57–63, Jan 2009.

[119] S. Picelli, O. R. Faridani, A. K. Björklund, G. Winberg, S. Sagasser, and R. Sandberg, "Full-length rna-seq from single cells using smart-seq2," *Nat Protoc*, vol. 9, pp. 171–81, Jan 2014.

[120] K. Zhang, A. C. Martiny, N. B. Reppas, K. W. Barry, J. Malek, S. W. Chisholm, and G. M. Church, "Sequencing genomes from single cells by polymerase cloning," *Nat Biotechnol*, vol. 24, pp. 680–6, Jun 2006.

[121] K. Taniguchi, T. Kajiyama, and H. Kambara, "Quantitative analysis of gene expression in a single cell by qpcr," *Nat Methods*, vol. 6, pp. 503–6, Jul 2009.

[122] A. Raj, P. van den Bogaard, S. A. Rifkin, A. van Oudenaarden, and S. Tyagi, "Imaging individual mrna molecules using multiple singly labeled probes," *Nat Methods*, vol. 5, pp. 877–9, Oct 2008.

[123] J. H. Lee, E. R. Daugharthy, J. Scheiman, R. Kalhor, J. L. Yang, T. C. Ferrante, R. Terry, S. S. F. Jeanty, C. Li, R. Amamoto, D. T. Peters, B. M. Turczyk, A. H. Marblestone, S. A. Inverso, A. Bernard, P. Mali, X. Rios, J. Aach, and G. M. Church, "Highly multiplexed subcellular rna sequencing in situ," *Science*, Feb 2014.

[124] G. Lenormand and J. J. Fredberg, "Deformability, dynamics, and remodeling of cytoskeleton of the adherent living cell," *Biorheology*, vol. 43, no. 1, pp. 1–30, 2006.

[125] B. Fabry, G. N. Maksym, J. P. Butler, M. Glogauer, D. Navajas, N. A. Taback, E. J. Millet, and J. J. Fredberg, "Time scale and other invariants of integrative mechanical behavior in living cells," *Phys Rev E Stat Nonlin Soft Matter Phys*, vol. 68, p. 041914, Oct 2003.

[126] J. H. T. Bates, M. Rincon, and C. G. Irvin, "Animal models of asthma," *Am J Physiol Lung Cell Mol Physiol*, vol. 297, pp. L401–10, Sep 2009.

[127] C. S. Stevenson and M. A. Birrell, "Moving towards a new generation of animal models for asthma and copd with improved clinical relevance," *Pharmacol Ther*, vol. 130, pp. 93–105, May 2011.

[128] A. R. Parrish, A. J. Gandolfi, and K. Brendel, "Precision-cut tissue slices: applications in pharmacology and toxicology," *Life Sci*, vol. 57, no. 21, pp. 1887–901, 1995.

[129] C. Martin, S. Uhlig, and V. Ullrich, "Videomicroscopy of methacholine-induced contraction of individual airways in precision-cut lung slices," *Eur Respir J*, vol. 9, pp. 2479–87, Dec 1996.

[130] H. D. Held, C. Martin, and S. Uhlig, "Characterization of airway and vascular responses in murine lungs," *Br J Pharmacol*, vol. 126, pp. 1191–9, Mar 1999.

[131] N. Struckmann, S. Schwering, S. Wiegand, A. Gschnell, M. Yamada, W. Kummer, J. Wess, and R. V. Haberberger, "Role of muscarinic receptor subtypes in the constriction of peripheral airways: studies on receptor-deficient mice," *Mol Pharmacol*, vol. 64, pp. 1444–51, Dec 2003.

[132] Y. Bai, M. Zhang, and M. J. Sanderson, "Contractility and ca2+ signaling of smooth muscle cells in different generations of mouse airways," *Am J Respir Cell Mol Biol*, vol. 36, pp. 122–30, Jan 2007.

[133] C. Dassow, L. Wiechert, C. Martin, S. Schumann, G. Müller-Newen, O. Pack, J. Guttmann, W. A. Wall, and S. Uhlig, "Biaxial distension of precision-cut lung slices," *J Appl Physiol (1985)*, vol. 108, pp. 713–21, Mar 2010.

[134] S. D. Crowther, I. D. Chapman, and J. Morley, "Heterogeneity of airway hyperresponsiveness," *Clin Exp Allergy*, vol. 27, pp. 606–16, Jun 1997.

[135] G. G. King, J. D. Carroll, N. L. Müller, K. P. Whittall, M. Gao, Y. Nakano, and P. D. Paré, "Heterogeneity of narrowing in normal and asthmatic airways measured by hrct," *Eur Respir J*, vol. 24, pp. 211–8, Aug 2004.

[136] N. T. Tgavalekos, M. Tawhai, R. S. Harris, G. Musch, G. Mush, M. Vidal-Melo, J. G. Venegas, and K. R. Lutchen, "Identifying airways responsible for heterogeneous ventilation and mechanical dysfunction in asthma: an image functional modeling approach," *J Appl Physiol (1985)*, vol. 99, pp. 2388–97, Dec 2005.

[137] N. T. Tgavalekos, G. Musch, R. S. Harris, M. F. Vidal Melo, T. Winkler, T. Schroeder, R. Callahan, K. R. Lutchen, and J. G. Venegas, "Relationship between airway narrowing, patchy ventilation and lung mechanics in asthmatics," *Eur Respir J*, vol. 29, pp. 1174–81, Jun 2007.

[138] M. L. Dowell, T. L. Lavoie, O. J. Lakser, N. O. Dulin, J. J. Fredberg, W. T. Gerthoffer, C. Y. Seow, R. W. Mitchell, and J. Solway, "Mek modulates force-fluctuation-induced relengthening of canine tracheal smooth muscle," *Eur Respir J*, vol. 36, pp. 630–7, Sep 2010.

[139] S. S. An, J. Kim, K. Ahn, X. Trepat, K. J. Drake, S. Kumar, G. Ling, C. Purington, T. Rangasamy, T. W. Kensler, W. Mitzner, J. J. Fredberg, and S. Biswal, "Cell stiffness, contractile stress and the role of extracellular matrix," *Biochem Biophys Res Commun*, vol. 382, pp. 697–703, May 2009.

[140] S. S. An, T. R. Bai, J. H. T. Bates, J. L. Black, R. H. Brown, V. Brusasco, P. Chitano, L. Deng, M. Dowell, D. H. Eidelman, B. Fabry, N. J. Fairbank, L. E. Ford, J. J. Fredberg, W. T. Gerthoffer, S. H. Gilbert, R. Gosens, S. J. Gunst, A. J. Halayko, R. H. Ingram, C. G. Irvin, A. L. James, L. J. Janssen, G. G. King, D. A. Knight, A. M. Lauzon, O. J. Lakser, M. S. Ludwig, K. R. Lutchen, G. N. Maksym, J. G. Martin, T. Mauad, B. E. McParland, S. M. Mijailovich, H. W. Mitchell, R. W. Mitchell, W. Mitzner, T. M. Murphy, P. D. Paré, R. Pellegrino, M. J. Sanderson, R. R. Schellenberg, C. Y. Seow, P. S. P. Silveira, P. G. Smith, J. Solway, N. L. Stephens, P. J. Sterk, A. G. Stewart, D. D. Tang, R. S. Tepper, T. Tran, and L. Wang, "Airway smooth muscle dynamics: a common pathway of airway obstruction in asthma," *Eur Respir J*, vol. 29, pp. 834–60, May 2007.

[141] A. Wohlsen, C. Martin, E. Vollmer, D. Branscheid, H. Magnussen, W. M. Becker, U. Lepp, and S. Uhlig, "The early allergic response in small airways of human precision-cut lung slices," *Eur Respir J*, vol. 21, pp. 1024–32, Jun 2003.

[142] Y. Bai and M. J. Sanderson, "The contribution of ca2+ signaling and ca2+ sensitivity to the regulation of airway smooth muscle contraction is different in rats and mice," *Am J Physiol Lung Cell Mol Physiol*, vol. 296, pp. L947–58, Jun 2009.

[143] M. Schlepütz, S. Uhlig, and C. Martin, "Electric field stimulation of precision-cut lung slices," *J Appl Physiol (1985)*, vol. 110, pp. 545–54, Feb 2011.

[144] S. Seehase, M. Schlepütz, S. Switalla, K. Mätz-Rensing, F. J. Kaup, M. Zöller, C. Schlumbohm, E. Fuchs, H.-D. Lauenstein, C. Winkler, A. R. Kuehl, S. Uhlig, A. Braun, K. Sewald, and C. Martin, "Bronchoconstriction in nonhuman primates: a species comparison," *J Appl Physiol (1985)*, vol. 111, pp. 791–8, Sep 2011.

[145] M. Schlepütz, A. D. Rieg, S. Seehase, J. Spillner, A. Perez-Bouza, T. Braunschweig, T. Schroeder, M. Bernau, V. Lambermont, C. Schlumbohm, K. Sewald, R. Autschbach, A. Braun, B. W. Kramer, S. Uhlig, and C. Martin, "Neurally mediated airway constriction in human and other species: a comparative study using precision-cut lung slices (pcls)," *PLoS One*, vol. 7, no. 10, p. e47344, 2012.

[146] N. Davidovich, J. Huang, and S. S. Margulies, "Reproducible uniform equibiaxial stretch of precision-cut lung slices," *Am J Physiol Lung Cell Mol Physiol*, vol. 304, pp. L210–20, Feb 2013.

[147] P. R. Cooper and R. A. Panettieri, Jr, "Steroids completely reverse albuterol-induced beta(2)-adrenergic receptor tolerance in human small airways," *J Allergy Clin Immunol*, vol. 122, pp. 734–40, Oct 2008.

[148] D. E. Pegg, "Principles of cryopreservation," *Methods Mol Biol*, vol. 368, pp. 39–57, 2007.

[149] H.-U. Kasper, E. Konze, N. Kutinová Canová, H. P. Dienes, and V. Dries, "Cryopreservation of precision cut tissue slices (pcts): investigation of morphology and reactivity," *Exp Toxicol Pathol*, vol. 63, pp. 575–80, Sep 2011.

[150] W. J. Maas, W. R. Leeman, J. P. Groten, and J. J. van de Sandt, "Cryopreservation of precision-cut rat liver slices using a computer-controlled freezer," *Toxicol In Vitro*, vol. 14, pp. 523–30, Dec 2000.

[151] J. W. MacRae, S. S. Tholpady, R. C. Ogle, and R. F. Morgan, "Ex vivo fat graft preservation: effects and implications of cryopreservation," *Ann Plast Surg*, vol. 52, pp. 281–2; discussion 283, Mar 2004.

[152] I. McGowan, K. Tanner, J. Elliott, J. Ibarrondo, E. Khanukhova, C. McDonald, T. Saunders, Y. Zhou, and P. A. Anton, "Nonreproducibility of "snap-frozen" rectal biopsies for later use in ex vivo explant infectibility studies," *AIDS Res Hum Retroviruses*, vol. 28, pp. 1509–12, Nov 2012.

[153] D. A. Deshpande, W. C. H. Wang, E. L. McIlmoyle, K. S. Robinett, R. M. Schillinger, S. S. An, J. S. K. Sham, and S. B. Liggett, "Bitter taste receptors on airway smooth muscle bronchodilate by localized calcium signaling and reverse obstruction," *Nat Med*, vol. 16, pp. 1299–304, Nov 2010.

[154] A. W. Saxe, G. W. Gibson, and S. Kay, "Characterization of a simplified method of cryopreserving human parathyroid tissue," *Surgery*, vol. 108, pp. 1033–8; discussion 1038–9, Dec 1990.

[155] H. Attarian, Z. Feng, C. D. Buckner, B. MacLeod, and S. D. Rowley, "Long-term cryopreservation of bone marrow for autologous transplantation," *Bone Marrow Transplant*, vol. 17, pp. 425–30, Mar 1996.

[156] J. O. Karlsson and M. Toner, "Long-term storage of tissues by cryopreservation: critical issues," *Biomaterials*, vol. 17, pp. 243–56, Feb 1996.

[157] R. Riggs, J. Mayer, D. Dowling-Lacey, T.-F. Chi, E. Jones, and S. Oehninger, "Does storage time influence postthaw survival and pregnancy outcome? an analysis of 11,768 cryopreserved human embryos," *Fertil Steril*, vol. 93, pp. 109–15, Jan 2010.

[158] I. A. M. de Graaf and H. J. Koster, "Cryopreservation of precision-cut tissue slices for application in drug metabolism research," *Toxicol In Vitro*, vol. 17, pp. 1–17, Feb 2003.

[159] I. A. M. de Graaf, A. L. Draaisma, O. Schoeman, G. M. Fahy, G. M. M. Groothuis, and H. J. Koster, "Cryopreservation of rat precision-cut liver and kidney slices by rapid freezing and vitrification," *Cryobiology*, vol. 54, pp. 1–12, Feb 2007.

[160] B. Fabry, G. N. Maksym, J. P. Butler, M. Glogauer, D. Navajas, and J. J. Fredberg, "Scaling the microrheology of living cells," *Phys Rev Lett*, vol. 87, p. 148102, Oct 2001.

[161] M. P. Sparrow, K. E. Willet, and H. W. Mitchell, "Airway diameter determines flow-resistance and sensitivity to contractile mediators in perfused bronchial segments," *Agents Actions Suppl*, vol. 31, pp. 63–6, 1990.

[162] H. W. Mitchell and M. P. Sparrow, "Increased responsiveness to cholinergic stimulation of small compared to large diameter cartilaginous bronchi," *Eur Respir J*, vol. 7, pp. 298–305, Feb 1994.

[163] C. Chen, M. Kudo, F. Rutaganira, H. Takano, C. Lee, A. Atakilit, K. S. Robinett, T. Uede, P. J. Wolters, K. M. Shokat, X. Huang, and D. Sheppard, "Integrin $\alpha 9\beta 1$ in airway smooth muscle suppresses exaggerated airway narrowing," *J Clin Invest*, vol. 122, pp. 2916–27, Aug 2012.

[164] M. Kudo, A. C. Melton, C. Chen, M. B. Engler, K. E. Huang, X. Ren, Y. Wang, X. Bernstein, J. T. Li, K. Atabai, X. Huang, and D. Sheppard, "Il-17a produced by $\alpha\beta$ t cells drives airway hyper-responsiveness in mice and enhances mouse and human airway smooth muscle contraction," *Nat Med*, vol. 18, pp. 547–54, Apr 2012.

[165] K. Radzikinas, L. Aven, Z. Jiang, T. Tran, J. Paez-Cortez, K. Boppidi, J. Lu, A. Fine, and X. Ai, "A shh/mir-206/bdnf cascade coordinates innervation and formation of airway smooth muscle," *J Neurosci*, vol. 31, pp. 15407–15, Oct 2011.

[166] M. D. Basson, G. D. Li, F. Hong, O. Han, and B. E. Sumpio, "Amplitude-dependent modulation of brush border enzymes and proliferation by cyclic strain in human intestinal caco-2 monolayers," *J Cell Physiol*, vol. 168, pp. 476–88, Aug 1996.

[167] D. Macconi, M. Abbate, M. Morigi, S. Angioletti, M. Mister, S. Buelli, M. Bonomelli, P. Mundel, K. Endlich, A. Remuzzi, and G. Remuzzi, "Permselective dysfunction of podocyte-podocyte contact upon angiotensin ii unravels the molecular target for renoprotective intervention," *Am J Pathol*, vol. 168, pp. 1073–85, Apr 2006.

[168] J. D. Humphrey, J. F. Eberth, W. W. Dye, and R. L. Gleason, "Fundamental role of axial stress in compensatory adaptations by arteries," *J Biomech*, vol. 42, pp. 1–8, Jan 2009.

[169] R. Wazir, D.-Y. Luo, Y. Tian, X. Yue, H. Li, and K.-J. Wang, "The purinergic component of human bladder smooth muscle cells' proliferation and contraction under physiological stretch," *Biochem Biophys Res Commun*, vol. 437, pp. 256–60, Jul 2013.

[170] C. Chen, R. Krishnan, E. Zhou, A. Ramachandran, D. Tambe, K. Rajendran, R. M. Adam, L. Deng, and J. J. Fredberg, "Fluidization and resolidification of the human bladder smooth muscle cell in response to transient stretch," *PLoS One*, vol. 5, no. 8, p. e12035, 2010.

[171] S. J. Gunst, "Contractile force of canine airway smooth muscle during cyclical length changes," *J Appl Physiol Respir Environ Exerc Physiol*, vol. 55, pp. 759–69, Sep 1983.

[172] J. J. Fredberg, "Frozen objects: small airways, big breaths, and asthma," *J Allergy Clin Immunol*, vol. 106, pp. 615–24, Oct 2000.

[173] D. E. Discher, P. Janmey, and Y.-L. Wang, "Tissue cells feel and respond to the stiffness of their substrate," *Science*, vol. 310, pp. 1139–43, Nov 2005.

[174] R. Krishnan, D. D. Klumpers, C. Y. Park, K. Rajendran, X. Trepat, J. van Bezu, V. W. M. van Hinsbergh, C. V. Carman, J. D. Brain, J. J. Fredberg, J. P. Butler, and G. P. van Nieuw Amerongen, "Substrate stiffening promotes endothelial monolayer disruption through enhanced physical forces," *Am J Physiol Cell Physiol*, vol. 300, pp. C146–54, Jan 2011.

[175] J. D. Mih, A. Marinkovic, F. Liu, A. S. Sharif, and D. J. Tschumperlin, "Matrix stiffness reverses the effect of actomyosin tension on cell proliferation," *J Cell Sci*, vol. 125, pp. 5974–83, Dec 2012.

[176] C. A. Boswell, G. Majno, I. Joris, and K. A. Ostrom, "Acute endothelial cell contraction in vitro: a comparison with vascular smooth muscle cells and fibroblasts," *Microvasc Res*, vol. 43, pp. 178–91, Mar 1992.

[177] J. K. Chen, S. R. Li, and R. J. Tsai, "Cyclic amp-induced inhibition of collagen lattice contraction by fibroblasts may be attenuated by both cyclic amp dependent and independent mechanisms," *J Cell Physiol*, vol. 155, pp. 8–13, Apr 1993.

[178] M. L. Toews, T. L. Ediger, D. J. Romberger, and S. I. Rennard, "Lysophosphatidic acid in airway function and disease," *Biochim Biophys Acta*, vol. 1582, pp. 240–50, May 2002.

[179] R. E. Slager, G. A. Hawkins, X. Li, D. S. Postma, D. A. Meyers, and E. R. Bleecker, "Genetics of asthma susceptibility and severity," *Clin Chest Med*, vol. 33, pp. 431–43, Sep 2012.

[180] Y. Zhang, M. F. Moffatt, and W. O. C. Cookson, "Genetic and genomic approaches to asthma: new insights for the origins," *Curr Opin Pulm Med*, vol. 18, pp. 6–13, Jan 2012.

[181] M. Wjst, M. Sargurupremraj, and M. Arnold, "Genome-wide association studies in asthma: what they really told us about pathogenesis," *Curr Opin Allergy Clin Immunol*, vol. 13, pp. 112–8, Feb 2013.

[182] B. Fabry and J. J. Fredberg, "Remodeling of the airway smooth muscle cell: are we built of glass?," *Respir Physiol Neurobiol*, vol. 137, pp. 109–24, Sep 2003.

[183] R. E. Laudadio, E. J. Millet, B. Fabry, S. S. An, J. P. Butler, and J. J. Fredberg, "Rat airway smooth muscle cell during actin modulation: rheology and glassy dynamics," *Am J Physiol Cell Physiol*, vol. 289, pp. C1388–95, Dec 2005.

[184] Y. Y. Degenhardt and S. Silverstein, "Interaction of zyxin, a focal adhesion protein, with the e6 protein from human papillomavirus type 6 results in its nuclear translocation," *J Virol*, vol. 75, pp. 11791–802, Dec 2001.

[185] Y. Wang and T. D. Gilmore, "Zyxin and paxillin proteins: focal adhesion plaque lim domain proteins go nuclear," *Biochim Biophys Acta*, vol. 1593, pp. 115–20, Feb 2003.

[186] J. L. Kadrmas and M. C. Beckerle, "The lim domain: from the cytoskeleton to the nucleus," *Nat Rev Mol Cell Biol*, vol. 5, pp. 920–31, Nov 2004.

[187] H. Janssen and P. Marynen, "Interaction partners for human znf384/ciz/nmp4–zyxin as a mediator for p130cas signaling?," *Exp Cell Res*, vol. 312, pp. 1194–204, Apr 2006.

[188] M. Hervy, L. Hoffman, and M. C. Beckerle, "From the membrane to the nucleus and back again: bifunctional focal adhesion proteins," *Curr Opin Cell Biol*, vol. 18, pp. 524–32, Oct 2006.

[189] U. Alon, *An introduction to systems biology: design principles of biological circuits*, vol. 10 of *Chapman and Hall: CRC mathematical and computational biology series*. Boca Raton, FL: Chapman and Hall:CRC, 2007.

[190] S. S. An, B. Fabry, M. Mellema, P. Bursac, W. T. Gerthoffer, U. S. Kayyali, M. Gaestel, S. A. Shore, and J. J. Fredberg, "Role of heat shock protein 27 in cytoskeletal remodeling of the airway smooth muscle cell," *J Appl Physiol (1985)*, vol. 96, pp. 1701–13, May 2004.

[191] M. Green and J. Mead, "Time dependence of flow-volume curves," *J Appl Physiol*, vol. 37, pp. 793–7, Dec 1974.

[192] J. E. Fish, M. G. Ankin, J. F. Kelly, and V. I. Peterman, "Regulation of bronchomotor tone by lung inflation in asthmatic and nonasthmatic subjects," *J Appl Physiol Respir Environ Exerc Physiol*, vol. 50, pp. 1079–86, May 1981.

[193] N. Carroll, J. Elliot, A. Morton, and A. James, "The structure of large and small airways in nonfatal and fatal asthma," *Am Rev Respir Dis*, vol. 147, pp. 405–10, Feb 1993.

[194] R. Kraemer and F. Geubelle, "Lung distensibility and airway function in asthmatic children," *Pediatr Res*, vol. 18, pp. 1154–9, Nov 1984.

[195] X. Ma, Z. Cheng, H. Kong, Y. Wang, H. Unruh, N. L. Stephens, and M. Laviolette, "Changes in biophysical and biochemical properties of single bronchial smooth muscle cells from asthmatic subjects," *Am J Physiol Lung Cell Mol Physiol*, vol. 283, pp. L1181–9, Dec 2002.

[196] R. W. Mitchell, M. L. Dowell, J. Solway, and O. J. Lakser, "Force fluctuation-induced relengthening of acetylcholine-contracted airway smooth muscle," *Proc Am Thorac Soc*, vol. 5, pp. 68–72, Jan 2008.

[197] A. L. Mansell, J. V. Rojas, E. M. Sillos, C. J. Stolar, M. H. Collins, and S. J. Rozovski, "Diaphragmatic activity is a determinant of postnatal lung growth," *J Appl Physiol (1985)*, vol. 61, pp. 1098–103, Sep 1986.

[198] R. Harding and S. B. Hooper, "Regulation of lung expansion and lung growth before birth," *J Appl Physiol (1985)*, vol. 81, pp. 209–24, Jul 1996.

[199] K. K. Nobuhara, D. O. Fauza, J. W. DiFiore, M. H. Hines, J. C. Fackler, R. Slavin, R. Hirschl, and J. M. Wilson, "Continuous intrapulmonary distension with perfluorocarbon accelerates neonatal (but not adult) lung growth," *J Pediatr Surg*, vol. 33, pp. 292–8, Feb 1998.

[200] Y. Yang, S. Beqaj, P. Kemp, I. Ariel, and L. Schuger, "Stretch-induced alternative splicing of serum response factor promotes bronchial myogenesis and is defective in lung hypoplasia," *J Clin Invest*, vol. 106, pp. 1321–30, Dec 2000.

[201] A. B. Ysasi, J. M. Belle, B. C. Gibney, A. V. Fedulov, W. Wagner, AkiraTsuda, M. A. Konerding, and S. J. Mentzer, "Effect of unilateral diaphragmatic paralysis on postpneumonectomy lung growth," *Am J Physiol Lung Cell Mol Physiol*, vol. 305, pp. L439–45, Sep 2013.

[202] M. Cattaruzza, C. Lattrich, and M. Hecker, "Focal adhesion protein zyxin is a mechanosensitive modulator of gene expression in vascular smooth muscle cells," *Hypertension*, vol. 43, pp. 726–30, Apr 2004.

[203] H. Hirata, H. Tatsumi, and M. Sokabe, "Mechanical forces facilitate actin polymerization at focal adhesions in a zyxin-dependent manner," *J Cell Sci*, vol. 121, pp. 2795–804, Sep 2008.

[204] Z. Sun, S. Huang, Z. Li, and G. A. Meininger, "Zyxin is involved in regulation of mechanotransduction in arteriole smooth muscle cells," *Front Physiol*, vol. 3, p. 472, 2012.

[205] T. Watanabe-Nakayama, M. Saito, S. Machida, K. Kishimoto, R. Afrin, and A. Ikai, "Requirement of lim domains for the transient accumulation of paxillin at damaged stress fibres," *Biol Open*, vol. 2, pp. 667–74, Jul 2013.

[206] J. C. Schittny, G. Miserocchi, and M. P. Sparrow, "Spontaneous peristaltic airway contractions propel lung liquid through the bronchial tree of intact and fetal lung explants," *Am J Respir Cell Mol Biol*, vol. 23, pp. 11–8, Jul 2000.

[207] C. H. Fanta, "Asthma," *N Engl J Med*, vol. 360, pp. 1002–14, Mar 2009.

[208] *Guidelines for the diagnosis and management of asthma: summary report 2007*, vol. no. 08-5846 of *NIH Publication*. U.S. Dept. of Health and Human Services, National Institues of Health, National Heart, Lung, and Blood Institute, 2008.

[209] F. E. Simons, T. V. Gerstner, and M. S. Cheang, "Tolerance to the bronchoprotective effect of salmeterol in adolescents with exercise-induced asthma using concurrent inhaled glucocorticoid treatment," *Pediatrics*, vol. 99, pp. 655–9, May 1997.

[210] J. A. Nelson, L. Strauss, M. Skowronski, R. Ciufo, R. Novak, and E. R. McFadden, Jr, "Effect of long-term salmeterol treatment on exercise-induced asthma," *N Engl J Med*, vol. 339, pp. 141–6, Jul 1998.

[211] M. Weinberger and M. Abu-Hasan, "Life-threatening asthma during treatment with salmeterol," *N Engl J Med*, vol. 355, pp. 852–3, Aug 2006.

[212] K. Malmstrom, G. Rodriguez-Gomez, J. Guerra, C. Villaran, A. Piñeiro, L. X. Wei, B. C. Seidenberg, and T. F. Reiss, "Oral montelukast, inhaled beclomethasone, and placebo for chronic asthma. a randomized, controlled trial. montelukast/beclomethasone study group," *Ann Intern Med*, vol. 130, pp. 487–95, Mar 1999.

[213] C. A. Sorkness, R. F. Lemanske, Jr, D. T. Mauger, S. J. Boehmer, V. M. Chinchilli, F. D. Martinez, R. C. Strunk, S. J. Szefler, R. S. Zeiger, L. B. Bacharier, G. R. Bloomberg, R. A. Covar, T. W. Guilbert, G. Heldt, G. Larsen, M. H. Mellon, W. J. Morgan, M. H. Moss, J. D. Spahn, L. M. Taussig, and Childhood Asthma Research and Education Network of the National Heart, Lung, and Blood Institute, "Long-term comparison of 3 controller regimens for mild-moderate persistent childhood asthma: the pediatric asthma controller trial," *J Allergy Clin Immunol*, vol. 119, pp. 64–72, Jan 2007.

[214] C. L. Grainge, L. C. K. Lau, J. A. Ward, V. Dulay, G. Lahiff, S. Wilson, S. Holgate, D. E. Davies, and P. H. Howarth, "Effect of bronchoconstriction on airway remodeling in asthma," *N Engl J Med*, vol. 364, pp. 2006–15, May 2011.

[215] D. J. Tschumperlin, "Physical forces and airway remodeling in asthma," *N Engl J Med*, vol. 364, pp. 2058–9, May 2011.

[216] C. E. Turner and J. T. Miller, "Primary sequence of paxillin contains putative sh2 and sh3 domain binding motifs and multiple lim domains: identification of a vinculin and pp125fak-binding region," *J Cell Sci*, vol. 107 (Pt 6), pp. 1583–91, Jun 1994.

[217] C. E. Turner, J. R. Glenney, Jr, and K. Burridge, "Paxillin: a new vinculin-binding protein present in focal adhesions," *J Cell Biol*, vol. 111, pp. 1059–68, Sep 1990.

[218] S. Arber, F. A. Barbayannis, H. Hanser, C. Schneider, C. A. Stanyon, O. Bernard, and P. Caroni, "Regulation of actin dynamics through phosphorylation of cofilin by lim-kinase," *Nature*, vol. 393, pp. 805–9, Jun 1998.